



**VYSOKÉ UČENÍ TECHNICKÉ V BRNĚ**

Fakulta chemická

**Podklady k habilitační práci v oboru**

**Chemie a technologie ochrany životního prostředí**

RNDr. Ondřej Zvěřina, Ph.D.

Brno 2024

prof. Ing. Michal Veselý, CSc.

Děkan FCH VUT v Brně  
Purkyňova 464/118  
612 00 Brno

V Brně dne 28. srpna 2024

### **Návrh na zahájení habilitačního řízení**

Vážený pane děkane,

dovoluji si Vám předložit návrh na zahájení habilitačního řízení v oboru Chemie a technologie ochrany životního prostředí na Fakultě chemické Vysokého učení technického v Brně.

V souladu se Směrnicí č. 9/2018, Postup při jmenovacím řízení na VUT ke svému návrhu přikládám:

- Habilitační práci s názvem „Využití možností, které přinesla technika vysokorozlišovací AAS s kontinuálním zdrojem záření do výzkumu materiálů životního prostředí“
- Podklady k habilitační práci v oboru Chemie a technologie ochrany životního prostředí, jejichž součástí jsou:
  - Životopis
  - Vyjádření vztahu k VUT
  - Přehled autoevaluačních kritérií včetně komentáře
  - Seznam publikovaných prací
  - Nejvýznamnější publikace
  - Přehled absolvovaných vědeckých stáží
  - Návrh tří témat pro veřejnou pedagogickou přednášku
  - Doklady osvědčující pedagogickou praxi
  - Ověřené doklady o dosaženém vysokoškolském vzdělání
  - Reprinty pěti nejvýznamnějších publikací

S pozdravem

RNDr. Ondřej Zvěřina, Ph.D.

# Obsah

Životopis	2
Vyjádření vztahu k VUT	4
Vlastní hodnocení uchazeče	6
Podrobnosti k jednotlivým kritériím – odborné činnosti	9
Recenzovaný odborný článek (výsledek Jimp), Q1	9
Recenzovaný odborný článek (výsledek Jimp), Q2	11
Recenzovaný odborný článek (výsledek Jimp), Q3	12
Recenzovaný odborný článek (výsledek Jimp), Q4	14
Recenzovaný odborný článek (výsledek Jost) **)	15
Citace jiným autorem podle WoS	16
Získání externího grantu (řešitel, spoluřešitel)	44
Podrobnosti k jednotlivým kritériím – pedagogické činnosti	45
Za každý rok pedagogického působení na vysoké škole na plný úvazek	45
Garantování SP	46
Garantování předmětů	47
Zavedení nového předmětu nebo zásadní inovace předmětu	48
Vedení úspěšně obhájené diplomové práce	49
Vedení úspěšně obhájené bakalářské práce	50
Školitel studenta, který získal Ph.D.	51
Skripta s ISBN (za 1 stranu)	52
Vytvoření významné výukové podpory	53
Doklady osvědčující pedagogickou praxi	55
Pedagogické působení na Ústavu veřejného zdraví	55
Pedagogické působení na ÚCHTOŽP	57
Seznam publikovaných prací	59
Vyjádření podílu na uvedených publikacích	63
Přehled absolvovaných vědeckých stáží	64
Návrh tří témat pro veřejnou pedagogickou přednášku	65
Úředně ověřené doklady o dosaženém vysokoškolském vzdělání	66
Nejvýznamnější publikace	73
Reprinty nejvýznamnějších publikací	74

# Životopis

jméno a příjmení: RNDr. Ondřej Zvěřina, Ph.D.  
narozen: 23. května 1986 v Třebíči  
bydliště: Sladová 4, 602 00 Brno  
kontakt: [ondrej.zverina@gmail.com](mailto:ondrej.zverina@gmail.com) | +420 776 025 904



## Vzdělání

2005–2015 Masarykova Univerzita, Přírodovědecká fakulta, Ústav chemie

2010-2015 postgraduální studium: Analytická chemie (Ph.D.)  
2013 studium k rozšíření, doplnění učitelské kvalifikace  
2012 rigorózní řízení v oboru: Analytická chemie (RNDr.)  
2008–2010 magisterský studijní obor: Analytická chemie (Mgr.)  
2005–2008 bakalářský studijní obor: Chemie (Bc.)

2001–2005 Střední průmyslová škola chemická v Brně  
studijní obor: Analytická chemie, maturita

## Zaměstnání

4/2014–doposud Masarykova Univerzita, Lékařská fakulta,  
Ústav veřejného zdraví, pozice: odborný asistent

## Vědeckovýzkumná činnost

- h-index: 11 (podle WoS, srpen 2024)
- počet citací: 291 (podle WoS, bez autocitací, srpen 2024)
- oblasti zájmu: atomová absorpční spektrometrie, potenciálně toxické prvky, antarktický ekosystém, polétavý prach

## Členství v odborných společnostech

- člen hlavního výboru Spektroskopické společnosti Jana Marka Marci (SSJMM)

## Účast na projektech

- MŠMT AKTION Česká republika - Rakousko 96p6: *Investigation of potentially toxic elements in Antarctic terrestrial flora* (2023)
- MZK (Moravská zemská knihovna), projekt institucionálního rozvoje: *Výzkum spor, plísni a prachových částic ve fondu MZK* (2019–2023)
- MŠMT Mobility 8J21AT006: *Potenciálně toxické prvky v houbách a zelenině pěstovaných ve městech v Rakousku a České republice* (2021–2022)
- GAČR P503/12/0682: *Transformace sloučenin rtuti půdní mikroflorou: možné využití pro bioremediační technologie* (2012–2015)

## Přednášky na odborných akcích

- *Simultaneous determination of Pb, Al, and Fe in the analysis of Antarctic terrestrial flora using HR-CS GF-AAS*, 18th Czech - Slovak Spectroscopic Conference (CSSC), Kurdějov, 2024
- *Biologicky přístupná frakce kovů v zelenině a její stanovení metodou in-vitro trávení*, Workshop Speciační analýza, Skalka u Kyjova, 2022
- *Simultánní stanovení více prvků pomocí contraA 800G*, Škola elementové stopové analýzy ChromSpec, FCH VUT Brno, 2022
- *Biomonitoring těžkých kovů s využitím lišejníků Usnea antarctica*, Biovědy v polárním a alpinském výzkumu: Současný stav a perspektivy polárního a alpinského výzkumu, Brno, 2016
- *Seal remains as sources of mercury for Antarctic environment*, Students in Polar and Alpine Research Conference, SPARC, Brno, 2016
- *Stanovení rtuti a methylrtuti ve specifických antarktických půdách z okolí uhynulých tuleňů*, Workshop Speciační analýza, Skalka u Kyjova, 2017
- *Sekvenční extrakce forem rtuti vázaných na městský polétavý prach*, Workshop Speciační analýza, Skalka u Kyjova, 2013
- *Mercury associated with size-fractionated urban particulate matter: three years of sampling in Prague, Czech Republic*, ESAS, Tatranská Lomnica, Slovensko, 2012

## Školitelství a konzultantství závěrečných prací

- doktorští studenti
  - absolventi 1 (školitel)
  - aktivní 1 (školitel)
- magisterští studenti
  - absolventi 7 (školitel), 9 (konzultant)
  - aktivní 1 (školitel)
- bakalářští studenti
  - absolventi 10 (školitel), 5 (konzultant)
  - aktivní 1 (školitel)

## Vyjádření vztahu k VUT

Můj vztah k VUT spočívá v zapojení do výuky, do vysokoškolských kvalifikačních prací (VŠKP) a výzkumu, a to převážně na Ústavu chemie a technologie ochrany životního prostředí (ÚCHTOŽP).

**Garantuji a vyučuji** zde předmět *Atomová absorpční spektrometrie v environmentální analýze* (FCH-MC\_AAS), který je součástí magisterského navazujícího programu Environmentální chemie a technologie. Pro tento předmět jsem také vytvořil elektronické studijní materiály. Dále se podílím na výuce předmětů *Instrumentální a strukturální analýza* (MC\_ISA) a její anglické verze *Instrumental and Structural Analysis* (MA\_ISA) a také v povinném předmětu bakalářského studia *Chemické látky v životním prostředí* (FCH-BC\_LZP). Přednáším a vedu cvičení také v Double degree magisterském navazujícím programu Environmental Sciences and Engineering v předmětu *Water analysis*.

Moje zapojení do **závěrečných prací** je na úrovni odborného poradce. V posledních letech jsem se podílel například na bakalářské práci Simony Kožnarové (obhájena 2021) a to konzultacemi a kontrolními měřeními vzorků platinových chemoterapeutik, kdy společné výsledky studentka prezentovala na konferenci ESAS 2022. Spolupracoval jsem také na závěrečné práci Kristýny Bilavčikové (mezilaboratorní ověření výsledků koncentrací ruthenia v buněčných mineralizátech v rámci bakalářské práce „*Studium interakce potenciálních léčiv na bázi metalocenu s buňkami*“, obhájena 2023). Pomáhal jsem s designem experimentů u DP Romana Jurnečky (obhájena 2023) s názvem „*Vývoj metod simultánní analýzy na přístroji HR-CS-ET-AAS a jejich využití v environmentální analýze*“.

Právě skrze vývoj a aplikace metod pro techniku vysokorozlišovací AAS – jež je tématem této habilitační práce – se zapojuji do **výzkumné spolupráce s ÚCHTOŽP**. Dlouhodobě spolupracuji s doc. Mgr. Michaelou Vašinovou Galiovou, Ph.D. při sledování chemoterapeutik na bázi platiny a ruthenocenu v živých buňkách. Společně jsme také publikovali studii sledující chování potenciálně toxických prvků v prostředí závislosti na převládajícím typu dopravy.

Můj hlavní pracovní poměr je na Ústavu veřejného zdraví Lékařské fakulty Masarykovy univerzity. Svým odborným zaměřením však cílím na vývoj analytických metod pro materiály životního prostředí. V tomto ohledu je proto spolupráce s ÚCHTOŽP VUT logická a stejně tak i habilitace v oboru Chemie a technologie ochrany životního prostředí. Získání titulu docenta umožní moji lepší integraci do struktur VUT, například i na úrovni garantství a účasti v závěrečných komisích. Budu se také moci stát školitelem postgraduálních studentů. V současnosti probíhá debata o dalším prohloubení a formalizace mojí spolupráce s ÚCHTOŽP VUT formou částečného pracovního úvazku.

## Vlastní hodnocení uchazeče

Autoevaluační analýza je zpracována podle Směrnice č. 9/2018, postup při **habilitačním řízení** na VUT.

Uchazeč: RNDr. Ondřej Zvěřina, Ph.D.  
Narozen: 23. května 1986  
Bydliště: Sladová 4, 602 00 Brno

Na základě provedené autoevaluační analýzy splňuji bodová kritéria v obou hodnocených oblastech; odborné (1361 bodů oproti požadovaným 600) i pedagogické (559 bodů z požadovaných 200). Splňuji také jednotlivá požadovaná kritéria oblastí, specifikovaná v Pokynu děkana č. 4/2022 v bodě čtyři, konkrétně:

- a) Na vysoké škole pedagogicky působím 10 let plným úvazkem (požadavek: minimálně 3 roky).
- b) Za tuto dobu jsem vedl celkem 17 úspěšně obhájených bakalářských a diplomových prací (požadavek: 6 prací).
- c) Jsem autorem elektronické studijní pomůcky a také spoluautorem kapitoly ve skriptech (požadavek: 1 dílo).
- d) Jsem autorem nebo spoluautorem 34 publikací souvisejících s mojí vědeckou orientací v časopisech s impact factorem (požadavek: 15 prací).
- e) Z toho jsem prvním nebo korespondujícím autorem u 12 z nich (požadavek: 5).
- f) Jako řešitel nebo spoluřešitel jsem získal 2 externí granty (požadavek: 1).
- g) Moje publikace mají 257 citací na WoS bez autocitací (požadavek: 50).

Následující tabulky poskytují podrobný přehled plnění jednotlivých rámcových kritérií.

### Souhrnný přehled – odborná oblast

Položka	A. Název odborné činnosti <sup>*)</sup>	Bodové hodnocení položky	Počet	Body celkem
1	Recenzovaný odborný článek (výsledek Jimp), Q1 <sup>**)</sup>	80	12	480
2	Recenzovaný odborný článek (výsledek Jimp), Q2 <sup>**)</sup>	40	7	140
3	Recenzovaný odborný článek (výsledek Jimp), Q3 <sup>**)</sup>	20	13	130

4	Recenzovaný odborný článek (výsledek Jimp), Q4 <sup>**</sup> )	10	2	10
5	Recenzovaný odborný článek (výsledek Jsc) <sup>**</sup> )	5		
6	Recenzovaný odborný článek (výsledek Jost) <sup>**</sup> )	5	2	5
7	Odborná kniha (výsledek B, za 1 stranu) <sup>**</sup> )	0,4		
8	Kapitola v odborné knize (výsledek C, za 1 stranu) <sup>**</sup> )	0,4		
9	Stat' ve sborníku (výsledek D) <sup>**</sup> )	2		
10	Citace jiným autorem podle WoS	2	257	514
11	Patent (výsledek P) <sup>**</sup> )	20		
12	Komeracionalizovaný patent <sup>**</sup> )	160		
13	Poloprovoz (výsledek Z)	5		
14	Ověřená technologie (výsledek Z)	5		
15	Užitný vzor (výsledek F)	5		
16	Průmyslový vzor (výsledek F)	5		
17	Prototyp (výsledek G)	5		
18	Funkční vzorek (výsledek G)	5		
19	Členství ve výboru světové vědecké společnosti (za každý rok)	3		
20	Členství ve výboru české vědecké společnosti (za každý rok)	2	1	2
21	Členství v redakční radě vědeckého časopisu Jimp (za každý rok)	10		
22	Členství v redakční radě českého vědeckého časopisu (za každý rok)	2		
23	Členství ve vědecké radě (za každý rok)	2		
24	Získání zahraničního grantu (řešitel, spoluřešitel) <sup>***</sup> )	80		
25	Získání externího grantu (řešitel, spoluřešitel) <sup>***</sup> )	40	2	80
26	Získání zakázky SmV vyšší jak 75 tis. Kč nebo 2500 €	10		
	CELKEM			<b>1361</b>
	minimální bodové požadavky			600

## Souhrnný přehled – pedagogická oblast

Položka	B. Název pedagogické činnosti	Bodové hodnocení položky	Počet	Body celkem
1	Za každý rok pedagogického působení na vysoké škole na plný úvazek (částečné úvazky se sčítají)	25	10	250
2	Zavedení nového SP nebo jeho zásadní inovace	20		
3	Garantování SP (za každý rok)	5	7	35
4	Garantování SP v angličtině (za každý rok)	10		
5	Garantování předmětů (za každý rok)	5	29	155
6	Zavedení nového předmětu nebo zásadní inovace předmětu	10	1	10
7	Vedení úspěšně obhájené diplomové práce	5	7	35
8	Vedení úspěšně obhájené bakalářské práce	3	10	30
11	Školitel studenta, který získal Ph.D.	20	1	20
12	Školitel specialista studenta, který získal Ph.D.	10		
13	Učebnice s ISBN (za 1 stranu)	0,4		
14	Skripta s ISBN (za 1 stranu)	0,4	10	4
15	Vytvoření významné výukové podpory v rozsahu odpovídajícím elearningovému kurzu k předmětu	20	1	20
16	Recenze učebnice nebo skript, která mají ISBN (za 1 stranu)	0,05		
	<b>CELKEM</b>			<b>559</b>
	minimální bodové požadavky			200

## Podrobnosti k jednotlivým kritériím – odborné činnosti

### Recenzovaný odborný článek (výsledek Jimp), Q1

Publikace jsou rozděleny podle WoS kvartilů platných v roce jejich publikace. V případě nových publikací je uveden poslední známý kvartil (tzn. pro rok 2023). U spoluautorských publikací, kde jsem korespondenčním autorem, je u mého jména symbol ☒.

Položka	A. Název odborné činnosti <sup>*)</sup>	Bodové hodnocení položky	Počet	Body celkem
1	Recenzovaný odborný článek (výsledek Jimp), Q1 <sup>**)</sup>	80	12	<b>480</b>
	<b>Zvěřina, O</b> ☒; Brůhová, L; Coufalík, P; Strínger, CD; Rieger, J; Goessler, W, 2024. Multi-element analysis (Pb, Al, Fe) of Antarctic flora using HR-CS ETAAS with an extended working range. SPECTROCHIMICA ACTA PART B-ATOMIC SPECTROSCOPY. 10.1016/j.sab.2024.106979	40		
	<b>Zvěřina, O</b> ☒; Vychytilová, M; Rieger, J; Goessler, W, 2023. Fast and simultaneous determination of zinc and iron using HR-CS GF-AAS in vegetables and plant material. SPECTROCHIMICA ACTA PART B-ATOMIC SPECTROSCOPY. 10.1016/j.sab.2023.106616	40		
	Duborská, E; Šebesta, M; Matulová, M; <b>Zvěřina, O</b> ; Urík, M, 2022. Current Strategies for Selenium and Iodine Biofortification in Crop Plants. NUTRIENTS. 10.3390/nu14224717	40		
	Hagarová, I; Nemček, L; Šebesta, M; <b>Zvěřina, O</b> ; Kasak, P; Urík, M, 2022. Preconcentration and Separation of Gold Nanoparticles from Environmental Waters Using Extraction Techniques Followed by Spectrometric Quantification. INTERNATIONAL JOURNAL OF MOLECULAR SCIENCES. 10.3390/ijms231911465	40		
	Duborská, E; Balíková, K; Matulová, M; <b>Zvěřina, O</b> ; Farkas, B; Littera, P; Urík, M, 2021. Production of Methyl-Iodide in the Environment. FRONTIERS IN MICROBIOLOGY. 10.3389/fmicb.2021.804081	40		

Farkas, B; Bujdos, M; Polák, F; Matulová, M; Cesnek, M; Duborská, E; <b>Zvěřina, O</b> ; Kim, H; Danko, M; Kisová, Z; Matůš, P; Urík, M, 2021. Bioremediation of Manganese Oxides at Different Oxidation States by Filamentous Fungus <i>Aspergillus niger</i> . JOURNAL OF FUNGI. 10.3390/jof7100808	40		
Brtnický, M; Pecina, V; Galiová, MV; Prokes, L; <b>Zvěřina, O</b> ; Juricka, D; Klimánek, M; Kynický, J, 2020. The impact of tourism on extremely visited volcanic island: Link between environmental pollution and transportation modes. CHEMOSPHERE. 10.1016/j.chemosphere.2020.126118	40		
Sysalová, J; <b>Zvěřina, O</b> ; Červenka, R; Komárek, J, 2020. Occurrence and transformation of mercury in formerly contaminated soils due to operation of amalgamation techniques and assessment of consequences. HUMAN AND ECOLOGICAL RISK ASSESSMENT. 10.1080/10807039.2019.1660848	40		
<b>Zvěřina, O</b> ✉; Kuta, J; Coufalík, P; Kosečková, P; Komárek, J, 2019. Simultaneous determination of cadmium and iron in different kinds of cereal flakes using high-resolution continuum source atomic absorption spectrometry. FOOD CHEMISTRY. 10.1016/j.foodchem.2019.125084	40		
Coufalík, P; Meszarosová, N; Coufalíková, K; <b>Zvěřina, O</b> ; Komárek, J, 2018. Determination of methylmercury in cryptogams by means of GC-AFS using enzymatic hydrolysis. MICROCHEMICAL JOURNAL. 10.1016/j.microc.2018.03.040	40		
Sysalová, J; Kučera, J; Drtinová, B; Červenka, R; <b>Zvěřina, O</b> ; Komárek, J; Kameník, J, 2017. Mercury species in formerly contaminated soils and released soil gases. SCIENCE OF THE TOTAL ENVIRONMENT. 10.1016/j.scitotenv.2017.01.157	40		
Coufalík, P; <b>Zvěřina, O</b> ; Komárek, J, 2016. The direct determination of HgS by thermal desorption coupled with atomic absorption spectrometry. SPECTROCHIMICA ACTA PART B-ATOMIC SPECTROSCOPY. 10.1016/j.sab.2016.01.004	40		

\*\*\*) V případě více autorů se započítá poloviční bodové hodnocení.

## Recenzovaný odborný článek (výsledek Jimp), Q2

Položka	A. Název odborné činnosti <sup>*)</sup>	Bodové hodnocení položky	Počet	Body celkem
2	Recenzovaný odborný článek (výsledek Jimp), Q2 <sup>**)</sup>	40	7	<b>140</b>
	Kosečková, P; <b>Zvěřina, O</b> ✉; Letková, K, 2024. Nutritional insights into broths in relation to elemental composition. EUROPEAN FOOD RESEARCH AND TECHNOLOGY. 10.1007/s00217-024-04556-2	20		
	Coufalík, P; <b>Zvěřina, O</b> ; Sádovská, K; Komárek, J, 2023. UV-photochemical vapor generation coupled to hydride generation AAS in the study of dietary intake of Se, Hg, Cd, and Pb from fish. JOURNAL OF FOOD COMPOSITION AND ANALYSIS. 10.1016/j.jfca.2023.105668	20		
	Kosečková, P; <b>Zvěřina, O</b> ✉; Pechová, M; Krulíková, M; Duborská, E; Borkovcová, M, 2022. Mineral profile of cricket powders, some edible insect species and their implication for gastronomy. JOURNAL OF FOOD COMPOSITION AND ANALYSIS. 10.1016/j.jfca.2021.104340	20		
	<b>Zvěřina, O</b> ✉; Coufalík, P; Brat, K; Červenka, R; Kuta, J; Mikes, O; Komárek, J, 2017. Leaching of mercury from seal carcasses into Antarctic soils. ENVIRONMENTAL SCIENCE AND POLLUTION RESEARCH. 10.1007/s11356-016-7879-3	20		
	Šípková, A; Száková, J; Coufalík, P; <b>Zvěřina, O</b> ; Kacálková, L; Tlustoš, P, 2014. Mercury distribution and mobility in contaminated soils from vicinity of waste incineration plant. PLANT SOIL AND ENVIRONMENT. 10.17221/634/2013-PSE	20		
	<b>Zvěřina, O</b> ✉; Láska, K; Červenka, R; Kuta, J; Coufalík, P; Komárek, J, 2014. Analysis of mercury and other heavy metals accumulated in lichen Usnea antarctica from James Ross Island, Antarctica. ENVIRONMENTAL MONITORING AND ASSESSMENT. 10.1007/s10661-014-4068-z	20		
	Coufalík, P; <b>Zvěřina, O</b> ; Komárek, J, 2013. Atmospheric mercury deposited in a peat bog, the Jeseniky Mountains, Czech Republic. JOURNAL OF GEOCHEMICAL EXPLORATION. 10.1016/j.gexplo.2013.06.005	20		

<sup>\*\*)</sup> V případě více autorů se započítá poloviční bodové hodnocení.

### Recenzovaný odborný článek (výsledek Jimp), Q3

Položka	A. Název odborné činnosti <sup>*)</sup>	Bodové hodnocení položky	Počet	Body celkem
3	Recenzovaný odborný článek (výsledek Jimp), Q3 <sup>**)</sup>	20	13	<b>130</b>
	Coufalík, P; Vašínska, M; Krmíček, L; Ševčík, R; <b>Zvěřina, O</b> ; Brůhová, L; Komárek, J, 2024. Toxic metals in cyanobacterial mat of Big Lachman Lake, James Ross Island, Antarctica. ENVIRONMENTAL MONITORING AND ASSESSMENT. 10.1007/s10661-023-12224-3	10		
	<b>Zvěřina, O</b> ✉; Venclíček, O; Kuta, J; Coufalík, P; Hagarova, I; Brat, K, 2021. A simple dilute-and-shoot procedure for the determination of platinum in human pleural effusions using HR-CS GF-AAS. JOURNAL OF TRACE ELEMENTS IN MEDICINE AND BIOLOGY. 10.1016/j.jtemb.2021.126869	10		
	<b>Zvěřina, O</b> ✉; Coufalík, P; Šimůnek, J; Kachlík, P; Chlupová, R; Pavelková, J, 2020. Inorganic pollutants in the indoor environment of the Moravian Library: assessment of Cd, Pb, Cu, and Zn in total suspended particles and dust using HR-CS GF-AAS. ENVIRONMENTAL MONITORING AND ASSESSMENT. 10.1007/s10661-020-08748-7	10		
	Coufalík, P; Uher, A; <b>Zvěřina, O</b> ; Komárek, J, 2020. Determination of cadmium in lichens by solid sampling graphite furnace atomic absorption spectrometry (SS-GF-AAS). ENVIRONMENTAL MONITORING AND ASSESSMENT. 10.1007/s10661-020-8186-5	10		
	Kosečková, P; <b>Zvěřina, O</b> ; Pruša, T; Coufalík, P; Hřežová, E, 2020. Estimation of cadmium load from soybeans and soy-based foods for vegetarians. ENVIRONMENTAL MONITORING AND ASSESSMENT. 10.1007/s10661-019-8034-7	10		
	Coufalík, P; Krmíček, L; <b>Zvěřina, O</b> ; Meszarosová, N; Hladil, J; Komárek, J, 2018. Model of Mercury Flux Associated with Volcanic Activity. BULLETIN OF ENVIRONMENTAL CONTAMINATION AND TOXICOLOGY. 10.1007/s00128-018-2430-5	10		

	<b>Zvěřina, O</b> ✉; Coufalík, P; Barták, M; Petrov, M; Komárek, J, 2018. The contents and distributions of cadmium, mercury, and lead in <i>Usnea antarctica</i> lichens from Solorina Valley, James Ross Island (Antarctica). ENVIRONMENTAL MONITORING AND ASSESSMENT. 10.1007/s10661-017-6397-1	10		
	Száková, J; Havlíčková, J; Šípková, A; Gabriel, J; Švec, K; Baldrian, P; Sysalová, J; Coufalík, P; Červenka, R; <b>Zvěřina, O</b> ; Komárek, J; Tlustoš, P, 2016. Effects of the soil microbial community on mobile proportions and speciation of mercury (Hg) in contaminated soil. JOURNAL OF ENVIRONMENTAL SCIENCE AND HEALTH PART A-TOXIC/HAZARDOUS SUBSTANCES & ENVIRONMENTAL ENGINEERING. 10.1080/10934529.2015.1109413	10		
	Coufalík, P; <b>Zvěřina, O</b> ; Krmíček, L; Pokorný, R; Komárek, J, 2015. Ultra-trace analysis of Hg in alkaline lavas and regolith from James Ross Island. ANTARCTIC SCIENCE. 10.1017/S0954102014000819	10		
	Coufalík, P; <b>Zvěřina, O</b> ; Mikuška, P; Komárek, J, 2014. Seasonal Variability of Mercury Contents in Street Dust in Brno, Czech Republic. BULLETIN OF ENVIRONMENTAL CONTAMINATION AND TOXICOLOGY. 10.1007/s00128-014-1289-3	10		
	Coufalík, P; <b>Zvěřina, O</b> ; Komárek, J, 2014. Determination of mercury species using thermal desorption analysis in AAS. CHEMICAL PAPERS. 10.2478/s11696-013-0471-0	10		
	<b>Zvěřina, O</b> ✉; Coufalík, P; Komárek, J; Gadas, P; Sysalová, J, 2014. Mercury associated with size-fractionated urban particulate matter: three years of sampling in Prague, Czech Republic. CHEMICAL PAPERS. 10.2478/s11696-013-0436-3	10		
	<b>Zvěřina, O</b> ✉; Červenka, R; Komárek, J; Sysalová, J, 2013. Mercury characterisation in urban particulate matter. CHEMICAL PAPERS. 10.2478/s11696-012-0259-7	10		

\*\*\*) V případě více autorů se započítá poloviční bodové hodnocení.

#### Recenzovaný odborný článek (výsledek Jimp), Q4

Položka	A. Název odborné činnosti <sup>*)</sup>	Bodové hodnocení položky	Počet	Body celkem
4	Recenzovaný odborný článek (výsledek Jimp), Q4 <sup>**)</sup>	10	2	<b>10</b>
	Lokvencová, L; <b>Zvěřina, O</b> ✉; Kuta, J, 2021. Different trends of Cr, Fe and Zn contents in hair between obese, overweight and normal-weight men. CENTRAL EUROPEAN JOURNAL OF PUBLIC HEALTH. 10.21101/cejph.a6912	5		
	Coufalík, P; Procházková, P; <b>Zvěřina, O</b> ; Trnková, K; Skácelová, K; Nývlt, D; Komárek, J, 2016. Freshwater mineral nitrogen and essential elements in autotrophs in James Ross Island, West Antarctica. POLISH POLAR RESEARCH. 10.1515/popore-2016-0025	5		

<sup>\*\*)</sup> V případě více autorů se započítá poloviční bodové hodnocení.

### Recenzovaný odborný článek (výsledek Jost) \*\*)

Položka	A. Název odborné činnosti <sup>*)</sup>	Bodové hodnocení položky	Počet	Body celkem
6	Recenzovaný odborný článek (výsledek Jost) **)	5	2	5
	Coufalík, P; Váczi, P; <b>Zvěřina, O</b> ; Trnková, K; Skácelová, K; Barták, M; Komárek, J, 2013. Nitrate and ammonium ions contents in field minibioreactors with Antarctic freshwater autotrophs. CZECH POLAR REPORTS. 10.5817/CPR2013-2-20	2,5		
	<b>Zvěřina, O</b> ✉; Coufalík, P; Vaculovič, T; Kuta, J; Zeman, J; Komárek, J, 2012. Macro- and microelements in soil profile of the moss-covered area in James Ross Island, Antarctica. CZECH POLAR REPORTS, vol. 2(no. 1), s. 1-7.	2,5		

\*\* ) V případě více autorů se započítá poloviční bodové hodnocení.

### Citace jiným autorem podle WoS

Citující články jsou uvedeny podle databáze Web of Science bez autocitací (a také bez autocitací spoluautorů), po vyfiltrování kategorie *Science Citation Index Expanded (SCI-EXP)*, tedy např. bez kategorií *Social Science Citation Index (SSCI)* a bez *Conference Proceedings Citation Index*. Platné k 1. srpnu 2024.

<b>Coufalík, P; Zvěřina, O; Sádovská, K; Komárek, J, 2023. UV-photochemical vapor generation coupled to hydride generation AAS in the study of dietary intake of Se, Hg, Cd, and Pb from fish. JOURNAL OF FOOD COMPOSITION AND ANALYSIS. 10.1016/j.jfca.2023.105668</b>	
1 Zhao, SM; Jia, RK; Han, QC; Shang, ND; Teng, KY; Feng, JW, 2024. Comparison of the Application of High-Resolution Inductively Coupled Plasma Mass Spectrometry (HR-ICP-MS) and Collision/Reaction Cell Technology of Inductively Coupled Plasma Mass Spectrometry (ICP-CCT-MS) in the Determination of Selenium in Coal-Bearing Strata. MINERALS. 10.3390/min14050510	2
<b>celkem za položku 2</b>	
<b>Zvěřina, O; Vychytilová, M; Rieger, J; Goessler, W, 2023. Fast and simultaneous determination of zinc and iron using HR-CS GF-AAS in vegetables and plant material. SPECTROCHIMICA ACTA PART B-ATOMIC SPECTROSCOPY. 10.1016/j.sab.2023.106616</b>	
1 Umaz, K; Umaz, A; Aydin, I; Aydin, F, 2024. Determination of zinc in dried nuts by slotted quartz tube-flame atomic absorption spectrometry (SQT-FAAS) with citric acid-coated magnetic nanoparticle (CAMNP) based solid phase extraction (SPE). INSTRUMENTATION SCIENCE & TECHNOLOGY. 10.1080/10739149.2024.2355530	2
2 Abd El-Fattah, W; Guesmi, A; Ben Hamadi, N; Khalil, MA; Shahat, A, 2024. A highly sensitive chemosensor based on a metal-organic framework for determining zinc ions in cosmetics creams and wastewater. APPLIED ORGANOMETALLIC CHEMISTRY. 10.1002/aoc.7407	2
3 He, S; Niu, YT; Xing, L; Liang, ZS; Song, XM; Ding, MH; Huang, WL, 2024. Research progress of the detection and analysis methods of heavy metals in plants. FRONTIERS IN PLANT SCIENCE. 10.3389/fpls.2024.1310328	2
4 Alshehri, RF; El-Feky, HH; Askar, AM; Amin, AS; Aish, M, 2024. Utilization of a novel PVC- optical sensor for high sensitive and selective determination of zinc ion in real samples. SPECTROCHIMICA ACTA PART A-MOLECULAR AND BIOMOLECULAR SPECTROSCOPY. 10.1016/j.saa.2023.123424	2
<b>celkem za položku 8</b>	

<b>Duborská, E; Šebesta, M; Matulová, M; Zvěřina, O; Urik, M, 2022. Current Strategies for Selenium and Iodine Biofortification in Crop Plants. NUTRIENTS. 10.3390/nu14224717</b>		
1	Wang, YM; Xie, XC; Chen, HJ; Zhang, K; Zhao, BL; Qiu, RL, 2024. Selenium-Induced Enhancement in Growth and Rhizosphere Soil Methane Oxidation of Prickly Pear. PLANTS-BASEL. 10.3390/plants13060749	2
2	Zhao, FL; Jin, JZ; Yang, M; Santiago, FEM; Xue, JP; Xu, L; Duan, YB, 2024. Selenium Differentially Regulates Flavonoid Accumulation and Antioxidant Capacities in Sprouts of Twenty Diverse Mungbean ( <i>Vigna radiata</i> (L.) Wilczek) Genotypes. PHYTON-INTERNATIONAL JOURNAL OF EXPERIMENTAL BOTANY. 10.32604/phyton.2024.048295	2
3	Ma, YZ; Huang, XT; Du, HN; Yang, J; Guo, FX; Wu, FY, 2024. Impacts, causes and biofortification strategy of rice selenium deficiency based on publication collection. SCIENCE OF THE TOTAL ENVIRONMENT. 10.1016/j.scitotenv.2023.169619	2
4	Ramezani, S; Yousefshahi, B; Ramezan, D; Zargar, M; Pakina, E; Bayat, M, 2023. Selenium, Iodine, and Supplementary Blue Light Enriched Fenugreek ( <i>Trigonella foenum-gracum</i> L.) in Terms of Biochemical Quality, Mineral Uptake, and Trace Elements Accumulation in a Hydroponic System. AGRICULTURE-BASEL. 10.3390/agriculture13102009	2
5	Verstegen, J; Günther, K, 2023. Ubiquitous Occurrence of Nano Selenium in Food Plants. FOODS. 10.3390/foods12173203	2
6	Halawani, RF; Aloufi, FA, 2023. Galaxolide-contaminated soil and tolerance strategies in soybean plants using biofertilization and selenium nanoparticle supplementation. FRONTIERS IN PLANT SCIENCE. 10.3389/fpls.2023.1221780	2
7	Ramezani, S; Yousefshahi, B; Farrokhzad, Y; Ramezan, D; Zargar, M; Pakina, E, 2023. Selenium and Iodine Biofortification Interacting with Supplementary Blue Light to Enhance the Growth Characteristics, Pigments, Trigonelline and Seed Yield of Fenugreek ( <i>Trigonella foenum-gracum</i> L.). AGRONOMY-BASEL. 10.3390/agronomy13082070	2
8	Czarnek, K; Tatarczak-Michalewska, M; Dreher, P; Rajput, VD; Wójcik, G; Gierut-Kot, A; Szopa, A; Blicharska, E, 2023. UV-C Seed Surface Sterilization and Fe, Zn, Mg, Cr Biofortification of Wheat Sprouts as an Effective Strategy of Bioelement Supplementation. INTERNATIONAL JOURNAL OF MOLECULAR SCIENCES. 10.3390/ijms241210367	2
9	Parra-Orobio, BA; Soto-Paz, J; Hernández-Cruz, JA; Gómez-Herreño, MC; Domínguez-Rivera, IC; Ocaña-Oviedo, ER, 2023. Evaluation of Biochar as an Additive in the Co-Composting of Green Waste and Food Waste. SUSTAINABILITY. 10.3390/su15097437	2
10	Krzeminska, J; Smolen, S; Kowalska, I; Pitala, J; Sularz, O; Koronowicz, A, 2023. Effect of Biofortification with Iodine by 8-Hydroxy-7-iodo-5-quinolinesulfonic Acid and 5-Chloro-7-iodo-8-quinolinol on the Chemical Composition and Antioxidant Properties of Potato Tubers ( <i>Solanum tuberosum</i> L.) in a Pot Experiment. APPLIED SCIENCES-BASEL. 10.3390/app13084659	2
<b>celkem za položku</b>		<b>20</b>

<b>Hagarová, I; Nemček, L; Šebesta, M; Zvěřina, O; Kasak, P; Urík, M, 2022. Preconcentration and Separation of Gold Nanoparticles from Environmental Waters Using Extraction Techniques Followed by Spectrometric Quantification. INTERNATIONAL JOURNAL OF MOLECULAR SCIENCES. 10.3390/ijms231911465</b>		
1	Justo-Vega, A; Domínguez-González, R; Bermejo-Barrera, P; Moreda-Piñeiro, A, 2024. Prospects of surfactant assisted dispersive liquid-liquid microextraction for the selective extraction of silver and titanium dioxide nanoparticles from tap water and determination by spICP-MS. JOURNAL OF ANALYTICAL ATOMIC SPECTROMETRY. 10.1039/d3ja00227f	2
2	Tziasiou, C; Pournara, AD; Manos, MJ; Giokas, DL, 2023. Dispersive solid phase extraction of noble metal nanoparticles from environmental samples on a thiol-functionalized Zirconium(IV) metal organic framework and determination with atomic absorption spectrometry. MICROCHEMICAL JOURNAL. 10.1016/j.microc.2023.109387	2
3	Godlewska, K; Pacyga, P; Najda, A; Michalak, I, 2023. Investigation of Chemical Constituents and Antioxidant Activity of Biologically Active Plant-Derived Natural Products. MOLECULES. 10.3390/molecules28145572	2
4	Hagarová, I; Nemček, L, 2023. Analytical Application of Layered Double Hydroxides as High-Capacity Sorbents in Dispersive Solid Phase Extraction for the Separation and Preconcentration of (Ultra)Trace Heavy Metals. CRITICAL REVIEWS IN ANALYTICAL CHEMISTRY. 10.1080/10408347.2023.2227906	2
<b>celkem za položku</b>		<b>8</b>
<b>Kosečková, P; Zvěřina, O; Pechová, M; Krulíková, M; Duborská, E; Borkovcová, M, 2022. Mineral profile of cricket powders, some edible insect species and their implication for gastronomy. JOURNAL OF FOOD COMPOSITION AND ANALYSIS. 10.1016/j.jfca.2021.104340</b>		
1	Gori, A; Armani, A; Pedonese, F; Benini, O; Mancini, S; Nuvoloni, R, 2025. Heavy metals (Pb, Cd, Ni) in insect-based products for human consumption sold by e-commerce in the EU market: Occurrence and potential health risk associated with dietary exposure. FOOD CONTROL. 10.1016/j.foodcont.2024.110781	2
2	Hassan, SA; Altemimi, AB; Hashmi, AA; Shahzadi, S; Mujahid, W; Ali, A; Bhat, ZF; Naz, S; Nawaz, A; Abdi, G; Aadil, RM, 2024. Edible crickets as a possible way to curb protein-energy malnutrition: Nutritional status, food applications, and safety concerns. FOOD CHEMISTRY-X. 10.1016/j.fochx.2024.101533	2
3	Tarahi, M; Hedayati, S; Niakousari, M, 2024. Supplementation of Cereal Products with Edible Insects: Nutritional, Techno-Functional, and Sensory Properties. FOOD REVIEWS INTERNATIONAL. 10.1080/87559129.2024.2355282	2
4	Boit, TC; Melse-Boonstra, A; Michaelsen, KF; Roos, N, 2024. Should we provide edible insects in children's diets?. CURRENT OPINION IN CLINICAL NUTRITION AND METABOLIC CARE. 10.1097/MCO.0000000000001029	2

5	Lu, MX; Zhu, CX; Smetana, S; Zhao, M; Zhang, HB; Zhang, F; Du, YZ, 2024. Minerals in edible insects: a review of content and potential for sustainable sourcing. FOOD SCIENCE AND HUMAN WELLNESS. 10.26599/FSHW.2022.9250005	2
6	Skotnicka, M; Mazurek, A; Kowalski, S; Pribis, P, 2023. The Acceptance of Cream Soups with the Addition of Edible Insects (Mealworm, <i>T. molitor</i> ; House Cricket, <i>A. domesticus</i> ; Buffalo Worm, <i>A. diaperinus</i> ; Grasshopper, <i>R. differens</i> ) among Young People and Seniors in Poland. NUTRIENTS. 10.3390/nu15245047	2
7	Zafar, A; Shaheen, M; Bin Tahir, A; Silva, APGD; Manzoor, HY; Zia, S, 2024. Unraveling the nutritional, biofunctional, and sustainable food application of edible crickets: A comprehensive review. TRENDS IN FOOD SCIENCE & TECHNOLOGY. 10.1016/j.tifs.2023.104254	2
8	Malematja, E; Sebola, NA; Manyelo, TG; Kolobe, SD; Mabelebele, M, 2023. Copping out of novel feeds: HOW climate change pledgers and food summits overlooked insect protein. HELIYON. 10.1016/j.heliyon.2023.e22773	2
9	Oliveira, LA; Pereira, SMS; Dias, KA; Paes, SD; Grancieri, M; Jimenez, LGS; de Carvalho, CWP; de Oliveira, EE; Martino, HSD; Lucia, CMD, 2024. Nutritional content, amino acid profile, and protein properties of edible insects ( <i>Tenebrio molitor</i> and <i>Gryllus assimilis</i> ) powders at different stages of development. JOURNAL OF FOOD COMPOSITION AND ANALYSIS. 10.1016/j.jfca.2023.105804	2
10	Kepinska-Pacelik, J; Biel, W; Podsiadlo, C; Tokarczyk, G; Biernacka, P; Bienkiewicz, G, 2023. Nutritional Value of Banded Cricket and Mealworm Larvae. FOODS. 10.3390/foods12224174	2
11	Aljohani, ASM, 2023. Heavy metal toxicity in poultry: a comprehensive review. FRONTIERS IN VETERINARY SCIENCE. 10.3389/fvets.2023.1161354	2
12	Krongdang, S; Phokasem, P; Venkatachalam, K; Charoenphun, N, 2023. Edible Insects in Thailand: An Overview of Status, Properties, Processing, and Utilization in the Food Industry. FOODS. 10.3390/foods12112162	2
13	Sikora, D; Proch, J; Niedzielski, P; Rzymiski, P, 2023. Elemental content of the commercial insect-based products available in the European Union. JOURNAL OF FOOD COMPOSITION AND ANALYSIS. 10.1016/j.jfca.2023.105367	2
14	Zhu, CX; Zhao, M; Lu, MX; Zhang, HB; Zhang, F; Du, YZ, 2023. Transcriptome analyses of different edible tissues of <i>Clanis bilineata tsingtauica</i> (Lepidoptera: Sphingidae) based on cooking customs. JOURNAL OF INSECTS AS FOOD AND FEED. 10.3920/JIFF2022.0075	2
15	Hameed, A; Majeed, W; Naveed, M; Ramzan, U; Bordiga, M; Hameed, M; Rehman, SU; Rana, N, 2022. Success of Aquaculture Industry with New Insights of Using Insects as Feed: A Review. FISHES. 10.3390/fishes7060395	2
<b>celkem za položku</b>		<b>30</b>

<b>Duborská, E; Balíková, K; Matulová, M; Zvěřina, O; Farkas, B; Littera, P; Urik, M, 2021. Production of Methyl-Iodide in the Environment. FRONTIERS IN MICROBIOLOGY. 10.3389/fmicb.2021.804081</b>		
1	Bey, E; Hughes, C; Hogg, K; Chance, R; Petrou, K, 2023. Ocean acidification reduces iodide production by the marine diatom <i>Chaetoceros</i> sp. (CCMP 1690). MARINE CHEMISTRY. 10.1016/j.marchem.2023.104311	2
<b>celkem za položku</b>		<b>2</b>
<b>Farkas, B; Bujdos, M; Polák, F; Matulová, M; Cesnek, M; Duborská, E; Zvěřina, O; Kim, H; Danko, M; Kisová, Z; Matúš, P; Urik, M, 2021. Bioleaching of Manganese Oxides at Different Oxidation States by Filamentous Fungus <i>Aspergillus niger</i>. JOURNAL OF FUNGI. 10.3390/jof7100808</b>		
1	Singh, N; Puneekar, NS, 2023. A plate assay to screen manganese-tolerant <i>Aspergillus niger</i> strains. INDIAN JOURNAL OF EXPERIMENTAL BIOLOGY. 10.56042/ijeb.v61i10.830	2
2	Naseri, T; Pourhossein, F; Mousavi, SM; Kaksonen, AH; Kuchta, K, 2022. Manganese bioleaching: an emerging approach for manganese recovery from spent batteries. REVIEWS IN ENVIRONMENTAL SCIENCE AND BIOTECHNOLOGY. 10.1007/s11157-022-09620-5	2
<b>celkem za položku</b>		<b>4</b>
<b>Zvěřina, O; Venclíček, O; Kuta, J; Coufalík, P; Hagarova, I; Brat, K, 2021. A simple dilute-and-shoot procedure for the determination of platinum in human pleural effusions using HR-CS GF-AAS. JOURNAL OF TRACE ELEMENTS IN MEDICINE AND BIOLOGY. 10.1016/j.jtemb.2021.126869</b>		
1	Butcher, DJ, 2024. Recent advances in graphite furnace atomic absorption spectrometry: a review of fundamentals and applications. APPLIED SPECTROSCOPY REVIEWS. 10.1080/05704928.2023.2192268	2
2	Patriarca, M; Barlow, N; Cross, A; Hill, S; Robson, A; Taylor, A; Tyson, J, 2023. Atomic spectrometry update: review of advances in the analysis of clinical and biological materials, foods and beverages. JOURNAL OF ANALYTICAL ATOMIC SPECTROMETRY. 10.1039/d3ja90008h	2
<b>celkem za položku</b>		<b>4</b>
<b>Lokvencová, L; Zvěřina, O; Kuta, J, 2021. Different trends of Cr, Fe and Zn contents in hair between obese, overweight and normal-weight men. CENTRAL EUROPEAN JOURNAL OF PUBLIC HEALTH. 10.21101/cejph.a6912</b>		
1	Mierzynska, Z; Niemirska, M; Zgonina, K; Bienkowski, T; Hryniow, K; Swider, P; Pawlak, K, 2024. Multi-Elemental Analysis of Hair and Fingernails Using Energy-Dispersive X-ray Fluorescence (ED XRF) Method Supported by Inductively Coupled Plasma Mass Spectrometry (ICP MS). MOLECULES. 10.3390/molecules29040773	2
2	Vigna, L; Tirelli, AS; Grossi, E; Turolo, S; Tomaino, L, 2023. Metal Body Burden as Cardiovascular Risk Factor in Adults with Metabolic Syndrome and Overweight-Obesity Analysed with an Artificial Neural Network: The Role of Hair Mineralograms. METABOLITES. 10.3390/metabo13060679	2
3	Zhang, Y; Huang, BY; Jin, J; Xiao, Y; Ying, HM, 2023. Recent advances in the application of ionomics in metabolic diseases. FRONTIERS IN NUTRITION. 10.3389/fnut.2022.1111933	2

	<b>celkem za položku</b>	<b>6</b>
<b>Zvěřina, O; Coufalík, P; Šimůnek, J; Kachlík, P; Chlupová, R; Pavelková, J, 2020. Inorganic pollutants in the indoor environment of the Moravian Library: assessment of Cd, Pb, Cu, and Zn in total suspended particles and dust using HR-CS GF-AAS. ENVIRONMENTAL MONITORING AND ASSESSMENT. 10.1007/s10661-020-08748-7</b>		
1	Zheng, PC; Liu, RN; Wang, JM; Feng, CH; He, YT; Wu, MN; He, YX, 2022. Solution Cathode Glow Discharge-Atomic Emission Spectroscopy Coupled With Hydride Generation for Detecting Trace Mercury and Tin in Water. SPECTROSCOPY AND SPECTRAL ANALYSIS. 10.3964/j.issn.1000-0593(2022)04-1139-05	2
	<b>celkem za položku</b>	<b>2</b>
<b>Brtnický, M; Pecina, V; Galiová, MV; Prokes, L; Zvěřina, O; Juricka, D; Klimánek, M; Kynický, J, 2020. The impact of tourism on extremely visited volcanic island: Link between environmental pollution and transportation modes. CHEMOSPHERE. 10.1016/j.chemosphere.2020.126118</b>		
1	Wang, Y; Hu, YX; Liu, YT; Chen, Q; Xu, JX; Zhang, F; Mao, JH; Shi, Q; He, C; Cai, RH; Lonborg, C; Liu, LH; Guo, AX; Jiao, NZ; Zheng, Q, 2024. Heavy metal induced shifts in microbial community composition and interactions with dissolved organic matter in coastal sediments. SCIENCE OF THE TOTAL ENVIRONMENT. 10.1016/j.scitotenv.2024.172003	2
2	Suhud, U; Allan, M, 2024. Structural Model of Tourists' Visit Intention Relating to Mount Ijen, a Volcano Tourism Destination: The Lack Role of Novelty-Seeking, Self-Congruity, and Destination Personality?. GEOHERITAGE. 10.1007/s12371-024-00926-0	2
3	Li, J; Liu, JZ; Tai, XS; Jiao, L; Zhang, M; Zang, F, 2024. Pollution and source-specific risk analysis of potentially toxic metals in urban soils of an oasis-tourist city in northwest China. ENVIRONMENTAL GEOCHEMISTRY AND HEALTH. 10.1007/s10653-023-01850-y	2
4	Yigit, Y; Aslan, A; Altinoz, B; Umut, A; Ozturk, I; Al-Mulali, U; Raboshuk, A, 2024. Examining the nexus between tourist arrivals and transportation sector-based emissions in Mediterranean countries: evidence from quantile regressions via method of moments. AIR QUALITY ATMOSPHERE AND HEALTH. 10.1007/s11869-024-01502-9	2
5	Bernardo, F; Garcia, P; Rodrigues, A, 2023. Air Quality at Ponta Delgada City (Azores) Is Unaffected so Far by Growing Cruise Ship Transit in Recent Years. ATMOSPHERE. 10.3390/atmos14010188	2
6	Zeng, T; Ma, L; Li, YZ; Abuduwaili, J; Liu, W; Feng, S, 2022. Source apportionment of soil heavy metals with PMF model and Pb isotopes in an intermountain basin of Tianshan Mountains, China. SCIENTIFIC REPORTS. 10.1038/s41598-022-24064-1	2
7	Li, F; Wang, KL; Li, X; Zhang, HD; Li, Y, 2022. The Evaluation and Key-Factor Identification of the Influence of Tourism on the Soil of Mount Tai. SUSTAINABILITY. 10.3390/su142113929	2

8	Yang, JZ; Sun, YL; Wang, ZL; Gong, JJ; Gao, JW; Tang, SX; Ma, SM; Duan, Z, 2022. Heavy metal pollution in agricultural soils of a typical volcanic area: Risk assessment and source appointment. CHEMOSPHERE. 10.1016/j.chemosphere.2022.135340	2
9	Yang, J; Xu, H; Wang, X, 2022. Impact of tourism activities on the distribution and pollution of soil heavy metals in natural scenic spots on the northern slope of Tianshan Mountain. PLOS ONE. 10.1371/journal.pone.0267829	2
10	Guo, ZH, 2022. Local Revitalization: Support from Local Residents. SUSTAINABILITY. 10.3390/su14148298	2
11	Zhang, SJ; Ye, H; Zhang, AJ; Ma, YY; Liu, Q; Shu, Q; Cao, XL, 2022. Pollution Characteristics, Sources, and Health Risk Assessment of Heavy Metals in the Surface Soil of Lushan Scenic Area, Jiangxi Province, China. FRONTIERS IN ENVIRONMENTAL SCIENCE. 10.3389/fenvs.2022.891092	2
12	Huang, WL; Chen, CY; Fu, YK, 2022. The Sustainable Island Tourism Evaluation Model Using the FDM-DEMATEL-ANP Method. SUSTAINABILITY. 10.3390/su14127244	2
13	Liu, J; Yue, MT; Liu, YM; Wen, D; Tong, Y, 2022. The Impact of Tourism on Ecosystem Services Value: A Spatio-Temporal Analysis Based on BRT and GWR Modeling. SUSTAINABILITY. 10.3390/su14052587	2
14	Zhang, YQ; Zhan, CC; Wang, H; Gao, Y, 2022. Evolution and reconstruction of settlement space in tourist islands: a case study of Dachangshan Island, Changhai County. ENVIRONMENT DEVELOPMENT AND SUSTAINABILITY. 10.1007/s10668-021-01845-8	2
15	Alexakis, DE; Bathrellos, GD; Skilodimou, HD; Gamvroula, DE, 2021. Land Suitability Mapping Using Geochemical and Spatial Analysis Methods. APPLIED SCIENCES-BASEL. 10.3390/app11125404	2
16	Martin, JAR; Gutiérrez, C; Escuer, M; Martín-Dacal, M; Ramos-Miras, JJ; Roca-Perez, L; Boluda, R; Nanos, N, 2021. Trends in soil mercury stock associated with pollution sources on a Mediterranean island (Majorca, Spain). ENVIRONMENTAL POLLUTION. 10.1016/j.envpol.2021.117397	2
17	Liu, SD; Geng, YH; Zhang, JJ; Kang, XF; Shi, XL; Zhang, J, 2021. Ecological trap in tourism-urbanization: Simulating the stagnation and restoration of urbanization from the perspective of government incentives. ECOLOGICAL ECONOMICS. 10.1016/j.ecolecon.2021.107054	2
18	Silva, LFO; Pinto, D; Neckel, A; Oliveira, MLS, 2020. An analysis of vehicular exhaust derived nanoparticles and historical Belgium fortress building interfaces. GEOSCIENCE FRONTIERS. 10.1016/j.gsf.2020.07.003	2
19	Silva, LFO; Pinto, D; Neckel, A; Oliveira, MLS; Sampaio, CH, 2020. Atmospheric nanocompounds on Lanzarote Island: Vehicular exhaust and igneous geologic formation interactions. CHEMOSPHERE. 10.1016/j.chemosphere.2020.126822	2
20	Chen, SH; Xi, JC; Liu, MH; Li, T, 2020. Analysis of Complex Transportation Network and Its Tourism Utilization Potential: A Case Study of Guizhou Expressways. COMPLEXITY. 10.1155/2020/1042506	2
<b>celkem za položku</b>		<b>40</b>

<b>Coufalík, P; Uher, A; Zvěřina, O; Komárek, J, 2020. Determination of cadmium in lichens by solid sampling graphite furnace atomic absorption spectrometry (SS-GF-AAS). ENVIRONMENTAL MONITORING AND ASSESSMENT. 10.1007/s10661-020-8186-5</b>		
1	Gao, WW; Yang, Z; Jiang, CJ; Sun, HJ; Wang, ZW; Zhang, MJ; Wei, Y; Wang, CT, 2023. Near-infrared reflectance spectroscopy model predictive of cadmium concentration in peanut kernels. JOURNAL OF FOOD MEASUREMENT AND CHARACTERIZATION. 10.1007/s11694-023-02064-7	2
2	Budzynska-Lipka, W; Swislawski, P; Rajfur, M, 2022. Biological Monitoring Using Lichens as a Source of Information About Contamination of Mountain with Heavy Metals. ECOLOGICAL CHEMISTRY AND ENGINEERING SCHEMIA I INZYNIERIA EKOLOGICZNA S. 10.2478/eces-2022-0012	2
3	Popovici, V; Bucur, L; Gird, CE; Calcan, SI; Cucolea, EI; Costache, T; Rambu, D; Ungureanu-Iuga, M; Oroian, M; Mironeasa, S; Schröder, V; Ozon, EA; Caraiane, A; Badea, V, 2022. Advances in the Characterization of Usnea barbata (L.) Weber ex FH Wigg from Calimani Mountains, Romania. APPLIED SCIENCES-BASEL. 10.3390/app12094234	2
4	Jurowski, K; Folta, M; Tatar, B; Krosniak, M, 2022. The Level of Cadmium Impurities in Traditional Herbal Medicinal Products with Plantago lanceolata L., folium (Ribwort Plantain Leaves) Available in Polish Pharmacies - Comprehensive Toxicological Risk Assessment Including Regulatory Point of View and ICH Q3D Elemental Impurities Guideline. BIOLOGICAL TRACE ELEMENT RESEARCH. 10.1007/s12011-021-02861-5	2
5	Padariya, C; Rutkowska, M; Konieczka, P, 2022. The importance and availability of marine certified reference materials. CRITICAL REVIEWS IN ENVIRONMENTAL SCIENCE AND TECHNOLOGY. 10.1080/10643389.2021.1922254	2
<b>celkem za položku</b>		<b>10</b>
<b>Kosečková, P; Zvěřina, O; Pruša, T; Coufalík, P; Hrežová, E, 2020. Estimation of cadmium load from soybeans and soy-based foods for vegetarians. ENVIRONMENTAL MONITORING AND ASSESSMENT. 10.1007/s10661-019-8034-7</b>		
1	Derkacz, R; Marciniak, W; Baszuk, P; Wysokinska, M; Chrzanowska, N; Lener, M; Huzarski, T; Gronwald, J; Debniak, T; Cybulski, C; Jakubowska, A; Scott, RJ; Lubinski, J, 2024. Blood Cadmium Level Is a Marker of Cancer Risk in Men. NUTRIENTS. 10.3390/nu16091309	2
2	Redan, BW; Zuklic, J; Hryshko, J; Boyer, M; Wan, JS; Sandhu, A; Jackson, LS, 2023. Analysis of eight types of plant-based milk alternatives from the United States market for target minerals and trace elements. JOURNAL OF FOOD COMPOSITION AND ANALYSIS. 10.1016/j.jfca.2023.105457	2
3	Flores-Collado, G; Mérida-Ortega, A; Ramirez, N; López-Carrillo, L, 2023. Urinary cadmium concentrations and intake of nutrients, food groups and dietary patterns in women from Northern Mexico. FOOD ADDITIVES AND CONTAMINANTS PART A-CHEMISTRY ANALYSIS CONTROL EXPOSURE & RISK ASSESSMENT. 10.1080/19440049.2022.2157050	2

4	Trung, NQ; Minh, BQ; Minh, TN, 2021. Rapid Identification of Geographical Origin of Commercial Soybean Marketed in Vietnam by ICP-MS. JOURNAL OF ANALYTICAL METHODS IN CHEMISTRY. 10.1155/2021/5583860	2
5	Paz, S; Rubio, C; Gutiérrez, AJ; González-Weller, D; Hardisson, A, 2021. Human exposure assessment to potentially toxic elements (PTEs) from tofu consumption. ENVIRONMENTAL SCIENCE AND POLLUTION RESEARCH. 10.1007/s11356-021-13076-5	2
6	Zhang, S; Song, J; Wu, LH; Chen, Z, 2021. Worldwide cadmium accumulation in soybean grains and feasibility of food production on contaminated calcareous soils. ENVIRONMENTAL POLLUTION. 10.1016/j.envpol.2020.116153	2
7	Gustin, K; Barman, M; Stråvik, M; Levi, M; Englund-Ögge, L; Murray, F; Jacobsson, B; Sandberg, AS; Sandin, A; Wold, AE; Vahter, M; Kippler, M, 2020. Low-level maternal exposure to cadmium, lead, and mercury and birth outcomes in a Swedish prospective birth-cohort. ENVIRONMENTAL POLLUTION. 10.1016/j.envpol.2020.114986	2
<b>celkem za položku</b>		<b>14</b>
<b>Zvěřina, O; Kuta, J; Coufalík, P; Kosečková, P; Komárek, J, 2019. Simultaneous determination of cadmium and iron in different kinds of cereal flakes using high-resolution continuum source atomic absorption spectrometry. FOOD CHEMISTRY. 10.1016/j.foodchem.2019.125084</b>		
1	Wang, X; Hu, XT; Zhai, XD; Huang, XW; Li, ZH; Zou, XB; Shi, JY, 2024. A simple and sensitive electrochemical sensing based on amine-functionalized metal-organic framework and polypyrrole composite for detection of lead ions in meat samples. JOURNAL OF FOOD MEASUREMENT AND CHARACTERIZATION. 10.1007/s11694-024-02611-w	2
2	Che, YR; Yang, JY; Dong, ZM; Wang, JH; Yan, XQ; Wang, Y; Shuang, SM, 2024. A sensitive turn-on Schiff-base fluorescent probe for the selective detection of Fe <sup>3+</sup> and bio-imaging. SPECTROCHIMICA ACTA PART A-MOLECULAR AND BIOMOLECULAR SPECTROSCOPY. 10.1016/j.saa.2023.123799	2
3	Ai, QS; Dong, YF; Yu, XR; Wei, PL; Zhang, DW; Qiu, SY, 2023. Sensitive detection of cadmium ions based on a quantum-dot-mediated fluorescent visualization sensor. RSC ADVANCES. 10.1039/d3ra04255c	2
4	Hou, J; Gao, X; Li, GJ; Liu, HL; Chen, QQ; Sun, J; Yang, G, 2023. Carbon dots/layered zirconium phosphate composites for the adsorption-detection integration of iron ions. NEW JOURNAL OF CHEMISTRY. 10.1039/d3nj03034b	2
5	Sumczynski, D; Fisera, M; Salek, RN; Orsavová, J, 2023. The Effect of Flake Production and In Vitro Digestion on Releasing Minerals and Trace Elements from Wheat Flakes: The Extended Study of Dietary Intakes for Individual Life Stage Groups. NUTRIENTS. 10.3390/nu15112509	2
6	Du, YC; Li, YX; Liu, YL; Liu, NY; Cheng, YY; Shi, QZ; Liu, X; Tao, ZM; Guo, YM; Zhang, JG; Askaria, N; Li, HT, 2023. Stalk-derived carbon dots as nanosensors for Fe <sup>3+</sup> ions detection and biological cell imaging. FRONTIERS IN BIOENGINEERING AND BIOTECHNOLOGY. 10.3389/fbioe.2023.1187632	2

7	Bustos, DE; Toro, JA; Briceño, M; Rivas, RE, 2022. Use of slow atomization ramp in high resolution continuum source graphite furnace atomic absorption spectrometry for the simultaneous determination of Cd and Ni in slurry powdered chocolate samples. <i>TALANTA</i> . 10.1016/j.talanta.2022.123547	2
8	Sanchez-Ponce, L; Galindo-Riano, MD; Casanueva-Marengo, MJ; Granado-Castro, MD; Diaz-de-Alba, M, 2021. Sensing Cd(II) Using a Disposable Optical Sensor Based on a Schiff Base Immobilisation on a Polymer-Inclusion Membrane. Applications in Water and Art Paint Samples. <i>POLYMERS</i> . 10.3390/polym13244414	2
9	Chen, XJ; Sun, Y; Mo, XM; Gao, Q; Deng, YA; Hu, M; Zou, JM; Nie, JF; Zhang, Y, 2021. On-site, rapid and visual method for nanomolar Hg <sup>2+</sup> detection based on the thymine-Hg <sup>2+</sup> -thymine triggered double aggregation of Au nanoparticles enhancing the Tyndall effect. <i>RSC ADVANCES</i> . 10.1039/d1ra07211k	2
10	Pasias, IN; Rousis, NI; Psoma, AK; Thomaidis, NS, 2021. Simultaneous or Sequential Multi-element Graphite Furnace Atomic Absorption Spectrometry Techniques: Advances Within the Last 20 Years. <i>ATOMIC SPECTROSCOPY</i> . 10.46770/AS.2021.707	2
11	Nakadi, FV; García-Poyo, MC; Pécheyran, C; Resano, M, 2021. Time-absorbance profile ratio background correction: introducing TAP to correct for spectral overlap in high-resolution continuum source graphite furnace atomic absorption spectrometry. <i>JOURNAL OF ANALYTICAL ATOMIC SPECTROMETRY</i> . 10.1039/d1ja00233c	2
12	Yildirim, A; Kocer, MB; Demir, AD; Arslan, E; Yilmaz, M, 2021. A bi-modal, cellulose-based sensor for fluorometric detection of Fe(III) and antimicrobial studies of its silver-loaded form. <i>INTERNATIONAL JOURNAL OF BIOLOGICAL MACROMOLECULES</i> . 10.1016/j.ijbiomac.2021.04.134	2
13	Patriarca, M; Barlow, N; Cross, A; Hill, S; Robson, A; Taylor, A; Tyson, J, 2021. Atomic spectrometry update: review of advances in the analysis of clinical and biological materials, foods and beverages. <i>JOURNAL OF ANALYTICAL ATOMIC SPECTROMETRY</i> . 10.1039/d1ja90007b	2
14	Altundal, M; Üge, A; Gök, O; Zeybek, B, 2021. Determination of Cadmium(II) by Differential Pulse Voltammetry (DPV) Using a Cerium(IV) Oxide: Polyaniline Composite Modified Glassy Carbon Electrode (GCE). <i>ANALYTICAL LETTERS</i> . 10.1080/00032719.2020.1870121	2
15	Gómez-Nieto, B; Motyzhov, V; Gismera, MJ; Procopio, JR; Sevilla, MT, 2020. Fast-sequential determination of cadmium and copper in milk powder and infant formula by direct solid sampling high-resolution continuum source graphite furnace atomic absorption spectrometry. <i>MICROCHEMICAL JOURNAL</i> . 10.1016/j.microc.2020.105335	2
16	Huang, LJ; Huang, W; Shen, RJ; Shuai, Q, 2020. Chitosan/thiol functionalized metal-organic framework composite for the simultaneous determination of lead and cadmium ions in food samples. <i>FOOD CHEMISTRY</i> . 10.1016/j.foodchem.2020.127212	2

17	Qian, J; Lu, XT; Wang, CQ; Cui, HN; An, KQ; Long, LL; Hao, N; Wang, K, 2020. Controlling over the terminal functionalities of thiol-capped CdZnTe QDs to develop fluorescence nanosensor for selective discrimination and determination of Fe(II) ions. SENSORS AND ACTUATORS B-CHEMICAL. 10.1016/j.snb.2020.128636	2
18	Cao, Q; Xiao, YS; Huang, R; Liu, N; Chi, H; Lin, CT; Huang, CH; Han, G; Wu, LD, 2020. Thiolated poly(aspartic acid)-functionalized two-dimensional MoS <sub>2</sub> , chitosan and bismuth film as a sensor platform for cadmium ion detection. RSC ADVANCES. 10.1039/d0ra06197b	2
19	Ghuniem, MM; Khorshed, MA; El-safty, SM; Souaya, ER; Khalil, MMH, 2022. Assessment of human health risk due to potentially toxic elements intake via consumption of Egyptian rice-based and wheat-based baby cereals. INTERNATIONAL JOURNAL OF ENVIRONMENTAL ANALYTICAL CHEMISTRY. 10.1080/03067319.2020.1817911	2
20	Kasa, NA; Bakirdere, EG, 2021. Determination of Iron in Licorice Samples by Slotted Quartz Tube Flame Atomic Absorption Spectrometry (FAAS) with Matrix Matching Calibration Strategy after Complexation with Schiff Base Ligand-Based Dispersive Liquid-Liquid Microextraction. ANALYTICAL LETTERS. 10.1080/00032719.2020.1801709	2
21	Atsever, N; Borahan, T; Bakirdere, EG; Bakirdere, S, 2020. Determination of iron in hair samples by slotted quartz tube-flame atomic absorption spectrometry after switchable solvent liquid phase extraction. JOURNAL OF PHARMACEUTICAL AND BIOMEDICAL ANALYSIS. 10.1016/j.jpba.2020.113274	2
22	Gan, TT; Zhao, NJ; Yin, GF; Chen, M; Wang, X; Hua, H, 2020. Preconcentration with <i>Chlorella vulgaris</i> combined with energy dispersive X-ray fluorescence spectrometry for rapid determination of Cd in water. ROYAL SOCIETY OPEN SCIENCE. 10.1098/rsos.200182	2
23	Yin, Y; Yang, QL; Liu, G, 2020. Ammonium Pyrrolidine Dithiocarbamate-Modified CdTe/CdS Quantum Dots as a Turn-on Fluorescent Sensor for Detection of Trace Cadmium Ions. SENSORS. 10.3390/s20010312	2
<b>celkem za položku</b>		<b>46</b>
<b>Coufalík, P; Krmíček, L; Zvěřina, O; Meszarosová, N; Hladil, J; Komárek, J, 2018. Model of Mercury Flux Associated with Volcanic Activity. BULLETIN OF ENVIRONMENTAL CONTAMINATION AND TOXICOLOGY. 10.1007/s00128-018-2430-5</b>		
1	Ni, XR; Yin, RS; Yang, RD; Qiao, WL; Chen, J; Gao, JB, 2024. Mercury isotopes of the Late Ordovician to Middle Triassic tuff layers in South China link the fate of ancient volcanism and the mass extinction. JOURNAL OF ASIAN EARTH SCIENCES. 10.1016/j.jseaes.2024.106234	2
2	Greenplate, R; Thomas, S; Danley-Thomson, A; Missimer, TM, 2023. Phytoremediation Potential of the Coastal Plain Willow <i>Salix caroliniana</i> for Heavy Metals with Emphasis on Mercury. WATER. 10.3390/w15203628	2
3	Kushner, DS; Lopez, TM; Wallace, KL; Damby, DE; Kern, C; Cameron, CE, 2023. Estimates of volcanic mercury emissions from Redoubt Volcano, Augustine Volcano, and Mount Spurr eruption ash. FRONTIERS IN EARTH SCIENCE. 10.3389/feart.2023.1054521	2

4	Nauter-Alves, A; Dunkley-Jones, T; Bruno, MDR; Mota, MAD; Cachao, M; Krahl, G; Fauth, G, 2023. Biotic turnover and carbon cycle dynamics in the early Danian event (Dan-C2): New insights from Blake Nose, North Atlantic. GLOBAL AND PLANETARY CHANGE. 10.1016/j.gloplacha.2023.104046	2
5	Bruno, MDR; Fauth, G; Watkins, DK; Caramenz, MGD; Nauter-Alves, A; Savian, JF, 2022. Paleooceanographic evolution in the South Atlantic Ocean (Kwanza Basin, Angola) during its post-salt foundering. MARINE AND PETROLEUM GEOLOGY. 10.1016/j.marpetgeo.2022.105852	2
6	Yin, RS; Chen, D; Pan, X; Deng, CZ; Chen, LM; Song, XY; Yu, SY; Zhu, CAW; Wei, X; Xu, Y; Feng, XB; Blum, JD; Lehmann, B, 2022. Mantle Hg isotopic heterogeneity and evidence of oceanic Hg recycling into the mantle. NATURE COMMUNICATIONS. 10.1038/s41467-022-28577-1	2
7	Racki, G, 2020. A volcanic scenario for the Frasnian-Famennian major biotic crisis and other Late Devonian global changes: More answers than questions?. GLOBAL AND PLANETARY CHANGE. 10.1016/j.gloplacha.2020.103174	2
8	Sun, YT; Guo, ZF; Du, JG; Zhao, WB, 2020. Diffuse emission and transport of gaseous elemental mercury (GEM) in the Mapamylum geothermal system, Western Tibet (China). JOURNAL OF VOLCANOLOGY AND GEOTHERMAL RESEARCH. 10.1016/j.jvolgeores.2020.106825	2
9	Sun, RY, 2019. Mercury Stable Isotope Fractionation During Coal Combustion in Coal-Fired Boilers: Reconciling Atmospheric Hg Isotope Observations with Hg Isotope Fractionation Theory. BULLETIN OF ENVIRONMENTAL CONTAMINATION AND TOXICOLOGY. 10.1007/s00128-018-2531-1	2
<b>celkem za položku</b>		<b>18</b>
<b>Coufalík, P; Krmíček, L; Zvěřina, O; Meszarosová, N; Hladil, J; Komárek, J, 2018. Model of Mercury Flux Associated with Volcanic Activity (vol 101, pg 549, 2018). BULLETIN OF ENVIRONMENTAL CONTAMINATION AND TOXICOLOGY. 10.1007/s00128-018-2457-7</b>		
1	Edwards, BA; Outridge, PM; Wang, FY, 2024. Mercury from Icelandic geothermal activity: High enrichments in soils, low emissions to the atmosphere. GEOCHIMICA ET COSMOCHIMICA ACTA. 10.1016/j.gca.2024.06.026	2
2	Edwards, BA; Pfeiffer, MA; Ilyinskaya, E; Kleine-Marshall, BI; Mandon, CL; Cotterill, A; Aiuppa, A; Outridge, PM; Wang, FY, 2024. Exceptionally low mercury concentrations and fluxes from the 2021 and 2022 eruptions of Fagradalsfjall volcano, Iceland. SCIENCE OF THE TOTAL ENVIRONMENT. 10.1016/j.scitotenv.2024.170457	2
3	Font, E; Duarte, LV; Dekkers, MJ; Remazeilles, C; Egli, R; Spangenberg, JE; Fantasia, A; Ribeiro, J; Gomes, E; Mirao, J; Adatte, T, 2022. Rapid light carbon releases and increased aridity linked to Karoo-Ferrar magmatism during the early Toarcian oceanic anoxic event. SCIENTIFIC REPORTS. 10.1038/s41598-022-08269-y	2
4	Edwards, BA; Kushner, DS; Outridge, PM; Wang, FY, 2021. Fifty years of volcanic mercury emission research: Knowledge gaps and future directions. SCIENCE OF THE TOTAL ENVIRONMENT. 10.1016/j.scitotenv.2020.143800	2

	<b>celkem za položku</b>	<b>8</b>
<b>Coufalík, P; Meszarosová, N; Coufalíková, K; Zvěřina, O; Komárek, J, 2018. Determination of methylmercury in cryptogams by means of GC-AFS using enzymatic hydrolysis. MICROCHEMICAL JOURNAL. 10.1016/j.microc.2018.03.040</b>		
1	Zhang, Y; Wu, YQ; Su, LS; Zhu, CL; Wu, XP, 2022. An ultrasensitive electrochemical sensor based on in situ synthesized manganese dioxide/gold nanoparticles nanocomposites for rapid detection of methylmercury in foodstuffs. ANALYTICAL METHODS. 10.1039/d2ay00417h	2
2	Chen, SZ; Liu, YX; Yan, JT; Wang, CL; Lu, DB, 2021. Fibrous g-C3N4@Tio2 Nanocomposites-Based Dispersive Micro-Solid Phase Extraction for Chromium Speciation in Cow Milk by ICP-MS after Digestion Treatment with Artificial Gastric Juice. JOURNAL OF AOAC INTERNATIONAL. 10.1093/jaoacint/qsaa118	2
3	Li, SQ; Hao, CC; Xing, PZ; Xia, XL; Liu, TP; Mao, XF, 2020. Rapid Screening Analysis of Methylmercury in Fish Samples Using Stannous Chloride Reduction and Direct Sampling Electrothermal Vaporization Atomic Absorption Spectrometry. ATOMIC SPECTROSCOPY. 10.46770/AS.2020.05.006	2
4	Chen, SZ; Liu, YX; Wang, CL; Yan, JT; Lu, DB, 2020. Determination of Antimony Speciation in Cow Milk Using Dispersive Micro-solid Phase Extraction Based on Fibrous TiO2@g-C3N4Nanocomposites and ICP-MS After Sample Pretreatment by Artificial Gastric Juice. FOOD ANALYTICAL METHODS. 10.1007/s12161-020-01818-z	2
5	Bacon, JR; Butler, OT; Cairns, WRL; Cook, JM; Davidson, CM; Cavoura, O; Mertz-Kraus, R, 2020. Atomic spectrometry update - a review of advances in environmental analysis. JOURNAL OF ANALYTICAL ATOMIC SPECTROMETRY. 10.1039/c9ja90060h	2
6	Clough, R; Harrington, CF; Hill, SJ; Madrid, Y; Tyson, JF, 2019. Atomic spectrometry update: review of advances in elemental speciation. JOURNAL OF ANALYTICAL ATOMIC SPECTROMETRY. 10.1039/c9ja90028d	2
	<b>celkem za položku</b>	<b>12</b>
<b>Zvěřina, O; Coufalík, P; Barták, M; Petrov, M; Komárek, J, 2018. The contents and distributions of cadmium, mercury, and lead in Usnea antarctica lichens from Solorina Valley, James Ross Island (Antarctica). ENVIRONMENTAL MONITORING AND ASSESSMENT. 10.1007/s10661-017-6397-1</b>		
1	Ignatenko, RV; Nikerova, KM; Ignatenko, AA, 2024. The main biogenic elements' content in Lobaria pulmonaria cephalolichen thalli in different ontogenetic stages in the boreal forests of Karelia (Paanajärvi National Park). CHEMISTRY AND ECOLOGY. 10.1080/02757540.2024.2349773	2
2	Reipert, S; Gruber, D; Cyran, N; Schmidt, B; Noetzel, RD; Sancho, LG; Goga, M; Backor, M; Schmidt, K, 2023. Freeze Substitution Accelerated via Agitation: New Prospects for Ultrastructural Studies of Lichen Symbionts and Their Extracellular Matrix. PLANTS-BASEL. 10.3390/plants12234039	2

3	Bodur, S; Erarpat, S; Kayin, I; Bakirdere, S, 2023. Cadmium determination at trace levels in lake water samples by cold vapor generation-atomic absorption spectrometry after magnetic dispersive solid phase extraction. CHEMICAL PAPERS. 10.1007/s11696-023-02963-5	2
4	Gonkowski, S; Könyves, L; Balázs, B; Rytel, L, 2023. Assessment of cadmium concentration levels in wild bats in Poland by analysis of guano samples. JOURNAL OF ELEMENTOLOGY. 10.5601/jelem.2023.28.4.3252	2
5	Monaci, F; Ancora, S; Paoli, L; Loppi, S; Wania, F, 2022. Lichen transplants as indicators of gaseous elemental mercury concentrations*. ENVIRONMENTAL POLLUTION. 10.1016/j.envpol.2022.120189	2
6	Catán, SP; Bubach, D; Messuti, MI; Arribére, MA; Guevara, SR, 2022. Mercury and REE contents in fruticose lichens from volcanic areas of the south volcanic zone. ATMOSPHERIC POLLUTION RESEARCH. 10.1016/j.apr.2022.101384	2
7	Abas, A, 2021. A systematic review on biomonitoring using lichen as the biological indicator: A decade of practices, progress and challenges. ECOLOGICAL INDICATORS. 10.1016/j.ecolind.2020.107197	2
8	Catán, SP; Bubach, D; Arribere, M; Ansaldo, M; Kitaura, MJ; Scur, MC; Lirio, JM, 2020. Trace elements baseline levels in Usnea antarctica from Clearwater Mesa, James Ross Island, Antarctica. ENVIRONMENTAL MONITORING AND ASSESSMENT. 10.1007/s10661-020-8212-7	2
9	Catán, SP; Bubach, D; Messuti, MI; Arribére, MA; Guevara, SR, 2020. Mercury in a geothermal and volcanic area in Patagonia, southern South America. ATMOSPHERIC POLLUTION RESEARCH. 10.1016/j.apr.2019.12.005	2
10	Klapstein, SJ; Walker, AK; Saunders, CH; Cameron, RP; Murimboh, JD; O'Driscoll, NJ, 2020. Spatial distribution of mercury and other potentially toxic elements using epiphytic lichens in Nova Scotia. CHEMOSPHERE. 10.1016/j.chemosphere.2019.125064	2
<b>celkem za položku</b>		<b>20</b>
<b>Sysalová, J; Kučera, J; Drtinová, B; Červenka, R; Zvěřina, O; Komárek, J; Kameník, J, 2017. Mercury species in formerly contaminated soils and released soil gases. SCIENCE OF THE TOTAL ENVIRONMENT. 10.1016/j.scitotenv.2017.01.157</b>		
1	Liu, R; Hu, B; Dannenmann, M; Giesemann, A; Geilfus, CM; Li, CB; Gao, L; Fletmetakis, E; Haensch, R; Wang, DY; Rennenberg, H, 2024. Significance of phosphorus deficiency for the mitigation of mercury toxicity in the Robinia pseudoacacia L.- rhizobia symbiotic association. JOURNAL OF HAZARDOUS MATERIALS. 10.1016/j.jhazmat.2024.133717	2
2	Li, JX; Wu, LC; Chen, LM; Zhang, J; Shi, ZH; Ling, H; Cheng, C; Wu, HS; Butler, AD; Zhang, QK; Arslan, Z; Pierce, EM; Su, Y; Han, FX, 2024. Effects of slopes, rainfall intensity and grass cover on runoff loss of mercury from floodplain soil in Oak Ridge TN: A laboratory pilot study. GEODERMA. 10.1016/j.geoderma.2023.116750	2

3	Fakhri, MA; Jabbar, HD; AbdulRazaq, MJ; Salim, ET; Azzahrani, AS; Ibrahim, RK; Ismail, RA, 2023. Effect of laser fluence on the optoelectronic properties of nanostructured GaN/porous silicon prepared by pulsed laser deposition. SCIENTIFIC REPORTS. 10.1038/s41598-023-47955-3	2
4	Manivannan, N; Subirana, MA; Boada, R; Marini, C; Llugany, M; Valiente, M; Simonelli, L, 2023. Mercury speciation in selenium enriched wheat plants hydroponically exposed to mercury pollution. SCIENTIFIC REPORTS. 10.1038/s41598-023-46056-5	2
5	Junge, M; Goldmann, S; Wotruba, H, 2023. Mineralogy and mineral chemistry of detrital platinum-group minerals and gold particles from the Elbe, Germany. EUROPEAN JOURNAL OF MINERALOGY. 10.5194/ejm-35-439-2023	2
6	Sun, RG; Zhao, T; Fan, L; Zhang, YT; Wang, J; Yang, Y; Jiang, T; Tong, YD, 2023. The transformation of soil Hg oxidation states controls elemental Hg release in the greenhouse with applying organic fertilizer. JOURNAL OF HAZARDOUS MATERIALS. 10.1016/j.jhazmat.2023.131520	2
7	Becher, M; Kobierski, M; Pakula, K; Jaremko, D, 2023. Distribution of Mercury in Drained Peatlands as the Effect of Secondary Transformation of Soil Organic Matter. AGRICULTURE-BASEL. 10.3390/agriculture13050995	2
8	Sun, Y; Zhang, Z; Zhang, G; Zong, J; Zhang, HJ; Deng, YQ; Yang, KL; Wang, ZJ; Cui, D; Yang, CC, 2023. Characteristics of Mercury Fluxes between Soil and Air in the Farming-Pastoral Ecotone of Songnen Grassland. SUSTAINABILITY. 10.3390/su15065416	2
9	Zhang, YF; Wang, XQ; Yang, Y; Huang, YM; Li, XM; Hu, SW; Liu, KX; Pang, Y; Liu, TX; Li, FB, 2023. Retention and transformation of exogenous Hg in acidic paddy soil under alternating anoxic and oxic conditions: Kinetic and mechanistic insights. ENVIRONMENTAL POLLUTION. 10.1016/j.envpol.2023.121335	2
10	Floreani, F; Zappella, V; Faganeli, J; Covelli, S, 2023. Gaseous mercury evasion from bare and grass-covered soils contaminated by mining and ore roasting (Isonzo River alluvial plain, Northeastern Italy). ENVIRONMENTAL POLLUTION. 10.1016/j.envpol.2022.120921	2
11	Zhang, YJ; Sun, T; Ma, M; Wang, X; Xie, Q; Zhang, C; Wang, YM; Wang, DY, 2022. Distribution of mercury and methylmercury in river water and sediment of typical manganese mining area. JOURNAL OF ENVIRONMENTAL SCIENCES. 10.1016/j.jes.2021.12.011	2
12	Hussain, S; Yang, JJ; Hussain, J; Sattar, A; Ullah, S; Hussain, I; Rahman, SU; Zandi, P; Xia, X; Zhang, LD, 2022. Mercury fractionation, bioavailability, and the major factors predicting its transfer and accumulation in soil-wheat systems. SCIENCE OF THE TOTAL ENVIRONMENT. 10.1016/j.scitotenv.2022.157432	2
13	Mir, Y; Wu, SJ; Ma, MH; Ran, YG; Zhu, K; Mangwandi, C; Mirza, ZA, 2022. Mercury contamination in the riparian ecosystem during the reservoir discharging regulated by a mega dam. ENVIRONMENTAL GEOCHEMISTRY AND HEALTH. 10.1007/s10653-022-01205-z	2

14	Padariya, C; Rutkowska, M; Konieczka, P, 2022. The importance and availability of marine certified reference materials. CRITICAL REVIEWS IN ENVIRONMENTAL SCIENCE AND TECHNOLOGY. 10.1080/10643389.2021.1922254	2
15	Cho, K; Kang, J; Kim, S; Purev, O; Myung, E; Kim, H; Choi, N, 2021. Effect of inorganic carbonate and organic matter in thermal treatment of mercury-contaminated soil. ENVIRONMENTAL SCIENCE AND POLLUTION RESEARCH. 10.1007/s11356-021-14024-z	2
16	Kokh, SN; Sokol, EV; Gustaytis, MA; Sokol, IA; Deviatiiarova, AS, 2021. Onshore mud volcanoes as a geological source of mercury: Case study from the Kerch Peninsula, Caucasus continental collision zone. SCIENCE OF THE TOTAL ENVIRONMENT. 10.1016/j.scitotenv.2020.141806	2
17	Liu, WW; Li, MJ; Zhang, MY; Wang, D; Guo, ZL; Long, SY; Yang, S; Wang, HN; Li, W; Hu, YK; Wei, YY; Xiao, HY, 2020. Estimating leaf mercury content in Phragmites australis based on leaf hyperspectral reflectance. ECOSYSTEM HEALTH AND SUSTAINABILITY. 10.1080/20964129.2020.1726211	2
18	Liu, WW; Li, MJ; Zhang, MY; Long, SY; Guo, ZL; Wang, HN; Li, W; Wang, DA; Hu, YK; Wei, YY; Yang, S, 2020. Hyperspectral inversion of mercury in reed leaves under different levels of soil mercury contamination. ENVIRONMENTAL SCIENCE AND POLLUTION RESEARCH. 10.1007/s11356-020-08807-z	2
19	Brown, AD; Yalala, B; Cukrowska, E; Godoi, RHM; Potgieter-Vermaak, S, 2020. A scoping study of component-specific toxicity of mercury in urban road dusts from three international locations. ENVIRONMENTAL GEOCHEMISTRY AND HEALTH. 10.1007/s10653-019-00351-1	2
20	Natasha; Shahid, M; Khalid, S; Bibi, I; Bundschuh, J; Niazi, NK; Dumat, C, 2020. A critical review of mercury speciation, bioavailability, toxicity and detoxification in soil-plant environment: Ecotoxicology and health risk assessment. SCIENCE OF THE TOTAL ENVIRONMENT.	2
21	Zou, HM; Zhou, C; Li, YX; Yang, XS; Wen, J; Li, CX; Song, SJ; Sun, CJ, 2020. Speciation analysis of mercury in wild edible mushrooms by high-performance liquid chromatography hyphenated to inductively coupled plasma mass spectrometry. ANALYTICAL AND BIOANALYTICAL CHEMISTRY. 10.1007/s00216-020-02515-w	2
22	Souza, LRR; Pomarolli, LC; da Veiga, MAMS, 2020. From classic methodologies to application of nanomaterials for soil remediation: an integrated view of methods for decontamination of toxic metal(oid)s. ENVIRONMENTAL SCIENCE AND POLLUTION RESEARCH. 10.1007/s11356-020-08032-8	2
23	Yang, B; Gao, Y; Zhang, CX; Zheng, XQ; Li, B, 2020. Mercury accumulation and transformation of main leaf vegetable crops in Cambosol and Ferrosol soil in China. ENVIRONMENTAL SCIENCE AND POLLUTION RESEARCH. 10.1007/s11356-019-06798-0	2

24	Kulikova, T; Hiller, E; Jurkovic, L; Filová, L; Sottník, P; Lacina, P, 2019. Total mercury, chromium, nickel and other trace chemical element contents in soils at an old cinnabar mine site (Mernik, Slovakia): anthropogenic versus natural sources of soil contamination. ENVIRONMENTAL MONITORING AND ASSESSMENT. 10.1007/s10661-019-7391-6	2
25	O'Connor, D; Hou, DY; Ok, YS; Mulder, J; Duan, L; Wu, QR; Wang, SX; Tack, FMG; Rinklebe, J, 2019. Mercury speciation, transformation, and transportation in soils, atmospheric flux, and implications for risk management: A critical review. ENVIRONMENT INTERNATIONAL. 10.1016/j.envint.2019.03.019	2
26	Clough, R; Harrington, CF; Hill, SJ; Madrid, Y; Tyson, JF, 2018. Atomic Spectrometry Update: review of advances in elemental speciation. JOURNAL OF ANALYTICAL ATOMIC SPECTROMETRY. 10.1039/c8ja90025f	2
27	Diao, X; Yuan, CG; Wu, JJ; Gui, B; Zhang, KG; Zhang, C, 2018. Mercury release and fraction transformation during desulfurization gypsum aging process (UV irradiation). FUEL. 10.1016/j.fuel.2017.12.120	2
<b>celkem za položku</b>		<b>54</b>
<b>Zvěřina, O; Coufalík, P; Brat, K; Červenka, R; Kuta, J; Mikeš, O; Komárek, J, 2017. Leaching of mercury from seal carcasses into Antarctic soils. ENVIRONMENTAL SCIENCE AND POLLUTION RESEARCH. 10.1007/s11356-016-7879-3</b>		
1	Barragán-Barrera, DC; Riet-Sapriza, FG; Mojica-Moncada, DF; Negrete, J; Curtosi, A; Bustamante, P; Caballero, S; Luna-Acosta, A, 2024. Sex-specific mercury levels in skin samples of southern elephant seals ( <i>Mirounga leonina</i> ) at Isla 25 de Mayo (King George Island), Antarctic Peninsula. MARINE MAMMAL SCIENCE. 10.1111/mms.13058	2
2	Soares, TA; Souza-Kasprzyk, J; Padilha, JDG; Convey, P; Costa, ES; Torres, JPM, 2023. Ornithogenic mercury input to soils of Admiralty Bay, King George Island, Antarctica. POLAR BIOLOGY. 10.1007/s00300-023-03162-4	2
3	Darham, S; Zakaria, NN; Zulkharnain, A; Sabri, S; Khalil, KA; Merican, F; Gomez-Fuentes, C; Lim, S; Ahmad, SA, 2023. Antarctic heavy metal pollution and remediation efforts: state of the art of research and scientific publications. BRAZILIAN JOURNAL OF MICROBIOLOGY. 10.1007/s42770-023-00949-9	2
4	Schaefer, CEGR; Senra, EO; Schmitz, D; Siqueira, RG; De Paula, MD; Putzke, J; De Oliveira, FS; Maia, LG; Ibraimo, ASM; Francelino, MR, 2023. Soils under seal carcasses with varying degrees of decomposition: oasis of nutrients and vegetation in Antarctica. ANAIS DA ACADEMIA BRASILEIRA DE CIENCIAS. 10.1590/0001-3765202320230747	2
5	Chattová, B; Cahová, T; Pinseel, E; Kopalová, K; Kohler, TJ; Hrbáček, F; Van de Vijver, B; Nyvlt, D, 2022. Diversity, ecology, and community structure of the terrestrial diatom flora from Ulu Peninsula (James Ross Island, NE Antarctic Peninsula). POLAR BIOLOGY. 10.1007/s00300-022-03038-z	2
6	Bhakta, S; Rout, TK; Karmakar, D; Pawar, C; Padhy, PK, 2022. Trace elements and their potential risk assessment on polar ecosystem of Larsemann Hills, East Antarctica. POLAR SCIENCE. 10.1016/j.polar.2022.100788	2

7	Castro, MF; Meier, M; Neves, JCL; Francelino, MR; Schaefer, CEGR; Oliveira, TS, 2022. Influence of different seabird species on trace metals content in Antarctic soils. ANAIS DA ACADEMIA BRASILEIRA DE CIENCIAS. 10.1590/0001-3765202220210623	2
8	Puasa, NA; Zulkharnain, A; Verasoundarapandian, G; Wong, CY; Zahri, KNM; Merican, F; Shaharuddin, NA; Gomez-Fuentes, C; Ahmad, SA, 2021. Effects of Diesel, Heavy Metals and Plastics Pollution on Penguins in Antarctica: A Review. ANIMALS. 10.3390/ani11092505	2
9	Prater, I; Hrbáček, F; Braun, C; Vidal, A; Meier, LA; Nyvlt, D; Mueller, CW, 2021. How vegetation patches drive soil development and organic matter formation on polar islands. GEODERMA REGIONAL. 10.1016/j.geodrs.2021.e00429	2
10	Zou, Y; Pang, JY; Zhang, F; Chai, F, 2021. Silver Nanoparticles for Colorimetric Detection and Discrimination of Mercury Ions in Lake Water. CHEMISTRYSELECT. 10.1002/slct.202101389	2
11	Chu, WL; Dang, NL; Kok, YY; Yap, KSI; Phang, SM; Convey, P, 2019. Heavy metal pollution in Antarctica and its potential impacts on algae. POLAR SCIENCE. 10.1016/j.polar.2018.10.004	2
12	Ruiz-Fernández, J; Oliva, M; Nyvlt, D; Cannone, N; García-Hernández, C; Guglielmin, M; Hrbáček, F; Roman, M; Fernández, S; López-Martínez, J; Antoniades, D, 2019. Patterns of spatio-temporal paraglacial response in the Antarctic Peninsula region and associated ecological implications. EARTH-SCIENCE REVIEWS. 10.1016/j.earscirev.2019.03.014	2
13	Amirjani, A; Haghshenas, DF, 2019. Facile and on - line colorimetric detection of Hg <sup>2+</sup> based on localized surface plasmon resonance (LSPR) of Ag nanotriangles. TALANTA. 10.1016/j.talanta.2018.09.079	2
14	Cipro, CVZ; Bustamante, P; Petry, MV; Montone, RC, 2018. Seabird colonies as relevant sources of pollutants in Antarctic ecosystems: Part 1-Trace elements. CHEMOSPHERE. 10.1016/j.chemosphere.2018.02.048	2
<b>celkem za položku</b>		<b>28</b>
<b>Coufalík, P; Procházková, P; Zvěřina, O; Trnková, K; Skácelová, K; Nyvlt, D; Komárek, J, 2016. Freshwater mineral nitrogen and essential elements in autotrophs in James Ross Island, West Antarctica. POLISH POLAR RESEARCH. 10.1515/popore-2016-0025</b>		
1	Richter, D, 2018. Diversity of cyanobacteria and microalgae in hydro-terrestrial habitats in Svalbard and its ecological evaluation. POLISH POLAR RESEARCH. 10.24425/118748	2
<b>celkem za položku</b>		<b>2</b>

<b>Coufalík, P; Zvěřina, O; Komárek, J, 2016. The direct determination of HgS by thermal desorption coupled with atomic absorption spectrometry. SPECTROCHIMICA ACTA PART B-ATOMIC SPECTROSCOPY. 10.1016/j.sab.2016.01.004</b>		
1	Xiong, G; Xu, WF; Liang, LJ; Huang, K; Zhang, XY; Qin, DB, 2024. A doubly interpenetrated 3D nickel metal-organic framework for selective and sensitive turn-on sensing Hg <sup>2+</sup> ions in water. JOURNAL OF MOLECULAR STRUCTURE. 10.1016/j.molstruc.2024.137538	2
2	Yang, FB; Mu, J; Ma, JT; Jia, Q, 2022. Research Progress on Application of Fluorescent Probes in Detection of Soil Pollutants. CHINESE JOURNAL OF ANALYTICAL CHEMISTRY. 10.19756/j.issn.0253-3820.221027	2
3	Chang, L; Zhao, YC; Zhang, Y; Yu, XH; Li, ZH; Gong, BG; Liu, H; Wei, SZ; Wu, H; Zhang, JY, 2021. Mercury species and potential leaching in sludge from coal-fired power plants. JOURNAL OF HAZARDOUS MATERIALS. 10.1016/j.jhazmat.2020.123927	2
4	Pérez, PA; Bravo, MA; Quiroz, W, 2020. Total mercury bias in soil analysis by CV-AFS: causes, consequences and a simple solution based on sulfhydryl cotton fiber as a clean-up step. ANALYTICAL METHODS. 10.1039/d0ay01035a	2
5	Rezende, PS; Silva, NC; Moura, WD; Windmüller, CC, 2018. Quantification and speciation of mercury in streams and rivers sediment samples from Paracatu, MG, Brazil, using a direct mercury analyzer®. MICROCHEMICAL JOURNAL. 10.1016/j.microc.2018.04.006	2
6	Saniewska, D; Beldowska, M, 2017. Mercury fractionation in soil and sediment samples using thermo-desorption method. TALANTA. 10.1016/j.talanta.2017.03.026	2
7	Butler, OT; Cairns, WRL; Cooke, JM; Davidson, CM, 2017. Atomic spectrometry update - a review of advances in environmental analysis. JOURNAL OF ANALYTICAL ATOMIC SPECTROMETRY. 10.1039/c6ja90058e	2
<b>celkem za položku 14</b>		
<b>Szaková, J; Havlíčková, J; Šípková, A; Gabriel, J; Švec, K; Baldrian, P; Sysalová, J; Coufalík, P; Červenka, R; Zvěřina, O; Komárek, J; Tlustoš, P, 2016. Effects of the soil microbial community on mobile proportions and speciation of mercury (Hg) in contaminated soil. JOURNAL OF ENVIRONMENTAL SCIENCE AND HEALTH PART A-TOXIC/HAZARDOUS SUBSTANCES &amp; ENVIRONMENTAL ENGINEERING. 10.1080/10934529.2015.1109413</b>		
1	Amin, S; Khan, S; Sarwar, T; Nawab, J; Khan, MA, 2021. Mercury methylation and its accumulation in rice and paddy soil in degraded lands: A critical review. ENVIRONMENTAL TECHNOLOGY & INNOVATION. 10.1016/j.eti.2021.101638	2
2	Mahbub, KR; King, WL; Siboni, N; Nguyen, VK; Rahman, MM; Megharaj, M; Seymour, JR; Franks, AE; Labbate, M, 2020. Long-lasting effect of mercury contamination on the soil microbiota and its co-selection of antibiotic resistance. ENVIRONMENTAL POLLUTION. 10.1016/j.envpol.2020.115057	2

3	Teng, DY; Mao, K; Ali, W; Xu, GM; Huang, GP; Niazi, NK; Feng, XB; Zhang, H, 2020. Describing the toxicity and sources and the remediation technologies for mercury-contaminated soil. RSC ADVANCES. 10.1039/d0ra01507e	2
4	Górecki, J, 2018. Semi-automatic system for methylmercury determination in biological samples. MEASUREMENT. 10.1016/j.measurement.2017.12.035	2
5	Kogbara, RB, 2017. Interrelationships among geotechnical and leaching properties of a cement-stabilized contaminated soil. JOURNAL OF ENVIRONMENTAL SCIENCE AND HEALTH PART A-TOXIC/HAZARDOUS SUBSTANCES & ENVIRONMENTAL ENGINEERING. 10.1080/10934529.2016.1240483	2
<b>celkem za položku</b>		<b>10</b>
<b>Coufalík, P; Zvěřina, O; Krmíček, L; Pokorný, R; Komárek, J, 2015. Ultra-trace analysis of Hg in alkaline lavas and regolith from James Ross Island. ANTARCTIC SCIENCE. 10.1017/S0954102014000819</b>		
1	Bhakta, S; Rout, TK; Karmakar, D; Pawar, C; Padhy, PK, 2022. Trace elements and their potential risk assessment on polar ecosystem of Larsemann Hills, East Antarctica. POLAR SCIENCE. 10.1016/j.polar.2022.100788	2
2	Zheng, LG; Sun, RY; Hintelmann, H; Zhu, JM; Wang, RW; Sonke, JE, 2018. Mercury stable isotope compositions in magmatic-affected coal deposits: New insights to mercury sources, migration and enrichment. CHEMICAL GEOLOGY. 10.1016/j.chemgeo.2017.12.032	2
3	Zheng, W; Xie, ZQ; Bergquist, BA, 2015. Mercury Stable Isotopes in Ornithogenic Deposits As Tracers of Historical Cycling of Mercury in Ross Sea, Antarctica. ENVIRONMENTAL SCIENCE & TECHNOLOGY. 10.1021/acs.est.5b00523	2
<b>celkem za položku</b>		<b>6</b>
<b>Zvěřina, O; Láska, K; Červenka, R; Kuta, J; Coufalík, P; Komárek, J, 2014. Analysis of mercury and other heavy metals accumulated in lichen <i>Usnea antarctica</i> from James Ross Island, Antarctica. ENVIRONMENTAL MONITORING AND ASSESSMENT. 10.1007/s10661-014-4068-z</b>		
1	Conti, ME; Rapa, M; Pla, R; Jasan, R; Tudino, MB; Canepari, S; Massimi, L; Astolfi, ML, 2023. Elemental and chemometric analysis of baseline gradient contamination in <i>Usnea barbata</i> lichens from Tierra del Fuego (South Patagonia). MICROCHEMICAL JOURNAL. 10.1016/j.microc.2022.108283	2
2	Tapia, J; Molina-Montenegro, M; Sandoval, C; Rivas, N; Espinoza, J; Basualto, S; Fierro, P; Vargas-Chacoff, L, 2021. Human Activity in Antarctica: Effects on Metallic Trace Elements (MTEs) in Plants and Soils. PLANTS-BASEL. 10.3390/plants10122593	2
3	McKenzie, AC; Silvestro, AM; Marti, LJ; Emslie, SD, 2021. Intraspecific Variation in Mercury, $\delta^{15}\text{N}$ , and $\delta^{13}\text{C}$ Among 3 Adelie Penguin ( <i>Pygoscelis adeliae</i> ) Populations in the Northern Antarctic Peninsula Region. ENVIRONMENTAL TOXICOLOGY AND CHEMISTRY. 10.1002/etc.5166	2
4	Magesh, NS; Tiwari, A; Botsa, SM; Leitao, TD, 2021. Hazardous heavy metals in the pristine lacustrine systems of Antarctica: Insights from PMF model and ERA techniques. JOURNAL OF HAZARDOUS MATERIALS. 10.1016/j.jhazmat.2021.125263	2

5	Catán, SP; Bubach, D; Arribere, M; Ansaldo, M; Kitaura, MJ; Scur, MC; Lirio, JM, 2020. Trace elements baseline levels in <i>Usnea antarctica</i> from Clearwater Mesa, James Ross Island, Antarctica. ENVIRONMENTAL MONITORING AND ASSESSMENT. 10.1007/s10661-020-8212-7	2
6	Weiss-Penzias, PS; Bank, MS; Clifford, DL; Torregrosa, A; Zheng, B; Lin, W; Wilmers, CC, 2019. Marine fog inputs appear to increase methylmercury bioaccumulation in a coastal terrestrial food web. SCIENTIFIC REPORTS. 10.1038/s41598-019-54056-7	2
7	Barrientos, C; Tapia, J; Bertrán, C; Peña-Cortés, F; Hauenstein, E; Fierro, P; Vargas-Chacoff, L, 2019. Is eating wild rainbow trout safe? The effects of different land-uses on heavy metals content in Chile. ENVIRONMENTAL POLLUTION. 10.1016/j.envpol.2019.112995	2
8	Meier, LA; Krauze, P; Prater, I; Horn, F; Schaefer, CEGR; Scholten, T; Wagner, D; Mueller, CW; Kühn, P, 2019. Pedogenic and microbial interrelation in initial soils under semiarid climate on James Ross Island, Antarctic Peninsula region. BIOGEOSCIENCES. 10.5194/bg-16-2481-2019	2
9	Tapia, J; Villagra, F; Bertrán, C; Espinoza, J; Focardi, S; Fierro, P; Tapia, C; Pizarro, R; Vargas-Chacoff, L, 2019. Effect of the earthquake-tsunami (Chile, 2010) on toxic metal content in the Chilean abalone mollusc <i>Concholepas concholepas</i> . ECOTOXICOLOGY AND ENVIRONMENTAL SAFETY. 10.1016/j.ecoenv.2018.11.040	2
10	Chu, ZD; Yang, ZK; Wang, YH; Sun, LG; Yang, WQ; Yang, LJ; Gao, YS, 2019. Assessment of heavy metal contamination from penguins and anthropogenic activities on Fildes Peninsula and Ardley Island, Antarctic. SCIENCE OF THE TOTAL ENVIRONMENT. 10.1016/j.scitotenv.2018.07.152	2
11	Cipro, CVZ; Bustamante, P; Petry, MV; Montone, RC, 2018. Seabird colonies as relevant sources of pollutants in Antarctic ecosystems: Part 1-Trace elements. CHEMOSPHERE. 10.1016/j.chemosphere.2018.02.048	2
12	Fabri, R; Krause, M; Dalfior, BM; Salles, RC; de Freitas, AC; da Silva, HE; Licinio, MVVJ; Brandao, GP; Carneiro, MTWD, 2018. Trace elements in soil, lichens, and mosses from Fildes Peninsula, Antarctica: spatial distribution and possible origins. ENVIRONMENTAL EARTH SCIENCES. 10.1007/s12665-018-7298-5	2
13	Halici, MG; Bartak, M; Güllü, M, 2018. Identification of some lichenised fungi from James Ross Island (Antarctic Peninsula) using nrITS markers. NEW ZEALAND JOURNAL OF BOTANY. 10.1080/0028825X.2018.1478861	2
14	Mróz, T; Szufa, K; Frontasyeva, MV; Tselmovich, V; Ostrovnaya, T; Kornas, A; Olech, MA; Mietelski, JW; Brudecki, K, 2018. Determination of element composition and extraterrestrial material occurrence in moss and lichen samples from King George Island (Antarctica) using reactor neutron activation analysis and SEM microscopy. ENVIRONMENTAL SCIENCE AND POLLUTION RESEARCH. 10.1007/s11356-017-0431-2	2

15	Boonpeng, C; Polyiam, W; Sriviboon, C; Sangiamdee, D; Watthana, S; Nimis, PL; Boonpragob, K, 2017. Airborne trace elements near a petrochemical industrial complex in Thailand assessed by the lichen <i>Parmotrema tinctorum</i> (Despr. ex Nyl.) Hale. ENVIRONMENTAL SCIENCE AND POLLUTION RESEARCH. 10.1007/s11356-017-8893-9	2
16	Culicov, OA; Yurukova, L; Dului, OG; Zinicovscaia, I, 2017. Elemental content of mosses and lichens from Livingston Island (Antarctica) as determined by instrumental neutron activation analysis (INAA). ENVIRONMENTAL SCIENCE AND POLLUTION RESEARCH. 10.1007/s11356-016-8279-4	2
17	Srivastava, V; Sarkar, A; Singh, S; Singh, P; de Araujo, ASF; Singh, RP, 2017. Agroecological Responses of Heavy Metal Pollution with Special Emphasis on Soil Health and Plant Performances. FRONTIERS IN ENVIRONMENTAL SCIENCE. 10.3389/fenvs.2017.00064	2
18	Bargagli, R, 2016. Moss and lichen biomonitoring of atmospheric mercury: A review. SCIENCE OF THE TOTAL ENVIRONMENT. 10.1016/j.scitotenv.2016.07.202	2
19	Pasquet, C; Le Monier, P; Monna, F; Durllet, C; Brigaud, B; Losno, R; Chateau, C; Laporte-Magoni, C; Gunkel-Grillon, P, 2016. Impact of nickel mining in New Caledonia assessed by compositional data analysis of lichens. SPRINGERPLUS. 10.1186/s40064-016-3681-4	2
20	Bargagli, R, 2016. Atmospheric chemistry of mercury in Antarctica and the role of cryptogams to assess deposition patterns in coastal ice-free areas. CHEMOSPHERE. 10.1016/j.chemosphere.2016.08.007	2
21	Bubach, D; Catán, SP; Di Fonzo, C; Dopchiz, L; Arribére, M; Ansaldo, M, 2016. Elemental composition of <i>Usnea</i> sp lichen from Potter Peninsula, 25 de Mayo (King George) Island, Antarctica. ENVIRONMENTAL POLLUTION. 10.1016/j.envpol.2015.11.045	2
22	Greda, K; Kurcbach, K; Ochromowicz, K; Lesniewicz, T; Jamroz, P; Pohl, P, 2015. Determination of mercury in mosses by novel cold vapor generation atmospheric pressure glow microdischarge optical emission spectrometry after multivariate optimization. JOURNAL OF ANALYTICAL ATOMIC SPECTROMETRY. 10.1039/c5ja00170f	2
<b>celkem za položku</b>		<b>44</b>

**Coufalík, P; Zvěřina, O; Mikuška, P; Komárek, J, 2014. Seasonal Variability of Mercury Contents in Street Dust in Brno, Czech Republic. BULLETIN OF ENVIRONMENTAL CONTAMINATION AND TOXICOLOGY. 10.1007/s00128-014-1289-3**

1	Ehtemae, N; Ghanavati, N; Nazarpour, A; Babaeinejad, T; Watts, MJ, 2023. Status, Source, and Risk Assessment of Heavy Metal(Loid)s and Polycyclic Aromatic Hydrocarbons (PAHs) in the Street Dust of Ilam, Iran. POLYCYCLIC AROMATIC COMPOUNDS. 10.1080/10406638.2023.2276864	2
2	Huang, JH; Berg, B; Chen, CY; Thimonier, A; Schmitt, M; Osterwalder, S; Alewell, C; Rinklebe, J; Feng, XB, 2023. Predominant contributions through lichen and fine litter to litterfall mercury deposition in a subalpine forest. ENVIRONMENTAL RESEARCH. 10.1016/j.envres.2023.116005	2
3	Behrooz, RD; Tashakor, M; Asvad, R; Esmaili-Sari, A; Kaskaoutis, DG, 2022. Characteristics and Health Risk Assessment of Mercury Exposure via Indoor and Outdoor Household Dust in Three Iranian Cities. ATMOSPHERE. 10.3390/atmos13040583	2
4	Faisal, M; Wu, ZN; Wang, HL; Hussain, Z; Shen, CY, 2021. Geochemical Mapping, Risk Assessment, and Source Identification of Heavy Metals in Road Dust Using Positive Matrix Factorization (PMF). ATMOSPHERE. 10.3390/atmos12050614	2
5	Chai, L; Wang, YH; Wang, X; Ma, L; Cheng, ZX; Su, LM; Liu, MX, 2021. Quantitative source apportionment of heavy metals in cultivated soil and associated model uncertainty. ECOTOXICOLOGY AND ENVIRONMENTAL SAFETY. 10.1016/j.ecoenv.2021.112150	2
6	Pilar, L; Borovec, K; Szeliga, Z; Górecki, J, 2021. Mercury emission from three lignite-fired power plants in the Czech Republic. FUEL PROCESSING TECHNOLOGY. 10.1016/j.fuproc.2020.106628	2
7	Men, C; Liu, RM; Xu, LB; Wang, QR; Guo, LJ; Miao, YX; Shen, ZY, 2020. Source-specific ecological risk analysis and critical source identification of heavy metals in road dust in Beijing, China. JOURNAL OF HAZARDOUS MATERIALS. 10.1016/j.jhazmat.2019.121763	2
8	Navrátil, T; Nováková, T; Roll, M; Shanley, JB; Kopáček, J; Rohovec, J; Kana, J; Cudlín, P, 2019. Decreasing litterfall mercury deposition in central European coniferous forests and effects of bark beetle infestation. SCIENCE OF THE TOTAL ENVIRONMENT. 10.1016/j.scitotenv.2019.05.093	2
9	Liu, YZ; Song, SS; Bi, CJ; Zhao, JL; Xi, D; Su, ZQ, 2019. Occurrence, Distribution and Risk Assessment of Mercury in Multimedia of Soil-Dust-Plants in Shanghai, China. INTERNATIONAL JOURNAL OF ENVIRONMENTAL RESEARCH AND PUBLIC HEALTH. 10.3390/ijerph16173028	2
10	Men, C; Liu, RM; Wang, QR; Guo, LJ; Miao, YX; Shen, ZY, 2019. Uncertainty analysis in source apportionment of heavy metals in road dust based on positive matrix factorization model and geographic information system. SCIENCE OF THE TOTAL ENVIRONMENT. 10.1016/j.scitotenv.2018.10.212	2

11	Men, C; Liu, RM; Wang, QR; Guo, LJ; Shen, ZY, 2018. The impact of seasonal varied human activity on characteristics and sources of heavy metals in metropolitan road dusts. SCIENCE OF THE TOTAL ENVIRONMENT. 10.1016/j.scitotenv.2018.05.059	2
12	Men, C; Liu, RM; Xu, F; Wang, QR; Guo, LJ; Shen, ZY, 2018. Pollution characteristics, risk assessment, and source apportionment of heavy metals in road dust in Beijing, China. SCIENCE OF THE TOTAL ENVIRONMENT. 10.1016/j.scitotenv.2017.08.123	2
13	Quiñonez-Plaza, A; Wakida, FT; Temores-Peña, J; Rodriguez-Mendivil, DD; Garcia-Flores, E; Pastrana-Corral, MA; Melendez-Lopez, SG, 2017. Total petroleum hydrocarbons and heavy metals in road-deposited sediments in Tijuana, Mexico. JOURNAL OF SOILS AND SEDIMENTS. 10.1007/s11368-017-1778-1	2
14	Wisniewska, K; Lewandowska, AU; Witkowska, A, 2017. Factors determining dry deposition of total mercury and organic carbon in house dust of residents of the Tri-city and the surrounding area (Baltic Sea coast). AIR QUALITY ATMOSPHERE AND HEALTH. 10.1007/s11869-017-0471-2	2
15	Lin, YS; Fang, FM; Wu, JY; Zhu, Z; Zhang, DL; Xu, ML, 2017. Indoor and outdoor levels, sources, and health risk assessment of mercury in dusts from a coal-industry city of China. HUMAN AND ECOLOGICAL RISK ASSESSMENT. 10.1080/10807039.2017.1296759	2
<b>celkem za položku</b>		<b>30</b>
<b>Coufalík, P; Zvěřina, O; Komárek, J, 2014. Determination of mercury species using thermal desorption analysis in AAS. CHEMICAL PAPERS. 10.2478/s11696-013-0471-0</b>		
1	Arrighi, S; Franceschini, F; Petrini, R; Fornasaro, S; Ghezzi, L, 2024. The Legacy of Hg Contamination in a Past Mining Area (Tuscany, Italy): Hg Speciation and Health Risk Assessment. TOXICS. 10.3390/toxics12060436	2
2	Kwasigroch, U; Lukawska-Matuszewska, K; Jedruch, A; Broclawik, O; Beldowska, M, 2023. Mobility and bioavailability of mercury in sediments of the southern Baltic sea in relation to the chemical fractions of iron: Spatial and temporal patterns. MARINE ENVIRONMENTAL RESEARCH. 10.1016/j.marenvres.2023.106132	2
3	Sun, RG; Zhao, T; Fan, L; Zhang, YT; Wang, J; Yang, Y; Jiang, T; Tong, YD, 2023. The transformation of soil Hg oxidation states controls elemental Hg release in the greenhouse with applying organic fertilizer. JOURNAL OF HAZARDOUS MATERIALS. 10.1016/j.jhazmat.2023.131520	2
4	Petranich, E; Predonzani, S; Acquavita, A; Mashyanov, N; Covelli, S, 2022. Rapid thermoscaning technique for direct analysis of mercury species in contaminated sediments: From pure compounds to real sample application. APPLIED GEOCHEMISTRY. 10.1016/j.apgeochem.2022.105393	2
5	Zhang, XY; Fang, BB; Cui, L; Tang, JY; Xing, XW; Dong, Y, 2021. Effects of HCl and O <sub>2</sub> on Hg <sup>0</sup> Oxidation in the SCR Catalyst. ENERGY & FUELS. 10.1021/acs.energyfuels.1c00173	2

6	Selvaraj, M; Rajalakshmi, K; Ahn, DH; Yoon, SJ; Nam, YS; Lee, Y; Xu, YG; Song, JW; Lee, KB, 2021. Tetraphenylethene-based fluorescent probe with aggregation-induced emission behavior for Hg <sup>2+</sup> detection and its application. ANALYTICA CHIMICA ACTA. 10.1016/j.aca.2020.12.053	2
7	Zhou, SH; Xu, HB; Gao, J, 2020. Facile Preparation of In-Situ S-Doped Flake Carbon Materials from Metal-Organic Frameworks and Its Application in Electrochemical Detection of Hg (II). NANO. 10.1142/S1793292020501337	2
8	Katseli, V; Thomaidis, N; Economou, A; Kokkinos, C, 2020. Miniature 3D-printed integrated electrochemical cell for trace voltammetric Hg(II) determination. SENSORS AND ACTUATORS B-CHEMICAL. 10.1016/j.snb.2020.127715	2
9	Akhond, M; Jangi, SRH; Barzegar, S; Absalan, G, 2020. Introducing a nanozyme-based sensor for selective and sensitive detection of mercury(II) using its inhibiting effect on production of an indamine polymer through a stable n-electron irreversible system. CHEMICAL PAPERS. 10.1007/s11696-019-00981-w	2
10	Falciglia, PP; Catalfo, A; Finocchiaro, G; Vagliasindi, FGA; Romano, S; De Guidi, G, 2019. Chemically assisted 2.45 GHz microwave irradiation for the simultaneous removal of mercury and organics from contaminated marine sediments. CLEAN TECHNOLOGIES AND ENVIRONMENTAL POLICY. 10.1007/s10098-019-01665-5	2
11	Jiang, Y; Duan, QY; Zheng, GS; Yang, L; Zhang, J; Wang, YF; Zhang, HT; He, J; Sun, HY; Ho, D, 2019. An ultra-sensitive and ratiometric fluorescent probe based on the DTBET process for Hg <sup>2+</sup> detection and imaging applications. ANALYST. 10.1039/c8an02126k	2
12	Jedruch, A; Beldowska, M; Kwasigroch, U; Normant-Saremba, M; Saniewska, D, 2018. Mercury fractionation in marine macrofauna using thermodesorption technique: Method and its application. TALANTA. 10.1016/j.talanta.2018.07.047	2
13	Zuniga-Hansen, NZ; Silbert, LE; Calbi, MM, 2018. Breakdown of kinetic compensation effect in physical desorption. PHYSICAL REVIEW E. 10.1103/PhysRevE.98.032128	2
14	Jayadevimanoranjitham, J; Narayanan, SS, 2018. 2,4,6-Trimercaptotriazine incorporated gold nanoparticle modified electrode for anodic stripping voltammetric determination of Hg(II). APPLIED SURFACE SCIENCE. 10.1016/j.apsusc.2018.04.096	2
15	Bavec, S; Gosar, M; Miler, M; Biester, H, 2017. Geochemical investigation of potentially harmful elements in household dust from a mercury-contaminated site, the town of Idrija (Slovenia). ENVIRONMENTAL GEOCHEMISTRY AND HEALTH. 10.1007/s10653-016-9819-z	2
16	Chen, Y; Yin, YG; Shi, JB; Liu, GL; Hu, L; Liu, JF; Cai, Y; Jiang, GB, 2017. Analytical methods, formation, and dissolution of cinnabar and its impact on environmental cycle of mercury. CRITICAL REVIEWS IN ENVIRONMENTAL SCIENCE AND TECHNOLOGY. 10.1080/10643389.2018.1429764	2

17	Porwal, S; Singh, R, 2016. Cloning of merA Gene from Methylothermobacter Mobilis for Mercury Biotransformation. INDIAN JOURNAL OF MICROBIOLOGY. 10.1007/s12088-016-0613-5	2
18	Bavec, S; Gosar, M, 2016. Speciation, mobility and bioaccessibility of Hg in the polluted urban soil of Idrija (Slovenia). GEODERMA. 10.1016/j.geoderma.2016.03.015	2
19	Gajdosechova, Z; Boskamp, MS; Lopez-Linares, F; Feldmann, J; Krupp, EM, 2016. Hg Speciation in Petroleum Hydrocarbons with Emphasis on the Reactivity of Hg Particles. ENERGY & FUELS. 10.1021/acs.energyfuels.5b02080	2
20	Windmüller, CC; Durao, WA; de Oliveira, A; do Valle, CM, 2015. The redox processes in Hg-contaminated soils from Descoberto (Minas Gerais, Brazil): Implications for the mercury cycle. ECOTOXICOLOGY AND ENVIRONMENTAL SAFETY. 10.1016/j.ecoenv.2014.11.009	2
21	Butler, OT; Cairns, WRL; Cook, JM; Davidson, CM, 2015. 2014 atomic spectrometry update - a review of advances in environmental analysis. JOURNAL OF ANALYTICAL ATOMIC SPECTROMETRY. 10.1039/c4ja90062f	2
22	Sedlar, M; Pavlin, M; Popovic, A; Horvat, M, 2015. Temperature stability of mercury compounds in solid substrates. OPEN CHEMISTRY. 10.1515/chem-2015-0051	2
<b>celkem za položku</b>		<b>44</b>
<b>Šípková, A; Száková, J; Coufalík, P; Zvěřina, O; Kacálková, L; Tlustoš, P, 2014. Mercury distribution and mobility in contaminated soils from vicinity of waste incineration plant. PLANT SOIL AND ENVIRONMENT. 10.17221/634/2013-PSE</b>		
1	Xie, H; Liu, JY, 2022. Synergistic removal of NO and Hg <sup>0</sup> by Nanoflower-like TiO <sub>2</sub> supported MnCeOx. CHEMICAL PHYSICS LETTERS. 10.1016/j.cplett.2021.139322	2
2	Tarvainen, T; Ladenberger, A; Snöålv, J; Jarva, J; Andersson, M; Eklund, M, 2018. Urban soil geochemistry of two Nordic towns: Hameenlinna and Karlstad. JOURNAL OF GEOCHEMICAL EXPLORATION. 10.1016/j.gexplo.2017.07.018	2
3	Kim, KH; Kabir, E; Jahan, SA, 2016. A review on the distribution of Hg in the environment and its human health impacts. JOURNAL OF HAZARDOUS MATERIALS. 10.1016/j.jhazmat.2015.11.031	2
<b>celkem za položku</b>		<b>6</b>
<b>Zvěřina, O; Coufalík, P; Komárek, J; Gadas, P; Sysalová, J, 2014. Mercury associated with size-fractionated urban particulate matter: three years of sampling in Prague, Czech Republic. CHEMICAL PAPERS. 10.2478/s11696-013-0436-3</b>		
1	Liu, DY; Wang, CR; Fan, YP; Liu, QQ; Wang, XD; Xu, KL; Jin, J; Ma, JJ; Ma, JC, 2023. Mercury transformation and removal in chemical looping combustion of coal: A review. FUEL. 10.1016/j.fuel.2023.128440	2

2	Pelcová, P; Grmela, J; Ridosková, A; Kopp, R; Hruzová, M; Maly, O, 2022. Trophic distribution of mercury from an abandoned cinnabar mine within the Zaskalska reservoir ecosystem (Czech Republic). ENVIRONMENTAL SCIENCE AND POLLUTION RESEARCH. 10.1007/s11356-022-20159-4	2
3	Pelcová, P; Ridosková, A; Hrachovinová, J; Grmela, J, 2020. Fractionation Analysis of Mercury in Soils: A Comparison of Three Techniques for Bioavailable Mercury Fraction Determination. ENVIRONMENTAL TOXICOLOGY AND CHEMISTRY. 10.1002/etc.4797	2
4	Navrátil, T; Nováková, T; Roll, M; Shanley, JB; Kopáček, J; Rohovec, J; Kana, J; Cudlín, P, 2019. Decreasing litterfall mercury deposition in central European coniferous forests and effects of bark beetle infestation. SCIENCE OF THE TOTAL ENVIRONMENT. 10.1016/j.scitotenv.2019.05.093	2
5	Ghoshdastidar, AJ; Ariya, PA, 2019. The Existence of Airborne Mercury Nanoparticles. SCIENTIFIC REPORTS. 10.1038/s41598-019-47086-8	2
<b>celkem za položku</b>		<b>10</b>
<b>Coufalík, P; Zvěřina, O; Komárek, J, 2013. Atmospheric mercury deposited in a peat bog, the Jeseniky Mountains, Czech Republic. JOURNAL OF GEOCHEMICAL EXPLORATION. 10.1016/j.gexplo.2013.06.005</b>		
1	Cortizas, AM; Horák-Terra, I; Pérez-Rodríguez, M; Bindler, R; Cooke, CA; Kylander, M, 2021. Structural equation modeling of long-term controls on mercury and bromine accumulation in Pinheiro mire (Minas Gerais, Brazil). SCIENCE OF THE TOTAL ENVIRONMENT. 10.1016/j.scitotenv.2020.143940	2
2	Cooke, CA; Martínez-Cortizas, A; Bindler, R; Gustin, MS, 2020. Environmental archives of atmospheric Hg deposition - A review. SCIENCE OF THE TOTAL ENVIRONMENT. 10.1016/j.scitotenv.2019.134800	2
3	Pérez-Rodríguez, M; Horák-Terra, I; Rodríguez-Lado, L; Aboal, JR; Cortizas, AM, 2015. Long-Term (~57 ka) Controls on Mercury Accumulation in the Souther Hemisphere Reconstructed Using a Peat Record from Pinheiro Mire (Minas Gerais, Brazil). ENVIRONMENTAL SCIENCE & TECHNOLOGY. 10.1021/es504826d	2
<b>celkem za položku</b>		<b>6</b>
<b>Zvěřina, O; Červenka, R; Komárek, J; Sysalová, J, 2013. Mercury characterisation in urban particulate matter. CHEMICAL PAPERS. 10.2478/s11696-012-0259-7</b>		
1	Gonzalez-Raymat, H; Liu, GL; Liriano, C; Li, YB; Yin, YG; Shi, JB; Jiang, GB; Cai, Y, 2017. Elemental mercury: Its unique properties affect its behavior and fate in the environment. ENVIRONMENTAL POLLUTION. 10.1016/j.envpol.2017.04.101	2
2	Chen, Y; Yin, YG; Shi, JB; Liu, GL; Hu, L; Liu, JF; Cai, Y; Jiang, GB, 2017. Analytical methods, formation, and dissolution of cinnabar and its impact on environmental cycle of mercury. CRITICAL REVIEWS IN ENVIRONMENTAL SCIENCE AND TECHNOLOGY. 10.1080/10643389.2018.1429764	2

3	Urík, M; Hlodák, M; Mikusová, P; Matúš, P, 2014. Potential of Microscopic Fungi Isolated from Mercury Contaminated Soils to Accumulate and Volatilize Mercury(II). WATER AIR AND SOIL POLLUTION. 10.1007/s11270-014-2219-z	2
	<b>celkem za položku</b>	<b>6</b>
	<b>celkem za všechny položky</b>	<b>514</b>

### Získání externího grantu (řešitel, spoluřešitel)

Položka	A. Název odborné činnosti <sup>*)</sup>	Bodové hodnocení položky	Počet	Body celkem
25	Získání externího grantu (řešitel, spoluřešitel) <sup>***)</sup>	40	2	80
	Projekt Aktion 96p6: <i>Investigation of potentially toxic elements in Antarctic terrestrial flora</i> . Program AKTION Česká republika - Rakousko. Období řešení: 2023. Poskytovatel dotace Ministerstvo školství, mládeže a tělovýchovy ČR.		1	
	Projekt MŠMT Mobility 8J21AT006: Potenciálně toxické prvky v houbách a zelenině pěstovaných ve městech v Rakousku a České republice. Období řešení: 2021–2022. Poskytovatel dotace Ministerstvo školství, mládeže a tělovýchovy ČR.		1	

\*\*\*) Nejedná se o člena řešitelského týmu.

## Podrobnosti k jednotlivým kritériím – pedagogické činnosti

### Za každý rok pedagogického působení na vysoké škole na plný úvazek

Položka	B. Název pedagogické činnosti	Bodové hodnocení položky	Počet	Body celkem
1	Za každý rok pedagogického působení na vysoké škole na plný úvazek (částečné úvazky se sčítají)	25	10	<b>250</b>
	Plný akademický úvazek na Ústavu veřejného zdraví, Lékařská fakulta, Masarykova univerzita		10	

## Garantování SP

Od roku 2017 garantuji studijní program Nutriční terapie (dříve Nutriční terapeut), viz příložený jmenovací dekret.

Položka	B. Název pedagogické činnosti	Bodové hodnocení položky	Počet	Body celkem
3	Garantování SP (za každý rok)	5	7	<b>35</b>
	Garance studijního programu Nutriční terapie od 8/2017–současnost (započítáno je tedy 7 dokončených let)		7	

 **LÉKAŘSKÁ FAKULTA**

Číslo jednací  
MU-IS/94433/2017/592517LF-1

**JMENOVAČÍ DEKRET GARANTA STUDIJNÍHO PROGRAMU**

Děkan Lékařské fakulty Masarykovy univerzity, prof. MUDr. Jiří Mayer, CSc., tímto jménem Lékařské fakulty Masarykovy univerzity

**JMENUJE ke dni 31. 8. 2017**

na základě čl. V. odst. 4 Organizačního řádu Lékařské fakulty Masarykovy univerzity,

**GARANTEM BAKALÁŘSKÉHO STUDIJNÍHO PROGRAMU NUTRIČNÍ TERAPEUT**

**pana RNDr. Ondřeje Zvěřinu, Ph.D.**  
nar. 23. 5. 1986, bytem Valeč 218, 675 53 Valeč u Hrotovic.

Při plnění výkonu funkce garanta studijního programu Lékařské fakulty Masarykovy univerzity (dále jen „garant“) se garant řídí zejména vnitřním předpisem Masarykovy univerzity Schvalování, řízení a hodnocení kvality studijních programů Masarykovy univerzity a Organizačním řádem Lékařské fakulty Masarykovy univerzity a zákonem č. 111/1998 Sb., o vysokých školách a o změně a doplnění dalších zákonů (zákon o vysokých školách), ve znění pozdějších předpisů.

V Brně dne 24. srpna 2017

  
prof. MUDr. Jiří Mayer, CSc.  
děkan Lékařské fakulty Masarykovy univerzity

Masarykova univerzita, Lékařská fakulta  
Kamenice 753/5, 625 00 Brno, Česká republika  
T: +420 549 49 2810, E: info@med.muni.cz, www.med.muni.cz  
Bankovní spojení: KB Brno-město, ČÚ: 650305210100, IČ: 00216224, DIČ: CZ00216224  
V odpovědi prosím uvádějte naše číslo jednací.



*Jmenovací dekret: garant programu Nutriční terapie*

## Garantování předmětů

Položka	B. Název pedagogické činnosti	Bodové hodnocení položky	Počet	Body celkem
5	Garantování předmětů (za každý rok)	5	31	<b>155</b>
	<p>Garance předmětů na Ústavu veřejného zdraví LF MU:</p> <ul style="list-style-type: none"> <li>- Potravinářská chemie I – přednáška + cvičení, od 2013 (tzn. podzimní semestry 2013, 2014, 2015, 2016, 2017, 2018, 2019, 2020, 2021, 2022, 2023 = 11)</li> <li>- Potravinářská chemie II – přednáška + cvičení, od 2014 (tzn. jarní semestry 2014, 2015, 2016, 2017, 2018, 2019, 2020, 2021, 2022, 2023, 2024 = 11)</li> <li>- Lékařská toxikologie – přednáška + cvičení, od 2017 (tzn. podzimní semestry 2017, 2018, 2019, 2020, 2021, 2022, 2023 = 7)</li> </ul>		29	
	<p>Garance předmětu na ÚCHTOŽP FCH VUT:</p> <ul style="list-style-type: none"> <li>- Atomová absorpční spektrometrie v environmentální analýze (FCH-MC_AAS) – zimní semestry 2022 a 2023</li> </ul>		2	

## Zavedení nového předmětu nebo zásadní inovace předmětu

6	Zavedení nového předmětu nebo zásadní inovace předmětu	10	1	<b>10</b>
	Sestavení sylabu předmětu Potravinářská chemie I a II, tvorba elektronické studijní opory a tvorba nových laboratorních cvičení. Podpořeno projektem „Inovace dvousemestrálního předmětu Potravinářská chemie u oboru Nutriční terapeut: tvorba studijní elektronické opory“.		1	

Informace o projektu

**Inovace dvousemestrálního předmětu Potravinářská chemie u oboru Nutriční terapeut: tvorba studijní elektronické opory**

**Kód projektu**  
MUNI/FR/1498/2016

**Období řešení**  
1/2017 - 12/2017

**Investor / Programový rámec / typ projektu**  
[Masarykova univerzita](#)  
> Fond rozvoje MU

**Fakulta / Pracoviště MU**  
Lékařská fakulta  
> [RNDr. Ondřej Zvěřina, Ph.D.](#)  
> [MUDr. Halina Matějová](#)

Pro dvousemestrální předmět Potravinářská chemie bude v rámci projektu vytvořena ucelená studijní opora. Elektronické materiály v informačním systému budou obsahovat výukové texty, ilustrační fotografie a videa. Inovace je v souladu s dlouhodobým záměrem Masarykovy Univerzity na léta 2106-2020.

*Projekt Inovace dvousemestrálního předmětu Potravinářská chemie,  
podpořen fondem rozvoje MU*

### Vedení úspěšně obhájené diplomové práce

Položka	B. Název pedagogické činnosti	Bodové hodnocení položky	Počet	Body celkem
7	Vedení úspěšně obhájené diplomové práce	5	7	<b>35</b>
	<p><i>Vybrané mikroprvky v rostlinných náhradách mäsa</i> Bc. Mária Dávidová, 11. 6. 2024</p> <p><i>Domáci zelenina: obsah esenciálních a toxických prvků</i> Monika Vychytilová, 13. 6. 2023</p> <p><i>Jedlý hmyz jako potravina budoucnosti</i> Martina Krulíková, 13. 6. 2022</p> <p><i>Vývary ako zdroje minerálních látok</i> Katarína Orlovská, 3. 9. 2021</p> <p><i>Sůl v technologii přípravy pokrmů</i> Filip Martiník, 11. 6. 2018</p> <p><i>Chrómová vztáhu k obezite</i> Lenka Slobodníková, 13. 6. 2017</p> <p><i>Odhad zátěže kadmiem ze sóje a sójových výrobků u alternativního způsobu stravování</i> Pavčina Kosečková, 13. 6. 2017</p>		7	

### Vedení úspěšně obhájené bakalářské práce

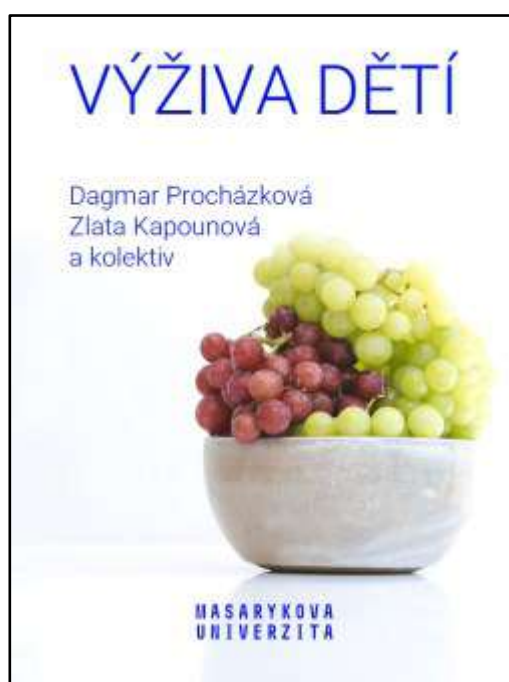
Položka	B. Název pedagogické činnosti	Bodové hodnocení položky	Počet	Body celkem
8	Vedení úspěšně obhájené bakalářské práce	3	10	<b>30</b>
	<p><i>Olejnata semena jako zdroje vápníku</i> Dominika Michaličková, 6. 6. 2023</p> <p><i>3-MCPD, 2-MCPD a jejich estery z pohledu nutričního terapeuta</i> Dita Pyšková, 4. 6. 2020</p> <p><i>Nutričně významné složky čaje</i> Martina Krulíková, 4. 6. 2020</p> <p><i>Současné poznatky o TMAO</i> Barbora Žitná, 5. 6. 2019</p> <p><i>Problematika arzeny v potravinách a potenciální riziko pro osoby dodržující bezlepkovou dietu</i> Tomáš Nekula, 4. 6. 2019</p> <p><i>Zinek v potravinách rostlinného původu</i> Nikola Kamenská, 4. 6. 2019</p> <p><i>Síra ve výživě člověka</i> Magdalena Kocurková, 4. 6. 201</p> <p><i>Vitamin C z pohledu nutričního terapeuta</i> Adriana Navrátilová, 9. 6. 2016</p> <p><i>Oxycholesterol</i> Anna Kadlecová, 8. 6. 2016</p> <p><i>Aditivní látky v cukrovinkách</i> Kateřina Vránová, 5. 6. 2015</p>		10	

**Školitel studenta, který získal Ph.D.**

Položka	B. Název pedagogické činnosti	Bodové hodnocení položky	Počet	Body celkem
11	Školitel studenta, který získal Ph.D.	20	1	<b>20</b>
	<i>Stopové prvky u jednostranně založených diet</i> Pavčina Kosečková, 10. 10. 2022		1	

### Skripta s ISBN (za 1 stranu)

Položka	B. Název pedagogické činnosti	Bodové hodnocení položky	Počet	Body celkem
14	Skripta s ISBN (za 1 stranu)	0,4	4	<b>4</b>
	spoluautorství skript Výživa dětí kapitola 6: Alternativní způsoby stravování (10 stran) ISBN 978-80-210-9846		10	



*Skripta Výživa dětí, do kterých jsem přispěl kapitolou pojednávající o stopových prvcích a jejich příjmu při alternativních dietách*

## Vytvoření významné výukové podpory

v rozsahu odpovídajícím elearningovému kurzu k předmětu

Položka	B. Název pedagogické činnosti	Bodové hodnocení položky	Počet	Body celkem
15	Vytvoření významné výukové podpory v rozsahu odpovídajícím elearningovému kurzu k předmětu	20	1	<b>20</b>
	elektronická studijní opora k předmětu Atomová absorpční spektrometrie v environmentální analýze (FCH-MC_AAS)		1	



*První z celkem 208 slajdů elektronické studijní opory vytvořené k předmětu Atomová absorpční spektrometrie v environmentální analýze (FCH-MC\_AAS)*

## **Doklady osvědčující pedagogickou praxi**

### **Pedagogické působení na Ústavu veřejného zdraví**

#### **Lékařské fakulty Masarykovy univerzity**

akademický pracovník: RNDr. Ondřej Zvěřina, Ph.D.

období: 4/2014–současnost

#### Výuka a garance předmětů

- Potravinářská chemie I - přednáška + cvičení (LF:BVCP0121p + LF:BVCP0121c)
  - Výuka od podzimního semestru 2013–doposud
  - Garance od podzimního semestru 2014–doposud
- Potravinářská chemie II - přednáška + cvičení (LF:BVCP0222p + LF:BVCP0222c)
  - Výuka i garance od jarního semestru 2014–doposud
- Lékařská toxikologie - přednáška + cvičení (LF:BVTO0311p + LF:BVTO0311c)
  - Výuka od podzimního semestru 2015–doposud
  - Garance od podzimního semestru 2017–doposud

#### Garance studijních programů

- Garant studijního programu Nutriční terapeut
  - 8/2017–doposud

Potvrzeno Mgr. Bc. Michalem Koščíkem, Ph.D., přednostou Ústavu veřejného zdraví a proděkanem pro personální záležitosti, vnitřní organizaci a legislativu Lékařské fakulty Masarykovy univerzity.

.....  
Mgr. Bc. Michal Koščík, Ph.D.

**Pedagogické působení na ÚCHTOŽP**  
**Fakulty chemické Vysokého učení technického**

Přednášející:  
RNDr. Ondřej Zvěřina, Ph.D.

Výuka a garance předmětů

- Atomová absorpční spektrometrie v environmentální analýze (FCH-MC\_AAS)  
Výuka a garance celosemestrálního předmětu od zimního semestru 2022 do současnosti

Výuka v předmětech

- Instrumentální a strukturní analýza (MC\_ISA)  
Výuka v rozsahu dvou přednášek/semestr v zimních semestrech 2021 a 2022
- Instrumental and Structural Analysis (MA\_ISA)  
Výuka v rozsahu dvou přednášek/semestr v zimních semestrech 2021 a 2022
- Chemické látky v životním prostředí (FCH-BC\_LZP)  
Výuka v rozsahu jedné přednášky v letních semestrech 2023 a 2024
- Water Analysis (MA\_ENG7)  
Výuka v rozsahu jedné přednášky a jednoho cvičení v letních semestrech 2022 a 2023

Potvrzeno doc. Mgr. Michaelou Vašinovou Galiovou Ph.D., proděkankou pro bakalářské a navazující magisterské studium, docentkou Ústavu chemie a technologie ochrany životního prostředí Fakulty Chemické Vysokého učení technického

.....  
doc. Mgr. Michaela Vašinová Galiová Ph.D.

## Seznam publikovaných prací

Seznam publikací je řazen chronologicky. Počet citací je dle Web of Science core databáze (srpen 2024).

Publikace	rok	citace
<b>Zvěřina, O</b> ✉; Brůhová, L; Coufalík, P; Strínger, CD; Rieger, J; Goessler, W, 2024. Multi-element analysis (Pb, Al, Fe) of Antarctic flora using HR-CS ETAAS with an extended working range. SPECTROCHIMICA ACTA PART B-ATOMIC SPECTROSCOPY. 10.1016/j.sab.2024.106979	2024	0
Kosečková, P; <b>Zvěřina, O</b> ✉; Letková, K, 2024. Nutritional insights into broths in relation to elemental composition. EUROPEAN FOOD RESEARCH AND TECHNOLOGY. 10.1007/s00217-024-04556-2	2024	0
Coufalík, P; Vašínska, M; Krmíček, L; Ševčík, R; <b>Zvěřina, O</b> ; Brůhová, L; Komárek, J, 2024. Toxic metals in cyanobacterial mat of Big Lachman Lake, James Ross Island, Antarctica. ENVIRONMENTAL MONITORING AND ASSESSMENT. 10.1007/s10661-023-12224-3	2024	0
<b>Zvěřina, O</b> ✉; Vychytilová, M; Rieger, J; Goessler, W, 2023. Fast and simultaneous determination of zinc and iron using HR-CS GF-AAS in vegetables and plant material. SPECTROCHIMICA ACTA PART B-ATOMIC SPECTROSCOPY. 10.1016/j.sab.2023.106616	2023	4
Coufalík, P; <b>Zvěřina, O</b> ; Sádovská, K; Komárek, J, 2023. UV-photochemical vapor generation coupled to hydride generation AAS in the study of dietary intake of Se, Hg, Cd, and Pb from fish. JOURNAL OF FOOD COMPOSITION AND ANALYSIS. 10.1016/j.jfca.2023.105668	2023	1
Kosečková, P; <b>Zvěřina, O</b> ✉; Pechová, M; Krulíková, M; Duborská, E; Borkovcová, M, 2022. Mineral profile of cricket powders, some edible insect species and their implication for gastronomy. JOURNAL OF FOOD COMPOSITION AND ANALYSIS. 10.1016/j.jfca.2021.104340	2022	16
Hagarová, I; Nemček, L; Šebesta, M; <b>Zvěřina, O</b> ; Kasak, P; Urík, M, 2022. Preconcentration and Separation of Gold Nanoparticles from Environmental Waters Using Extraction Techniques Followed by Spectrometric Quantification. INTERNATIONAL JOURNAL OF MOLECULAR SCIENCES. 10.3390/ijms231911465	2022	5
Duborská, E; Šebesta, M; Matulová, M; <b>Zvěřina, O</b> ; Urík, M, 2022. Current Strategies for Selenium and Iodine Biofortification in Crop Plants. NUTRIENTS. 10.3390/nu14224717	2022	13
<b>Zvěřina, O</b> ✉; Venclíček, O; Kuta, J; Coufalík, P; Hagarova, I; Brat, K, 2021. A simple dilute-and-shoot procedure for the determination of platinum in human pleural effusions using HR-CS GF-AAS. JOURNAL OF TRACE ELEMENTS IN MEDICINE AND BIOLOGY. 10.1016/j.jtemb.2021.126869	2021	3

Lokvencová, L; <b>Zvěřina, O</b> ✉; Kuta, J, 2021. Different trends of Cr, Fe and Zn contents in hair between obese, overweight and normal-weight men. CENTRAL EUROPEAN JOURNAL OF PUBLIC HEALTH. 10.21101/cejph.a6912	2021	3
Duborská, E; Balíková, K; Matulová, M; <b>Zvěřina, O</b> ; Farkas, B; Littera, P; Urik, M, 2021. Production of Methyl-Iodide in the Environment. FRONTIERS IN MICROBIOLOGY. 10.3389/fmicb.2021.804081	2021	2
Farkas, B; Bujdos, M; Polák, F; Matulová, M; Cesnek, M; Duborská, E; <b>Zvěřina, O</b> ; Kim, H; Danko, M; Kisová, Z; Matuš, P; Urik, M, 2021. Bioleaching of Manganese Oxides at Different Oxidation States by Filamentous Fungus Aspergillus niger. JOURNAL OF FUNGI. 10.3390/jof7100808	2021	5
Kosečková, P; <b>Zvěřina, O</b> ; Pruša, T; Coufalík, P; Hrežová, E, 2020. Estimation of cadmium load from soybeans and soy-based foods for vegetarians. ENVIRONMENTAL MONITORING AND ASSESSMENT. 10.1007/s10661-019-8034-7	2020	8
<b>Zvěřina, O</b> ✉; Coufalík, P; Šimůnek, J; Kachlík, P; Chlupová, R; Pavelková, J, 2020. Inorganic pollutants in the indoor environment of the Moravian Library: assessment of Cd, Pb, Cu, and Zn in total suspended particles and dust using HR-CS GF-AAS. ENVIRONMENTAL MONITORING AND ASSESSMENT. 10.1007/s10661-020-08748-7	2020	2
Coufalík, P; Uher, A; <b>Zvěřina, O</b> ; Komárek, J, 2020. Determination of cadmium in lichens by solid sampling graphite furnace atomic absorption spectrometry (SS-GF-AAS). ENVIRONMENTAL MONITORING AND ASSESSMENT. 10.1007/s10661-020-8186-5	2020	5
Brtnický, M; Pecina, V; Galiová, MV; Prokes, L; <b>Zvěřina, O</b> ; Juricka, D; Klimánek, M; Kynický, J, 2020. The impact of tourism on extremely visited volcanic island: Link between environmental pollution and transportation modes. CHEMOSPHERE. 10.1016/j.chemosphere.2020.126118	2020	28
Sysalová, J; <b>Zvěřina, O</b> ; Červenka, R; Komárek, J, 2020. Occurrence and transformation of mercury in formerly contaminated soils due to operation of amalgamation techniques and assessment of consequences. HUMAN AND ECOLOGICAL RISK ASSESSMENT. 10.1080/10807039.2019.1660848	2020	0
<b>Zvěřina, O</b> ✉; Kuta, J; Coufalík, P; Kosečková, P; Komárek, J, 2019. Simultaneous determination of cadmium and iron in different kinds of cereal flakes using high-resolution continuum source atomic absorption spectrometry. FOOD CHEMISTRY. 10.1016/j.foodchem.2019.125084	2019	26
Coufalík, P; Krmíček, L; <b>Zvěřina, O</b> ; Meszarosová, N; Hladil, J; Komárek, J, 2018. Model of Mercury Flux Associated with Volcanic Activity. BULLETIN OF ENVIRONMENTAL CONTAMINATION AND TOXICOLOGY. 10.1007/s00128-018-2430-5	2018	10

<b>Zvěřina, O</b> ✉; Coufalík, P; Barták, M; Petrov, M; Komárek, J, 2018. The contents and distributions of cadmium, mercury, and lead in <i>Usnea antarctica</i> lichens from Solorina Valley, James Ross Island (Antarctica). ENVIRONMENTAL MONITORING AND ASSESSMENT. 10.1007/s10661-017-6397-1	2018	14
Coufalík, P; Meszarosová, N; Coufalíková, K; <b>Zvěřina, O</b> ; Komárek, J, 2018. Determination of methylmercury in cryptogams by means of GC-AFS using enzymatic hydrolysis. MICROCHEMICAL JOURNAL. 10.1016/j.microc.2018.03.040	2018	7
<b>Zvěřina, O</b> ✉; Coufalík, P; Brat, K; Červenka, R; Kuta, J; Mikes, O; Komárek, J, 2017. Leaching of mercury from seal carcasses into Antarctic soils. ENVIRONMENTAL SCIENCE AND POLLUTION RESEARCH. 10.1007/s11356-016-7879-3	2017	15
Sysalová, J; Kučera, J; Drtinová, B; Červenka, R; <b>Zvěřina, O</b> ; Komárek, J; Kameník, J, 2017. Mercury species in formerly contaminated soils and released soil gases. SCIENCE OF THE TOTAL ENVIRONMENT. 10.1016/j.scitotenv.2017.01.157	2017	31
Coufalík, P; <b>Zvěřina, O</b> ; Komárek, J, 2016. The direct determination of HgS by thermal desorption coupled with atomic absorption spectrometry. SPECTROCHIMICA ACTA PART B-ATOMIC SPECTROSCOPY. 10.1016/j.sab.2016.01.004	2016	7
Száková, J; Havlíčková, J; Šípková, A; Gabriel, J; Švec, K; Baldrian, P; Sysalová, J; Coufalík, P; Červenka, R; <b>Zvěřina, O</b> ; Komárek, J; Tlustoš, P, 2016. Effects of the soil microbial community on mobile proportions and speciation of mercury (Hg) in contaminated soil. JOURNAL OF ENVIRONMENTAL SCIENCE AND HEALTH PART A-TOXIC/HAZARDOUS SUBSTANCES & ENVIRONMENTAL ENGINEERING. 10.1080/10934529.2015.1109413	2016	9
Coufalík, P; Procházková, P; <b>Zvěřina, O</b> ; Trnková, K; Skácelová, K; Nývlt, D; Komárek, J, 2016. Freshwater mineral nitrogen and essential elements in autotrophs in James Ross Island, West Antarctica. POLISH POLAR RESEARCH. 10.1515/popore-2016-0025	2016	4
Coufalík, P; <b>Zvěřina, O</b> ; Krmíček, L; Pokorný, R; Komárek, J, 2015. Ultra-trace analysis of Hg in alkaline lavas and regolith from James Ross Island. ANTARCTIC SCIENCE. 10.1017/S0954102014000819	2015	11
Coufalík, P; <b>Zvěřina, O</b> ; Mikuška, P; Komárek, J, 2014. Seasonal Variability of Mercury Contents in Street Dust in Brno, Czech Republic. BULLETIN OF ENVIRONMENTAL CONTAMINATION AND TOXICOLOGY. 10.1007/s00128-014-1289-3	2014	16
<b>Zvěřina, O</b> ✉; Láska, K; Červenka, R; Kuta, J; Coufalík, P; Komárek, J, 2014. Analysis of mercury and other heavy metals accumulated in lichen <i>Usnea antarctica</i> from James Ross Island, Antarctica. ENVIRONMENTAL MONITORING AND ASSESSMENT. 10.1007/s10661-014-4068-z	2014	37

Šípková, A; Száková, J; Coufalík, P; <b>Zvěřina, O</b> ; Kacálková, L; Tlustoš, P, 2014. Mercury distribution and mobility in contaminated soils from vicinity of waste incineration plant. PLANT SOIL AND ENVIRONMENT. 10.17221/634/2013-PSE	2014	7
<b>Zvěřina, O</b> ✉; Coufalík, P; Komárek, J; Gadas, P; Sysalová, J, 2014. Mercury associated with size-fractionated urban particulate matter: three years of sampling in Prague, Czech Republic. CHEMICAL PAPERS. 10.2478/s11696-013-0436-3	2014	6
Coufalík, P; <b>Zvěřina, O</b> ; Komárek, J, 2014. Determination of mercury species using thermal desorption analysis in AAS. CHEMICAL PAPERS. 10.2478/s11696-013-0471-0	2014	28
Coufalík, P; <b>Zvěřina, O</b> ; Komárek, J, 2013. Atmospheric mercury deposited in a peat bog, the Jeseníky Mountains, Czech Republic. JOURNAL OF GEOCHEMICAL EXPLORATION. 10.1016/j.gexplo.2013.06.005	2013	5
<b>Zvěřina, O</b> ✉; Červenka, R; Komárek, J; Sysalová, J, 2013. Mercury characterisation in urban particulate matter. CHEMICAL PAPERS. 10.2478/s11696-012-0259-7	2013	4

### **Vyjádření podílu na uvedených publikacích**

Z hlediska mého podílu lze výše uvedené publikace rozdělit do tří kategorií. Dělicím kritériem je domovské pracoviště, na kterém publikace vznikly:

- Práce vzniklé na Lékařské fakultě Masarykovy univerzity tvoří 35 % uvedených publikací a jsem u nich prvním nebo korespondenčním autorem. U těchto studií jsem designoval experimenty, prováděl měření a vyhodnocoval data a měl hlavní podíl na přípravě publikací. Podíl na nich proto odhaduji na 50–75 %.
- Práce vzniklé za mého působení na Přírodovědecké fakultě Masarykovy univerzity, věnující se především speciaci rtuti v životním prostředí se zvláštním důrazem na její výskyt v antarktickém ekosystému. Tyto publikace tvoří 26 % publikační činnosti. Podle mého pořadí v autorském kolektivu (u třetiny publikací jsem první autor) se můj podíl na publikacích pohyboval od 75 % (design a provádění experimentů, sestavování publikace) po 25 % v rolích spoluautora, kdy jsem prováděl experimenty, zpracovával výsledky a připravoval grafické podklady pro publikace, na jejichž sepsování jsem se podílel částečně.
- Publikace, na kterých jsem spolupracoval s dalšími institucemi, tvoří 39 procent. Byly vytvořeny ve spolupráci s Ústavem analytické chemie Akademie věd ČR, Vysokou školou chemicko-technologickou v Praze, Univerzitou Komenského v Bratislavě, Českou zemědělskou univerzitou v Praze a s Ústavem chemie a technologie ochrany životního prostředí Vysokého učení technického. Můj podíl na těchto publikacích spočíval především ve vývoji analytických metod a vlastním stanovení kovů v environmentálních matricích. V případě několika přehledových článků se jednalo o odborné konzultace. Svůj podíl v této kategorii publikací odhaduji na 10–20 %.

## **Přehled absolvovaných vědeckých stáží**

### **a) zahraniční konzultační stáže <1 měsíc**

- prof. Walter Goessler, University of Graz, Rakousko  
celkem 40 dní v období 2021–2024
- prof. Martin Resano, University of Zaragoza, Španělsko  
2 týdny, 2/2022
- prof. Przemyslaw Niedzielski, Adam Mickiewicz University in Poznań, Polsko  
2 týdny, 5/2022
- prof. Milena Horvath, Jožef Stefan Institute, Ljubljana, Slovinsko  
týden, 10/2019
- doc. Peter Matúš, Univerzita Komenského v Bratislave, Slovensko  
týden, 2–3/2019
- prof. Steven Siciliano, University of Saskatchewan, Saskatoon, Kanada  
dva týdny, 7/2018

### **b) člen polárních expedic**

- na ostrov Nelson, Antarktida  
1–2/2023
- na stanici J. G. Mendela, James Ross Island, Antarktida  
1–3/2015 a 1–3/2012

## **Návrh tří témat pro veřejnou pedagogickou přednášku**

1. Kontaminace antarktického ekosystému toxickými prvky
2. Úvod do vysokorozlišovací atomové absorpční spektrometrie
3. Rtuť v životním prostředí

## **Úředně ověřené doklady o dosaženém vysokoškolském vzdělání**

- Titul Mgr.
- Titul RNDr.
- Titul Ph.D.



Česká republika  
MASARYKOVA UNIVERZITA

# DIPLOM

## Ondřej Zvěřina

nar. 23. května 1986, Třebíč, r. č. 860523/5023,

získal vysokoškolské vzdělání studiem na  
**Přírodovědecké fakultě**

v magisterském studijním programu  
**Chemie**

ve studijním oboru  
**Analytická chemie.**

Podle § 46 odst. 4 písm. g) zákona č. 111/1998 Sb. o vysokých školách a o změně a doplnění dalších zákonů (zákon o vysokých školách), se mu uděluje

akademický titul **magistr,**  
ve zkratce **Mgr.** uváděné před jménem.

děkan



rektor

V Brně dne 21. června 2010

Číslo diplomu 1431/2010/0355.

Studijní program Chemie má v klasifikaci MŠMT ČR identifikaci N1407.

Studijní obor Analytická chemie má v klasifikaci MŠMT ČR identifikaci 1403T001.



Česká republika  
MASARYKOVA UNIVERZITA

# DIPLOM

## Ondřej Zvěřina

nar. 23. května 1986, Třebíč, r. č. 860523/5023,

vykonal státní rigorózní zkoušku na  
Přírodovědecké fakultě

v oboru  
**Analytická chemie.**

Podle § 46 odst. 5 písm. c) zákona č. 111/1998 Sb. o vysokých školách a o změně a doplnění dalších zákonů (zákon o vysokých školách), se mu uděluje

akademický titul **doktor přírodních věd,**  
ve zkratce **RNDr.** uváděné před jménem.

děkan



rektor

V Brně dne 13. prosince 2012

Číslo diplomu 1431/2012/1030.



Česká republika  
MASARYKOVA UNIVERZITA

# DIPLOM

**Ondřej Zvěřina**

nar. 23. května 1986, Třebíč, r. č. 860523/5023,

získal vysokoškolské vzdělání studiem na  
**Přírodovědecké fakultě**

v doktorském studijním programu  
**Chemie**

ve studijním oboru  
**Analytická chemie.**

Podle § 47 odst. 5 zákona č. 111/1998 Sb. o vysokých školách a o změně a doplnění dalších zákonů (zákon o vysokých školách), se mu uděluje

akademický titul **doktor,**  
ve zkratce **Ph.D.** uváděné za jménem.

děkan



rektor

V Brně dne 25. září 2015

Číslo diplomu 1431/2015/0913.  
Studijní program Chemie má v klasifikaci MŠMT ČR identifikaci P1417.  
Studijní obor Analytická chemie má v klasifikaci MŠMT ČR identifikaci 1403V001.

## **Reprinty nejvýznamnějších publikací**

## Nejvýznamnější publikace

1. **Zvěřina, O**; Brůhová, L; Coufalík, P; Stringer, CD; Rieger, J; Goessler, W, 2024. Multi-element analysis (Pb, Al, Fe) of Antarctic flora using HR-CS ETAAS with an extended working range. SPECTROCHIMICA ACTA PART B-ATOMIC SPECTROSCOPY. 10.1016/j.sab.2024.106979
2. **Zvěřina, O**; Vychytilová, M; Rieger, J; Goessler, W, 2023. Fast and simultaneous determination of zinc and iron using HR-CS GF-AAS in vegetables and plant material. SPECTROCHIMICA ACTA PART B-ATOMIC SPECTROSCOPY. 10.1016/j.sab.2023.106616
3. **Zvěřina, O**; Kuta, J; Coufalík, P; Kosečková, P; Komárek, J, 2019. Simultaneous determination of cadmium and iron in different kinds of cereal flakes using high-resolution continuum source atomic absorption spectrometry. FOOD CHEMISTRY. 10.1016/j.foodchem.2019.125084
4. **Zvěřina, O**; Venclíček, O; Kuta, J; Coufalík, P; Hagarova, I; Brat, K, 2021. A simple dilute-and-shoot procedure for the determination of platinum in human pleural effusions using HR-CS GF-AAS. JOURNAL OF TRACE ELEMENTS IN MEDICINE AND BIOLOGY. 10.1016/j.jtemb.2021.126869
5. **Zvěřina, O**; Láska, K; Červenka, R; Kuta, J; Coufalík, P; Komárek, J, 2014. Analysis of mercury and other heavy metals accumulated in lichen *Usnea antarctica* from James Ross Island, Antarctica. ENVIRONMENTAL MONITORING AND ASSESSMENT. 10.1007/s10661-014-4068-z



Contents lists available at ScienceDirect

## Spectrochimica Acta Part B: Atomic Spectroscopy

journal homepage: [www.elsevier.com/locate/sab](http://www.elsevier.com/locate/sab)

Analytical note

## Multi-element analysis (Pb, Al, Fe) of Antarctic flora using HR-CS ETAAS with an extended working range

Ondřej Zvěřina<sup>a,\*</sup>, Lenka Brůhová<sup>a</sup>, Pavel Coufalík<sup>b</sup>, Christopher D. Stringer<sup>c</sup>,  
Jaqueline Rieger<sup>d</sup>, Walter Goessler<sup>d</sup><sup>a</sup> Masaryk University, Department of Public Health, Kamenice 5, 625 00 Brno, Czech Republic<sup>b</sup> Institute of Analytical Chemistry of the Czech Academy of Sciences, Veverí 97, 60200 Brno, Czech Republic<sup>c</sup> School of Geography and water@leeds, University of Leeds, Woodhouse Lane, Leeds, West Yorkshire LS2 9JT, UK<sup>d</sup> University of Graz, Institute of Chemistry, Universitaetsplatz 1, 8010 Graz, Austria

## ARTICLE INFO

## Keywords:

Simultaneous multi-element analysis  
HR-CS ETAAS  
Antarctic flora analysis  
Biomonitoring  
Antarctica

## ABSTRACT

This paper introduces a new method for the simultaneous determination of lead, aluminum, and iron in plant samples using high-resolution continuum source electrothermal atomic absorption spectrometry (HR-CS ETAAS). The method is suitable for covering a wide range of concentrations for all three elements, by utilizing two spectral lines for Al and employing the wavelength-selected absorbance (WSA) approach, which combines the reading of absorbance signals at both the central and wing parts of the spectral lines. The method was validated against certified reference materials and was then applied in a large-scale analysis of Antarctic flora collected from Nelson Island in the South Shetland Islands, Antarctica. The method was found to be a useful biomonitoring tool for assessing Pb pollution in various plant materials, including lichens, mosses, grass and mushrooms, while Al and Fe contents may serve as normalizing elements in calculations of environmental indices. The observed Pb levels in lichens (median content 0.19 mg Pb/kg) were lower than those reported in other Antarctic regions. These findings indicate that the Stansbury Peninsula on Nelson Island is relatively unaffected by local pollution, compared to other Antarctic regions, and that the data might serve as an example of background levels in the South Shetland Islands.

## 1. Introduction

Lead is a global contaminant of particular concern due to its high ecosystem-disrupting potential, and is readily transported over long distances, even reaching remote areas like Antarctica [1]. Over the past 130 years, an estimated 660 tons of Pb have been deposited over the continent through long-range atmospheric transport [2]. Additionally, local pollution comes from anthropogenic activities such as the operation of scientific stations and tourism [1,3]. Such activities are mostly localized close to the coast, where most of the terrestrial floral and faunal diversity is concentrated [3,4]. In particular, cryptogams like lichens and mosses, widespread across Antarctica, act as sensitive bio-indicators, reflecting local environmental conditions [1,3,5]. A common approach to assessing Pb contamination in bioindicators is to normalize Pb levels to naturally occurring, less mobile elements such as Al and Fe, which act as reference elements due to their stable environmental concentrations.

The elemental analysis of plant materials, including cryptogams, is typically performed using various spectroscopic techniques such as atomic absorption spectrometry with both flame and electrothermal atomization (FAAS and ETAAS), and also methods based on inductively coupled plasma with either optical emission (ICP-OES) or mass spectrometry (ICP-MS) [6].

While ETAAS is a well-established and sensitive technique for the elemental analysis of environmental samples, it suffers from limitations such as single-element determination and a limited working range. However, commercially available high-resolution continuum source (HR-CS) AA spectrometers have introduced features to overcome these limitations, as they allow for detailed monitoring of the selected spectral line and its immediate surroundings.

Measuring elements of interest one by one is a significant limitation of AAS, especially for time-consuming methods like ETAAS. However, HR-CS AAS instruments monitor not only the analytical line itself, but also its immediate surroundings. Any other spectral line close enough to

\* Corresponding author.

E-mail address: [zverina@med.muni.cz](mailto:zverina@med.muni.cz) (O. Zvěřina).<https://doi.org/10.1016/j.sab.2024.106979>

Received 22 February 2024; Received in revised form 21 June 2024; Accepted 23 June 2024

Available online 24 June 2024

0584-8547/© 2024 The Authors. Published by Elsevier B.V. This is an open access article under the CC BY license (<http://creativecommons.org/licenses/by/4.0/>).

fit into this detection window (approximately 0.2 nm) can be monitored simultaneously. This capability has allowed for the simultaneous analysis of up to four elements in some HR-CS ETAAS applications [7–9] and reviews on multielemental methods indicate a high interest in the benefits of such a feature [10–12]. Previously, a method for the simultaneous analysis of Pb and other elements was described, using Pb's secondary line at 283.306 nm, which is surrounded by secondary lines of Co, Fe, and Ni [8]. Multielemental methods employing the primary line of Pb at 217.001 nm have so far been based on a sequential approach [13,14]. These techniques require cooling of the furnace and realigning of the monochromator between the two separate atomization steps; therefore, time-savings are not as significant as in the case of a truly simultaneous determination.

In ecological studies, measuring Pb concentrations with high sensitivity is crucial, as Pb is typically found in trace amounts. On the other hand, Al and Fe are usually present in substantially higher and varying amounts, for which measurement a wide working range is required. In this regard, HR-CS offers useful tools for extending the dynamic range, which has traditionally been limited in line-source AAS to about two orders of magnitude [15,16]. The dynamic range can be extended in either of the two following ways:

- by using a wavelength-selected absorbance (WSA) approach, which can adjust the sensitivity by reading the signal either at the center of the absorption line or at its wings. In practice, this is achieved by using various pixels to register the absorbance signal. The signal registered by these side-pixels grows linearly in a wide concentration range [17]. Such sensitivity attenuation has already been used in a number of studies, e.g. [18–21]; however, this was only to reduce the signal intensity. In our study, it was undertaken to extend the methods' working range by preparing a series of calibration curves based on the different pixel combinations.
- by using less sensitive spectral lines. In line-source AAS, the use of secondary lines is not very common, mainly because they 1) exhibit a poor signal-to-noise ratio, and 2) are not well studied in terms of potential spectral interferences. The above reasons become invalid with the use of a continuum source (which provides a similar emission intensity for all lines) and high-resolution monochromator (which makes any spectral interference obvious) [21]. Moreover, in the case where multiple lines of the same element fit in the detector window, these having different sensitivity, they can be used to cover different concentration ranges. For instance, such a use of the Ni triplet in the vicinity of 234.6 nm was described in a review by Resano [11], covering a concentration range of more than three orders of magnitude. Similarly, near the primary Pb line at 217.001 nm, two Al lines occur with significantly different sensitivities. These Al lines can be utilized in an analogous approach to expand the measurable Al concentration range.

Both above-mentioned approaches can also be effectively combined, most notably for Al, where the two spectral lines and also the WSA approach can be used to extend the dynamic range of the measurement.

The main objective of this work was the development of a method for assessing environmental lead (Pb) contamination using HR-CS ETAAS, enabling the simultaneous co-determination of the reference elements aluminum (Al) and iron (Fe). The study aimed to develop a routine method involving multi-calibration based on WSA and multi-line evaluation, as well as the use of a simultaneous multi element method for assessing Pb contamination at trace levels. To the best of our knowledge, no routine method including these features has been described so far. A deeper insight into the contamination of the Antarctic flora of Nelson Island is the further contribution of this work.

## 2. Materials and methods

### 2.1. Samples of terrestrial flora from Nelson Island

The samples for this work originated from Nelson Island, South Shetland Islands, Antarctica (Fig. 1). Nelson Island is adjacent to King George Island, where most research stations are located, and experiences minimal human activity due to the absence of permanent settlements. Thus, it offers a relatively pristine environment compared to other areas in the region with higher tourist and scientific traffic. The local terrestrial flora is represented by lichens, mosses, grass, and mushrooms.

Samples were collected from the Rip Point oasis, Stansbury Peninsula, located in the northern part of the island. We established 28 sampling sites, each encompassing a circular area with a diameter of approximately 20 m to ensure comprehensive spatial coverage and representative sampling. At each site, we collected representative samples of lichens, mosses, mushrooms, and grass, whenever present. All collected samples were stored in PE plastic bags and kept frozen until analysis.

Samples of lichens included fruticose species prevalent in the area, namely *Usnea antarctica* ( $n = 27$ ), *Usnea aurantiaco-atra* ( $n = 23$ ), and *Ramalina terebrata* ( $n = 4$ ). Moss samples included mainly the locally-dominant specie *Sanionia uncinata* ( $n = 15$ ) followed by *Polytrichum* sp. ( $n = 3$ ) and *Bryum pseudotriquetrum* ( $n = 3$ ) and their mixtures ( $n = 8$ ). Five samples of grass were all *Deschampsia antarctica* and the mushroom samples consisted of *Arrhenia antarctica* ( $n = 6$ ) and one sample of *Arrhenia* cf. *lilacinicolor*.

### 2.2. Sample treatment and mineralization

In the laboratory, the samples underwent a series of preparation steps. First, they were subjected to a double wash with ultrapure water (18.2 M $\Omega$  cm) to remove any soil particles. Subsequently, the samples were dried for 48 h at 35 °C in a laboratory oven. To achieve a consistent texture, the samples were milled using an IKA A11 stainless-steel mill (IKA, Germany). However, due to the robustness of lichen thalli, an additional grinding step was necessary. The lichens were finely ground using a Pulverisette 7 planetary mill with silicon nitride grinding balls (Fritsch GmbH, Germany), resulting in a uniformly homogenized fine-grained material.

An UltraWAVE high-pressure microwave mineralizer (Milestone, Italy) was used for the decomposition of samples. The traceCLEAN cleaning system (Milestone, Italy) was used for the decontamination of quartz mineralization tubes. The decomposition of samples was carried out in a clean laboratory (class 100). Sub-boiled distilled HNO<sub>3</sub> (MES 2000, Gerber Instruments AG, Switzerland) was used for the mineralization of samples. The mineralized samples were further diluted by deionized water with a specific electrical conductivity of 0.055  $\mu$ S/cm (Ultra Clear, Evoqua Water Technologies, USA).

200 mg samples of lichens, mosses, and grass (to the nearest 0.1 mg) were weighed into the quartz mineralization tubes; only 50 mg mushroom samples were used due to the scarcity of the material. The samples were digested in 3 mL of concentrated HNO<sub>3</sub>. Decomposition was carried out according to a temperature program with a maximum mineralization temperature of 250 °C for 15 min. After cooling, the samples were transferred into PP tubes (Roth, USA) and topped up with deionized water to a volume of 10 mL (5 mL in the case of mushroom samples). White undissolved residues were observed in a few moss and grass samples. These residues were centrifuged to the bottom of the sample tubes, and the clear supernatant solution was used for the analysis.

Four certified reference materials (CRMs) were used to verify the accuracy of metal determinations: BCR-482 Lichen (IRMM, Belgium), NIST 1570a Spinach (NIST, USA), INCT-TL-1 Tea Leaves (INCT, Poland) and Metranal AN-BM02 Green Tea (ANALYTIKA, Czech Republic). CRMs were mineralized in triplicates using the same procedure as the

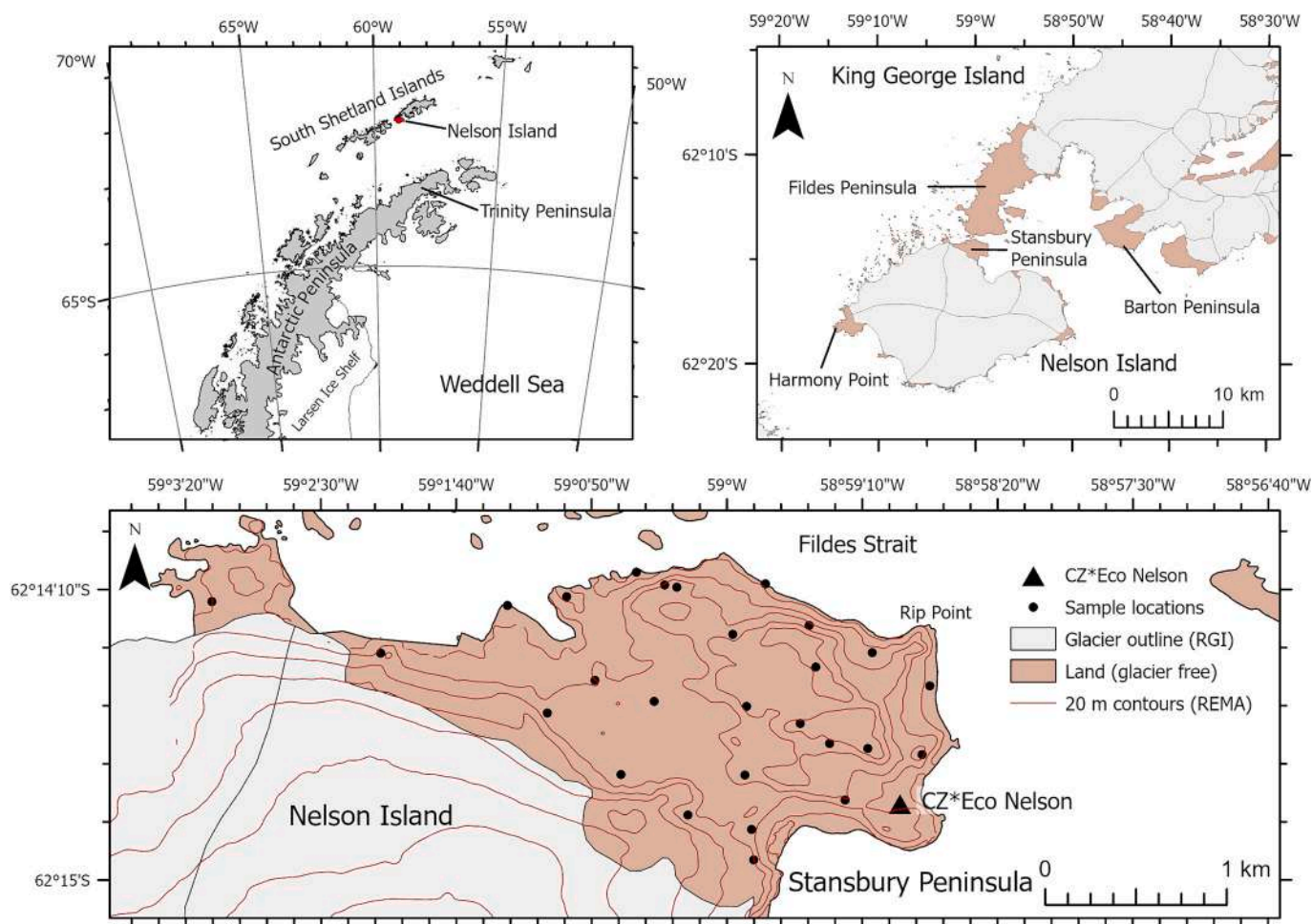


Fig. 1. Map of Nelson Island and sampling locations.

samples. Also, a total digestion of the CRMs was carried out for a trueness study purpose, using a mixture of 3 mL HNO<sub>3</sub> and 0.250 μL HF (Analpure grade, 48%, Analytika, Czech Republic) for the digestion.

### 2.3. Method for the simultaneous determination of Pb, Al, and Fe

A ContrAA 800G (Analytik Jena, Germany) high-resolution continuum source spectrometer was used for all analyses, this equipped with a Xe short-arc lamp as a continuum light source combined with a high-resolution double-Echelle monochromator and charge-coupled device detector. Graphite tubes with a PIN-platform were utilized for the analysis.

For the analysis, a 10 μL sample was injected into the furnace together with 15 μL of Pd/Mg(NO<sub>3</sub>)<sub>2</sub> modifier (consisting of Pd 1 g/L and Mg(NO<sub>3</sub>)<sub>2</sub> 0.6 g/L). The modifier not only prevents Pb losses during pyrolysis but also improves the shape of the Al peaks and reduces spectral interference from phosphorus monoxide. In samples with especially high phosphorus content, remaining molecular absorption bands were further minimized by the least squares background correction (see chapter 3.4. Handling the spectral interferences). The optimized temperature program is presented in Table 1, which is further discussed in the section 3.2. Developing a temperature program. The total duration of the program was 85 s. During the atomization step, the signals of adjacent spectral lines of Pb, Fe and two Al lines were recorded simultaneously using various combinations of detector pixels (see chapter 3.1. Spectral line selection). This approach allows considerable extension of the working range (see chapter 3.3. Method performance and working range). The wide working range allows for the batch

**Table 1**  
Temperature program for the simultaneous determination of Pb, Al, and Fe using HR-CS ETAAS.

Step	Temperature (°C)	Ramp (°C/s)	Hold (s)	Argon flow (L/min)	Read
Drying	130	10	7	2	
Pyrolysis	900	300	10	2	
Atomization	2500	1500	4	stop	active
Cleaning	2600	100	2	2	

analysis of sets of diverse samples, eliminating the need for individual dilutions. The need for operator intervention is thus also minimized. This capability was demonstrated by analyzing a set of 95 real plant materials with widely-varying elemental concentrations.

## 3. Results and discussion

### 3.1. Spectral line selection

In the immediate vicinity of the primary Pb resonance line at 217.001 nm, there are secondary lines for Al and Fe:

- Al 216.883 nm, with a sensitivity of 5.6% (with respect to primary line of the element),
- Al 216.984 nm, 0.19% sensitivity,
- Fe 217.130 nm, 0.33% sensitivity.

While the Pb line exhibits the highest possible sensitivity for this element, which is crucial for its detection at trace levels, the secondary lines for Al and Fe are less sensitive. However, the reduced sensitivity of the Al and Fe lines corresponds to the generally high contents of Al and Fe in the samples. Because of the presence of two Al lines with significantly different sensitivities, they can be effectively employed to extend the working range of Al determination.

At the relatively low atomization temperatures during normal Pb measurement, neither Al nor Fe volatilizes. However, when an adequate atomization temperature is applied, all four lines become observable in the detection window. An illustrative spectrum obtained during the analysis of a digested lichen sample is presented in Fig. 2.

### 3.2. Developing a temperature program

The initial drying step was optimized through the observation of the process via the instrument's camera, ensuring smooth drying with no spattering. It is important to note that when adopting this method, the drying program might require optimization for different spectrometer models and specific instrument conditions, such as the flow rate of the protective gas.

In the simultaneous determination of elements in ETAAS, the pyrolysis temperature is limited by the most volatile element, while the atomization temperature is defined by the most refractory element to be determined (in this work, Pb and Al, respectively). Due to the Pd/Mg (NO<sub>3</sub>)<sub>2</sub> modifier, Pb remained stable up to 1300 °C during pyrolysis. However, as there was no significant nonspecific background absorbance from the matrix, a pyrolysis temperature of 900 °C was chosen.

An atomization temperature of 2500 °C was necessary to achieve a good peak profile for Al, the most refractory element analyzed. This temperature was slightly higher than optimal for Pb, leading to a decrease in the Pb signal (the integrated absorbance was lower by approximately 30%) mainly due to the rapid expansion of the atom cloud (see Fig. 3). Despite the sensitivity (defined as the slope of the calibration curve) might be affected for volatile elements during multielement analyses at high temperature, it is known that the resulting narrower peaks can partially compensate for this. Narrower peaks allow for a shorter integration time, leading to an improved signal-to-noise ratio [15]. To take advantage of this phenomenon, the Pb signal integration time was shortened to only the first 2 s of the atomization step. The resulting limit of quantification was sufficient with respect to the actual concentration in the real samples (see the next chapter).

Also, the simultaneous determination of elements with substantially different volatilities can be performed using multi-step atomization,

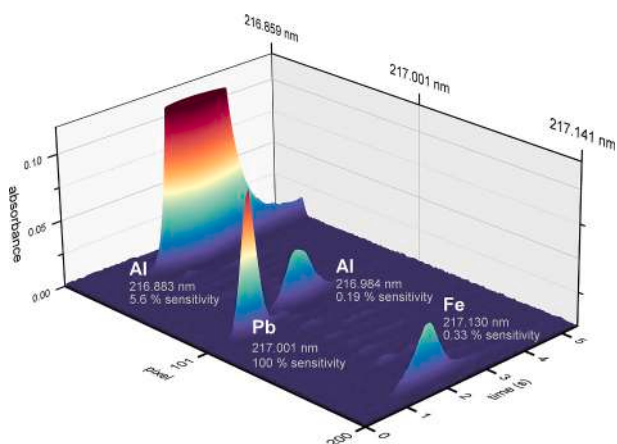


Fig. 2. Wavelength- and time-resolved absorption spectrum from the analysis of a lichen digest (Pb 20 µg/L, Al 7 mg/L, Fe 4 mg/L) using the proposed method. Wavelengths and relative sensitivities of the four monitored spectral lines are indicated.

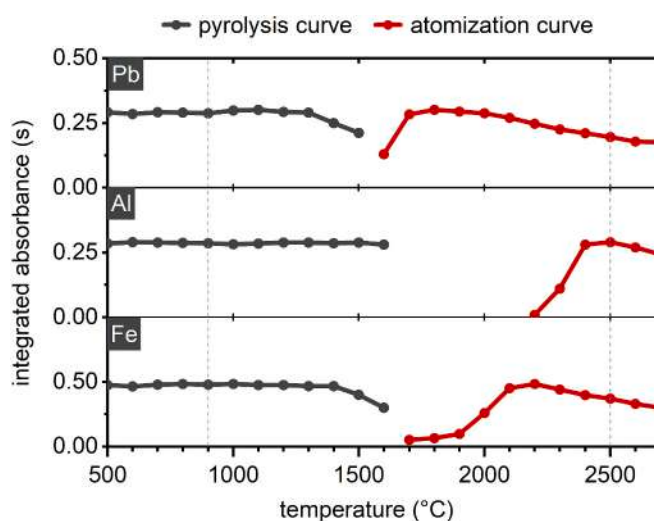


Fig. 3. Atomization and pyrolysis curves for Pb, Al, and Fe, obtained with a proposed method for a lichen sample digest.

leading to the atomization of each element under optimal conditions [22–24]. However, this approach was not feasible in this case. Our experiments revealed that separate Pb atomization resulted in a partial loss of Fe, as it becomes volatile at temperatures exceeding 1700 °C (as can be seen in Fig. 3):

### 3.3. Method performance and working range

Our goal was to develop a method that can be routinely used to analyze large sample sets without the need for repeated dilutions or manual recalculation of the results. To achieve a wide working range, calibration curves were constructed using a combination of signals from the two spectral lines (in the case of Al) and also the central and wing portions of the spectral lines, employing the WSA approach. As a result, a series of consecutive calibration curves was employed for each element, as illustrated in Fig. 4. The parameters of these curves are summarized in Table 2.

### 3.4. Lead

With the default setting, i.e. absorbance readings were obtained from the central pixel and the two adjacent pixels (CP ± 1), the calibration plot for the Pb\_a line exhibited linearity from the limit of quantification (LOQ) to 50 µg/L. For concentrations exceeding 50 µg/L, the WSA approach was employed, specifically by recording the signal from pixels 105 and 106, which lie at the wing of the Pb line. This approach yielded a second linear calibration function (the Pb\_b line), extending the dynamic range up to 500 µg/L.

### 3.5. Aluminum

Fig. 4 shows excellent linearity for the calibration plots of all three Al lines. The most sensitive Al line at 216.883 nm (Al\_a) is suitable for measuring concentrations from 0.02 to up to 5 mg/L, while the less sensitive line at 216.984 nm (Al\_b) provides a follow-up linear calibration line up to 100 mg/L. By employing the WSA approach, the working range of Al\_c is extended to up to 500 mg/L. This utilization of the available lines, with their sensitivities differing by a factor of approximately 30, expands the working range to more than four orders of magnitude. This wide working range was found to be necessary for directly analyzing the Al concentrations in the digests during the project.

On completion of the analysis, the control software reports values measured at each of the three lines (Al\_a, Al\_b, and Al\_c). However, the

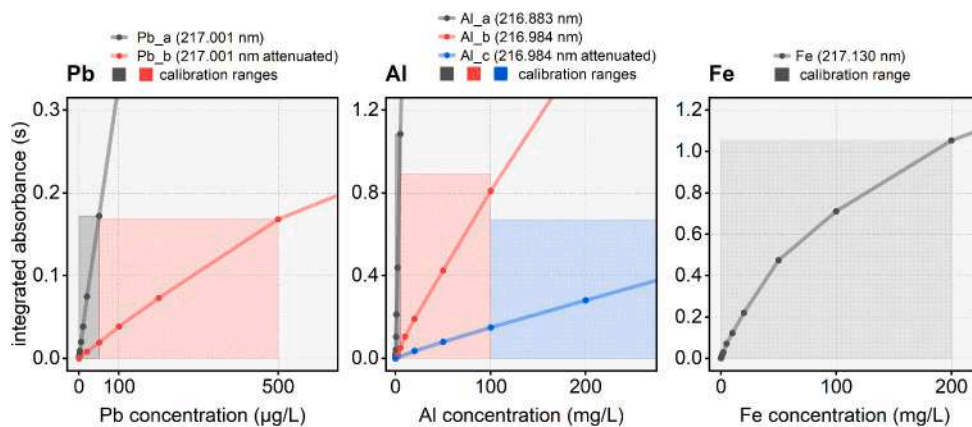


**Fig. 4.** Calibration plots for Pb, Al, and Fe. Aqueous calibration solutions matching the nitric acid content of the samples (3 mL concentrated HNO<sub>3</sub> in 10 mL final volume) were used to generate these plots using the proposed method. The individual calibration ranges are indicated.

**Table 2**

Analytical characteristics of the spectral lines investigated based on the detector pixels used and parameters of resulting calibration functions.

line (name)	wavelength (nm)	pixels	characteristic mass $m_0$ (ng)	LOD ( $\mu\text{g}/\text{L}$ ) <sup>a</sup>	LOQ ( $\mu\text{g}/\text{L}$ ) <sup>a</sup>	working range ( $\mu\text{g}/\text{L}$ )	calibration function	coefficient of determination $R^2$
Pb_a	217.001	100 + 101 + 102 (CP $\pm$ 1)	0.013	0.3	1	1–50	linear	0.9992
Pb_b	217.001	105 + 106 (attenuated <sup>b</sup> )	0.13	4	13	13–500	linear	0.9978
Al_a	216.883	21 + 22 + 23 (CP $\pm$ 1)	0.2	6	20	20–5000	linear	0.9999
Al_b	216.984	91 + 92 + 93 (CP $\pm$ 1)	5.4	600	2000	2000–100,000	linear	0.9982
Al_c	216.984	89 + 95 (attenuated <sup>b</sup> )	32	2000	7000	7000–500,000	linear	0.9992
Fe	217.130	191 + 192 + 193 (CP $\pm$ 1)	3–8	360	1200	1200–200,000	nonlinear rational	0.9989

<sup>a</sup> The limits of detection (LOD) and quantification (LOQ) were calculated as three and ten times the standard deviation of the blank solution (nitric acid diluted to the same extent as in the samples) measurement, divided by the slope of the calibration curve, respectively.

<sup>b</sup> attenuation of the signal involves using pixels further away from the peak maximum, measuring the absorbance at the wings of the analytical line.

software lacks the ability to automatically select the optimal line according to the linear ranges of the individual calibrations and the actual concentration of Al. To address this, a simple formula is applied during post-processing of the data in a spreadsheet application. This formula selects the line appropriate for the actual concentration, defined by the upper limits of the individual calibration ranges. The generalized formula is:

$$\text{Al} = \text{IF} (\text{Al}_a < 6000 \mu\text{g}/\text{L} \text{ THEN } \text{Al}_a; \\ \text{IF } \text{Al}_b < 100,000 \mu\text{g}/\text{L} \text{ THEN } \text{Al}_b; \\ \text{ELSE } \text{Al}_c)$$

In other words, the most sensitive line (Al<sub>a</sub>) is chosen if its measured value falls within its calibration range (i.e., below 6000  $\mu\text{g}/\text{L}$ ). If Al<sub>a</sub> exceeds its upper limit, the formula checks the less sensitive line (Al<sub>b</sub>) for saturation (below 100,000  $\mu\text{g}/\text{L}$ ). If both Al<sub>a</sub> and Al<sub>b</sub> exceed their upper limits, the least sensitive line (Al<sub>c</sub>) is chosen. This approach ensures that measurements stay within the reliable linear range of the chosen calibration curve.

Measuring Al concentrations as high as hundreds of milligrams per liter becomes possible and convenient using ETAAS. Although it may seem that aluminum concentrations higher than about 1 mg/L can be measured on flame AAS, such analysis requires a high-temperature acetylene/nitrous oxide flame not available in every laboratory equipped with AAS, and, more importantly, the information on its content is already accessible during Pb measurement with very little effort.

### 3.6. Iron

In contrast to Al, the calibration plot for Fe displayed significant non-

linearity across the tested concentration range. Linear dependence with an  $R^2$  exceeding 0.995 was only observed up to 10 mg/L. Neither using side pixels nor the central pixel alone resulted in a better linearity. Therefore, a non-linear calibration described by a rational function  $y = (a + bx)/(1 + cx)$  with a coefficient of determination of 0.9989 was employed (Table 2.)

Unusual behavior of Fe calibration plots for secondary Fe lines was already observed by Welz et al. [21], who reported a multi-slope response with distinct linear segments. However, a definitive conclusion regarding the presence or absence of these segments in our data might require a wider concentration range or additional investigation. Factors including the atomization temperature and instrumental parameters (e.g. instrument width  $\Delta\lambda_{\text{instr}}$  which was 1.4 pm per pixel in this case) and atomic line properties such as width and hyperfine structure can influence the calibration plot shape [17,25–27]. Further investigation with a wider concentration range or exploration of different instrumental settings could provide more insights into this aspect.

### 3.7. Carry-over effects

Carry-over (memory effect) was assessed by measuring blank samples directly following the highest calibration standard (500 mg/L for Al and Fe, 500  $\mu\text{g}/\text{L}$  for Pb). Our experiments exhibited minimal carryover for Al, Fe, and Pb. The first blank measurements showed memory effects of 1.5% for Al, 2.4% for Fe, and < 0.05% for Pb. The second blank measurement further reduced carryover to 0.5% for Al, 0.8% for Fe, and < 0.02% for Pb. If the samples to be analyzed are expected to vary

widely in concentrations, enabling “controlled cleaning” after high-concentration samples is recommended. Alternatively, prolonging the cleaning step might be considered.

### 3.8. Handling the spectral interferences

The spectral region around the Pb resonance line is significantly affected by absorption bands of phosphorus monoxide (PO) molecules, as shown in Fig. 5. These bands interfere with analytical lines, especially in samples with high levels of phosphorus. This interference was most pronounced in the samples of mushrooms, as it is known that they generally accumulate phosphorus in their bodies to a large extent [28]. To effectively minimize this interference, two complementary approaches were employed:

- The suppression of PO molecule formation by the addition of Pd/Mg (NO<sub>3</sub>)<sub>2</sub> modifier
- The correction of the structured background using least square background correction (LSBC)

The behavior of P in a graphite furnace has been extensively studied with HR-CS AAS in the last few decades. According to current knowledge, the balance between the atomization of P and its vaporization in the form of PO molecules is highly dependent on the addition of a modifier. Modifiers based on Pd, but also other metals such as Ir, W, and Ru, proved to favor the formation of atomic P instead of PO vaporization [29–32]. The relative intensity of PO bands is also highly dependent on the temperature of the atomizer [31]. However, it was not possible to separate PO molecules in the time-resolved spectra because they form at temperatures similar to the atomization temperatures of the analytes. Fig. 5 shows the spectrum of a mushroom sample affected by strong interference. Dosing 10  $\mu$ L of sample with 20  $\mu$ L of a Pd/Mg(NO<sub>3</sub>)<sub>2</sub> modifier reduced the interfering PO background by 50% compared to the addition of only 2  $\mu$ L of the modifier. Little difference was observed

between the addition of 2 and 5  $\mu$ L and, similarly, between 15 and 20  $\mu$ L. This indicates that the effective ratio between sample and modifier should be at least 1:1.5.

In most cases, the addition of 15  $\mu$ L of the modifier suppressed PO interferences effectively. As an additional step for samples exhibiting exceptionally high phosphorus content, like the one presented in Fig. 5, LSBC was employed. In such cases, the residual structured background was eliminated by subtracting the reference spectrum of a pure phosphate (Fig. 5b) from the samples signal through LSBC using instrument's software. The result was a clear, interference-free spectrum (the black line in Fig. 5c).

### 3.9. Trueness assessment using CRMs

The contents of elements determined in CRMs using the method's novel multi-line approach for an extended working range are listed in Table 3. Each value is labeled according to the used line. The concentrations of all samples, including CRMs, were determined against standard solutions with an HNO<sub>3</sub> content matching that used for sample preparation.

For Pb, the determined contents in CRMs exhibited a slight negative bias compared to the certified values (bias ranging from –11 to –7%). This might be attributed to incomplete digestion of silicate matrices when hydrofluoric acid was omitted, resulting in a small non-dissolved residue. Conversely, digestion with a mixture of HNO<sub>3</sub> and HF led to a complete digestion with no observable residue. In this case, the bias for Pb, Al, and Fe improved, ranging from –5 to +7%, 8 to 12%, and –4 to +5%, respectively.

However, even when HNO<sub>3</sub> alone was used, no significant difference was detected between the measured contents of the elements and their certified values according to Student's *t*-test at a 95% confidence interval. Therefore, the method demonstrated the capacity to provide true results for complex matrices, as evidenced by the good agreement between the measured and certified element contents in various CRMs.

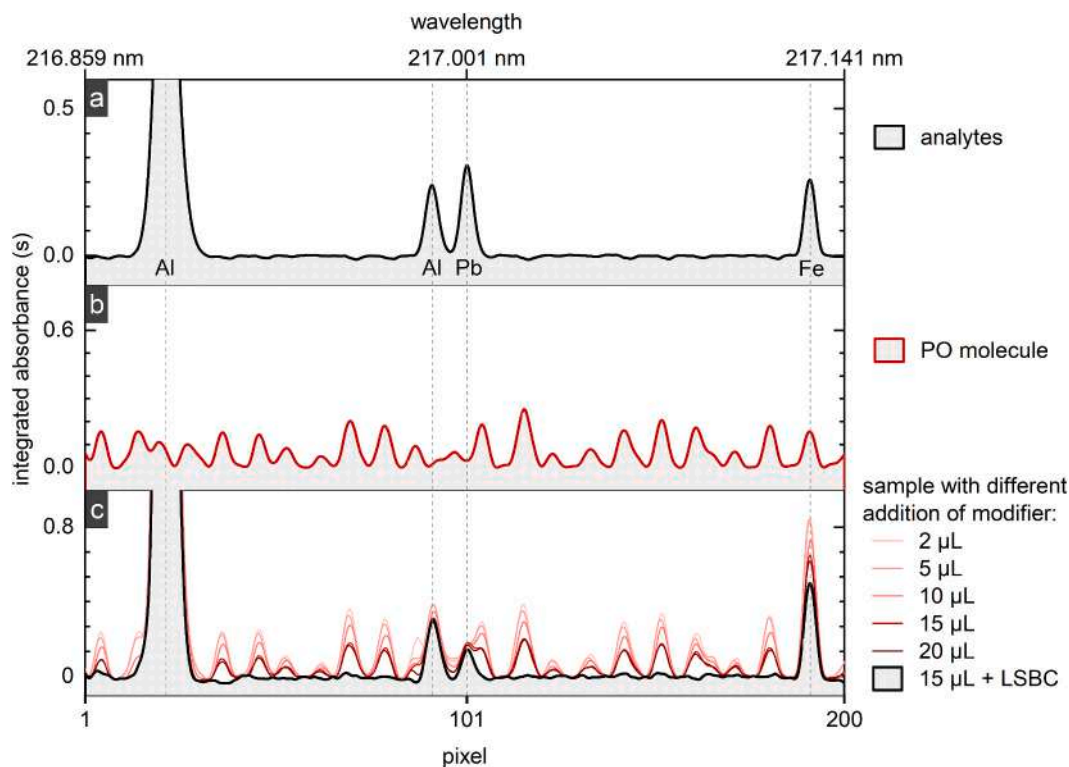


Fig. 5. Wavelength-resolved spectra obtained by measuring a) a simple solution of the analytes, b) ammonium phosphate solution (reference spectrum of PO molecules), and, c) a mushroom sample with strong interference arising from PO molecules, with different additions of Pd/Mg(NO<sub>3</sub>)<sub>2</sub> modifier and correction using LSBC.

**Table 3**

Determined levels of Pb, Al, and Fe in certified reference materials. Values are expressed as mean  $\pm$  standard deviation (mg/kg dry weight,  $n = 3$ ) and bias (percentual difference between found and certified value).

element	value	reference material			
		BCR-482 Lichen	INCT-TL-1 Tea leaves	NIST 1570a Spinach leaves	AN-BM02 Green tea
Pb	certified	40.9 $\pm$ 1.4	1.78 $\pm$ 0.24	0.2 <sup>a</sup>	1.54 $\pm$ 0.09
	HNO <sub>3</sub> digestion	37.9 $\pm$ 1.0 <sup>c</sup> (-7%)	1.59 $\pm$ 0.2 <sup>b</sup> (-11%)	0.19 $\pm$ 0.01 <sup>b</sup> (-5%)	1.43 $\pm$ 0.1 <sup>b</sup> (-7%)
	HNO <sub>3</sub> /HF digestion	38.9 $\pm$ 3.5 <sup>c</sup> (-5%)	1.80 $\pm$ 0.1 <sup>b</sup> (1%)	0.21 $\pm$ 0.02 <sup>b</sup> (7%)	1.51 $\pm$ 0.1 <sup>b</sup> (-2%)
Al	certified	1103 $\pm$ 24	2290 $\pm$ 280	310 $\pm$ 15	1700 $\pm$ 60
	HNO <sub>3</sub> digestion	1060 $\pm$ 90 <sup>e</sup> (-4%)	2160 $\pm$ 220 <sup>e</sup> (-6%)	278 $\pm$ 14 <sup>d</sup> (-10%)	1760 $\pm$ 100 <sup>c</sup> (4%)
	HNO <sub>3</sub> /HF digestion	1105 $\pm$ 69 <sup>e</sup> (0%)	2288 $\pm$ 227 <sup>e</sup> (0%)	323 $\pm$ 25 <sup>d</sup> (4%)	1573 $\pm$ 135 <sup>e</sup> (-8%)
Fe	certified	804 $\pm$ 160 <sup>a</sup>	432 <sup>a</sup>	-	216 $\pm$ 15
	HNO <sub>3</sub> digestion	777 $\pm$ 32 (-3%)	479 $\pm$ 27 (11%)	245 $\pm$ 13	220 $\pm$ 21 (2%)
	HNO <sub>3</sub> /HF digestion	799 $\pm$ 73 (2%)	414 $\pm$ 41 (-4%)	263 $\pm$ 14	227 $\pm$ 19 (5%)

<sup>a</sup> indicative values <sup>b, c, d, e</sup> determined using lines: b) Pb<sub>a</sub>; c) Pb<sub>b</sub>; d) Al<sub>a</sub>; e) Al<sub>b</sub>.

### 3.10. Pb, Al, and Fe in terrestrial Antarctic flora of Nelson Island

The contents of investigated elements in the samples of Antarctic flora are summarized in Fig. 6. In terms of Pb median contents in mg/kg, groups were sorted as follows: grass (0.34) > moss (0.28) > lichens (0.19) > mushrooms (0.13). The highest content of Pb was, however, observed in a sample of moss (1.5 mg/kg) and mosses as a group contained significantly more Pb than lichens and mushrooms (Mann-Whitney test,  $p < 0.001$ ).

Whilst the Pb content in mosses is consistent with data from similar studies conducted in non-polluted areas across the Antarctic (Table 4), levels found in the lichens on Nelson Island are among the lowest ever reported in the Antarctic. Historically, the sampling area on Nelson Island has experienced very little local pollution, as there is only a small human presence due to the lack of large-scale research facilities. As a result, these values may indicate the relative background level in this region.

Lead contents in *U. antarctica* (median 0.199 mg Pb/kg) and *U. aurantiaco-atra* (median 0.183 mg Pb/kg) were statistically similar

(according to Mann-Whitney test). The similarity of both lichen species in terms of metal accumulation patterns has already been observed [33]. The four samples of the lichen *Ramalina terebrata*, on the other hand, exhibited a median value of 0.086 mg Pb/kg, which is significantly less than the two *Usnea* species. *R. terebrata* was found only at a few sites adjacent to the sea, heavily exposed to sea spray.

Some of the first data on Pb in *U. antarctica* were reported back in 1991 from King George Island, South Shetland Islands. In the study, using the PIXE technique, the authors observed Pb levels in lichens growing in the vicinity of Arctowski Station to be as high as 12 mg/kg, while only 2 mg/kg were detected in areas further away from the station [34]. Although analytical methods have evolved substantially since these pioneer studies were published (e.g. recent studies have shown ICP-MS to be the analytical method of choice), recently published values have remained consistent. Levels of Pb reported for *U. aurantiaco-atra* growing in the vicinity of the nearby Korean research station at King George Island were up to 8.36 mg/kg (even 13 mg/kg observed in a single thalli), while lichens growing at least 1 km from the station contained only ca. 1 mg/kg, indicating local anthropogenic pollution [35].

A recent study at background sites on King George Island reported Pb contents in the lichens *U. aurantiaco-atra* and *U. antarctica* of 0.51  $\pm$  0.25 and 0.27  $\pm$  0.11 mg/kg (mean  $\pm$  SD), respectively, which are only slightly higher than our means for the same lichens (0.23  $\pm$  0.1 and 0.24  $\pm$  0.1 mg/kg, respectively). The study reported Pb contents in *Deschampsia antarctica* grass of 0.79  $\pm$  0.47 mg/kg, exceeding our mean value of 0.43  $\pm$  0.4 mg/kg. However, the limited number of samples analyzed in that study (2 and 3 samples of the respective lichens and 3 samples of grass), limits the representativeness of its findings.

In contrast to the gradually expanding knowledge on the elemental composition of cryptogams at various sites across the Antarctic, little data has been reported on the composition of Antarctic mushrooms. Although there is a sparsity of macrofungi in the Antarctic, observations on them have been steadily increasing in recent decades [36]. It is also expected that increasing temperatures together with more intense human activity will allow further colonization of the Antarctic by more fungal populations [37,38]. However, no data is yet available on their elemental composition. Similarly, only very limited data is available on the elemental composition of vascular plants, with the hair grass *Deschampsia antarctica* being one of only two native species [38–41]. Such a scarcity of comparative values makes it difficult to assess the current burden on the Antarctic ecosystem.

Regarding the Al and Fe contents in the samples, both elements correlated tightly (Pearson's  $r = 0.97$ ,  $p < 0.001$ ). Such strong correlation between Al and Fe, along with other lithophile elements, has been documented in some previous studies (e.g. [35,42,43] listed in Table 4). This finding aligns with the fact that both elements are non-mobile, originating mainly from local bedrock weathering instead of human

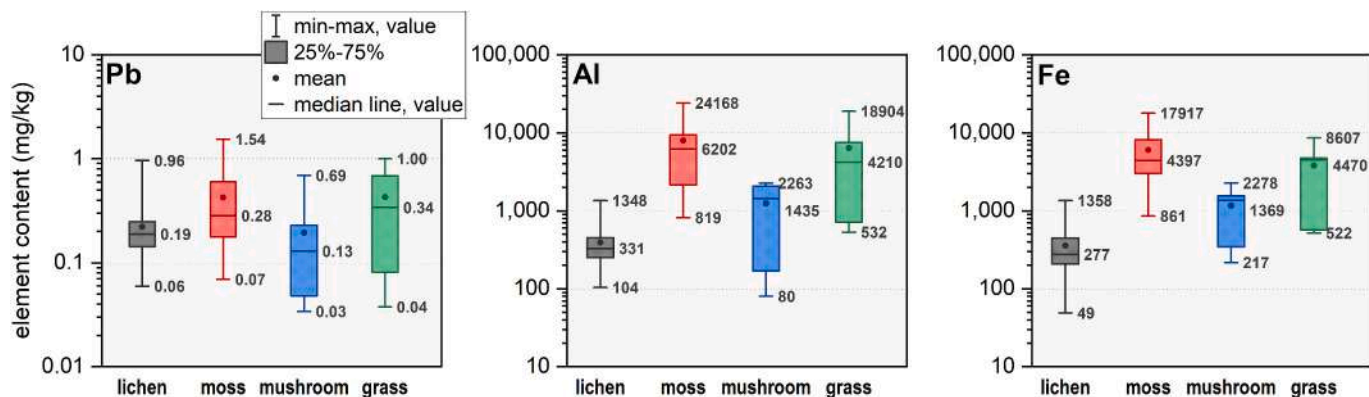


Fig. 6. Boxplots summarizing the contents of Pb, Al, and Fe in lichens, mosses, mushrooms, and grass (mg/kg dry weight). Median, minimum, and maximum values are given (note the logarithmic scale).

Table 4

Selected references for the studied elements across the Antarctic (expressed on a dry mass basis, chronological order).

Study site	Plant material	Pb (mg/kg)	Al (mg/kg)	Fe (mg/kg)	Analytical method	Reference
King George Island, South Shetland Islands	lichens <i>U. antarctica</i>	2–12	–	170–414	PIXE	[34]
25 de Mayo Island, South Shetland Islands	lichens ( <i>U. antarctica</i> and <i>U. aurantiaco-atra</i> )	<LOD–2.76	–	263–1365	FAAS	[33]
Edmonson point, Victoria Land	moss ( <i>Pottia heimii</i> , <i>B. argenteum</i> , <i>B. pseudotriquetrum</i> and <i>Ceratodon purpureus</i> )	0.3–1.4	1700–3700	3500–7100	ETAAS, ICP-OES	[44]
King George Island, South Shetland Islands	lichen ( <i>Usnea</i> spp.)	–	–	139	FAAS	[40]
	moss ( <i>Bryum</i> spp. and <i>Polytrichum</i> spp.)	–	–	3040–4348		
	grass ( <i>Deshampsia antarctica</i> )	–	–	610		
King George Island, South Shetland Islands	lichens ( <i>U. aurantiaco-atra</i> )	0.77–8.36	182–426	273–490	ICP-MS	[35]
King George Island, South Shetland Islands	lichens (various species)	ca. 0.4 <sup>a</sup>	–	ca. 550 <sup>a</sup>	FAAS, ETAAS	[45]
	moss (various species)	ca. 2.8 <sup>a</sup>	–	ca. 3750 <sup>a</sup>		
	grass ( <i>D. antarctica</i> and <i>C. quitensis</i> )	ca. 2.4 <sup>a</sup>	–	ca. 2600 <sup>a</sup>		
James Ross Island, Brandy Bay, the northern Antarctic Peninsula	lichens ( <i>U. antarctica</i> )	0.9–3	1800–6400	–	ICP-MS	[42]
Terra Nova Bay	moss (unspecified)	0.12–1.4	–	2480–13,400	ICP-MS, ICP-OES	[46]
James Ross Island, Solorina Valley, the northern Antarctic Peninsula	lichens ( <i>U. antarctica</i> )	0.99–2.51	–	–	ETAAS	[5]
Larseman Hills, East Antarctica	lichens (foliose <i>Umbilicaria</i> sp. and crustose <i>Buellia</i> sp.)	0.28–1.9	400–10,800	300–18,700	ICP-MS, ICP-OES	[43]
	moss (different genera)	0.65–1.49	1800–11,600	2900–13,800		
King George Island, South Shetland Islands	lichens:	a) 0.51 ± 0.25	a) 373 ± 191	a) 395 ± 226	ICP-MS	[41]
	a) <i>U. aurantiaco-atra</i> ,	b) 0.27 ± 0.11	b) 630 ± 355	b) 739 ± 500		
	b) <i>U. antarctica</i>					
	Moss ( <i>Ceratodon purpureus</i> , <i>Politrchastrum alpinum</i> , <i>Schistidium antarctici</i> )	0.41–0.84	2903–10,310	2140–8165		
	Grass ( <i>D. antarctica</i> )	0.79 ± 0.47	8625 ± 7174	9618 ± 7818		
Nelson Island, South Shetland Islands	lichens	0.06–0.96	104–1348	49–1358	HR-CS ETAAS	this study
	moss	0.07–1.54	819–24,168	861–17,917		
	mushroom	0.03–0.69	80–2263	217–2278		
	grass	0.04–1.00	532–18,904	522–8607		

<sup>a</sup> the values were retrieved from the graph.

activities, and thus, they both often serve as reference elements for, for example, enrichment factor calculations in ecological studies. Both elements were least abundant in the lichen samples, indicating low contents of captured mineral particles such as soil and dust in the thalli. Their highest content, in contrast, was observed in moss, likely due to its complex three-dimensional structure, which is prone to entrapping dust and soil particles. This is consistent with studies which analyzed both fruticose lichens and mosses (i.e. [40,41]), and also apparent from comparison with other reported data listed in Table 4. This highlights the significance of proper sample cleaning procedures to differentiate between element uptake by the organism and captured exogenous material accumulated on the upper surface of the thallus. Most listed studies (including this one) removed excess soil particles using tweezers and/or washing with deionized water. Nevertheless, according to the presence of undissolved residue in some digests of moss and grass, even a careful cleaning procedure may not be sufficient to remove all mineral particles. Thus, also in the grass, the Al and Fe contents displayed a wide range, similar to the values recently reported from King George Island [41]. Similarly, within the grass samples, both elements exhibited a strong positive correlation (Pearson's correlation coefficient = 0.95,  $p$ -value < 0.05). This finding may suggest a similar uptake mechanism, despite the known differences in mineral acquisition strategy among these organisms. Lichens and mosses primarily rely on passive methods like surface absorption and dust capture, while grasses have a well-developed root system for active nutrient uptake. Mushrooms often benefit from mycorrhizal associations with plant roots. However, the current lack of data on the elemental composition of Antarctic mushrooms hinders a comprehensive understanding of the element accumulation patterns in these representatives of Antarctic flora and their potential as biomonitors of environmental conditions.

### 3.11. Enrichment of Pb in the flora

To evaluate the enrichment of Pb in the samples, the enrichment factor for Pb ( $EF_{Pb}$ ) was calculated according to the method described by [47]. The formula is  $EF_{Pb} = (C_{Pb}/C_{Al})_{sample}/(C_{Pb}/C_{Al})_{background}$ , where  $C_{Pb}$  represents the content of Pb and  $C_{Al}$  represents the content of the reference element in the sample and in the background. Both Al and Fe are commonly used as reference elements for normalizing pollutant contents and enrichment. As the contents of the two metals correlated closely, so did the corresponding enrichment factors calculated on the basis of either Al or Fe as the reference elements (Pearson correlation coefficient 0.9 with  $p$ -value < 0.05). Eventually, Al was chosen, as it has often been suggested as a suitable reference element in studying cryptogams such as lichens and mosses [47–49]. As its background level, the average concentration in the Earth's crust was obtained from the work of Yaroshevsky [50].

The medians of  $EF_{Pb}$  were as follows: lichens 2.8 > mushrooms 0.5 > grass 0.4 > moss 0.3.

According to EF categories, lichens exhibited only minor enrichment while mushrooms, grass and moss exhibited no enrichment [49]. It is important to acknowledge the limitations of EFs, with one of the most significant being the difficulty of completely removing trapped mineral particles from samples. As a consequence, the presence of more soil or dust particles in the samples tends to decrease EF values [51]. This is probably the reason for the lower  $EF_{Pb}$  observed for mosses than for lichens.

Despite their limitations, EFs for Pb still provide some valuable insights: given the relative ease of obtaining clean lichen together with their ability to accumulate airborne contaminants, lichens present a suitable material for bioindicative purposes, owing to their relatively

high and consistent Pb–Al ratio, particularly evident for the dominant lichen species, *U. antarctica* and *U. aurantiaco-atra*.

#### 4. Conclusion

We present here a novel analytical method based on HR-CS ETAAS suitable for assessing the Pb contamination of plant material. The co-determination of Al and Fe as reference elements allows for the calculation of ecological risk indices. The method utilizes the highly-sensitive resonance Pb line at 217.001 nm, ensuring detection of the typically trace levels of this contaminant in environmental samples. Importantly, it also achieves a wide working range (e.g., four orders of magnitude for Al), eliminating the need for sample re-dilution and re-measurement for environmental samples with varying metal contents. Broadening of the working range was achieved by combining the use of spectral lines with different sensitivities and also by measuring absorbance at multiple points within each spectral line. This is a significant advantage considering the traditionally limited dynamic range of AAS compared to techniques like ICP-MS or ICP-OES. While developed for the analysis of Antarctic terrestrial flora, the method is generally applicable to environmental research studies involving various sample types.

Using the method, a large set of Antarctic floral samples, including lichens, mosses, mushrooms, and grass, was analyzed. In fact, the achieved working range proved necessary for analyzing these diverse samples without dilution steps. This also translates into less time required for operator intervention during analysis. According to the results, relatively low Pb contamination of the Nelson Island ecosystem was observed compared to data reported from the region. On the basis of enrichment factors, the analyzed fruticose lichens such as *U. antarctica* and *U. aurantiaco-atra* provide the most relevant information on the degree of contamination. In contrast, the other popular bioindicators, mosses, appear to be more influenced by trapped dust due to their structure. Apart from lichens and mosses, samples of substantially less-studied Antarctic mushrooms and grass were also subjected to the same analysis. In fact, the analysis of mushrooms presented the most significant challenge due to interference arising from their high phosphorus contents. However, using a combination of an excess of modifier and the LSBC model, the interference was suppressed, allowing data on Pb contents in these species to be reported for the first time.

Advanced methods, such as the one presented here, not only broaden the variety of routine techniques applicable for specific purposes, but also emphasize the demand for HR-CS AAS to develop into a truly multi-elemental technique. The successful application of multiple spectral lines for single element calibration demonstrates a promising approach for extending the dynamic range of both existing and also future AAS instruments that will be capable of wider spectral region monitoring.

#### CRedit authorship contribution statement

**Ondřej Zvěřina:** Writing – original draft, Visualization, Supervision, Investigation, Formal analysis, Data curation, Conceptualization. **Lenka Brůhová:** Investigation. **Pavel Coufalík:** Writing – original draft, Methodology, Investigation. **Christopher D. Stringer:** Writing – original draft, Investigation. **Jaqueline Rieger:** Investigation. **Walter Goessler:** Writing – original draft, Supervision.

#### Declaration of competing interest

The authors declare that they have no known competing financial interests or personal relationships that could have appeared to influence the work reported in this paper.

#### Data availability

Data will be made available on request.

#### Acknowledgement

This work was supported by funding from AKTION Austria–Czech Republic, project 96p6. The authors are also grateful for the support of Masaryk University (projects MUNI/A/2022/1366 and MUNI/A/1623/2023). The involvement of PC was funded by the Institute of Analytical Chemistry of the CAS under the Institutional Research Plan VOK: 68081715. CDS was in receipt of a PhD studentship from the Leeds-York-Hull Natural Environment Research Council (NERC) Doctoral Training Partnership (DTP) Panorama [NE/S007458/1]. Fieldwork was supported by the Czech Antarctic Foundation.

#### References

- [1] R. Bargagli, Environmental contamination in Antarctic ecosystems, *Sci. Total Environ.* 400 (2008) 212–226.
- [2] J.R. McConnell, O.J. Maselli, M. Sigl, P. Valielonga, T. Neumann, H. Anshütz, R. C. Bales, M.A.J. Curran, S.B. Das, R. Edwards, S. Kipfstuhl, L. Layman, E. R. Thomas, Antarctic-wide array of high-resolution ice core records reveals pervasive lead pollution began in 1889 and persists today, *Sci. Rep.* 4 (2014) 5848.
- [3] W.-L. Chu, N.-L. Dang, Y.-Y. Kok, K.-S. Ivan Yap, S.-M. Phang, P. Convey, Heavy metal pollution in Antarctica and its potential impacts on algae, *Polar Sci.* 20 (2019) 75–83.
- [4] R. Bargagli, E. Rota, Environmental contamination and climate change in Antarctic ecosystems: an updated overview, *environmental science, Advances* 3 (2024) 543–560.
- [5] O. Zvěřina, P. Coufalík, M. Barták, M. Petrov, J. Komárek, The contents and distributions of cadmium, mercury, and lead in *Usnea antarctica* lichens from Solorina Valley, James Ross island (Antarctica), *Environ. Monit. Assess.* 190 (2018), <https://doi.org/10.1007/s10661-017-6397-1>.
- [6] M. Hossain, D. Karmakar, S.N. Begum, S.Y. Ali, P.K. Patra, Recent trends in the analysis of trace elements in the field of environmental research: a review, *Microchem. J.* 165 (2021) 106086.
- [7] N. Ozbek, Simultaneous determination of co, Fe, Ni and K with HR CS GFAAS, *Microchem. J.* 145 (2019) 1066–1069.
- [8] M. Resano, E. Bolea-Fernández, E. Mozas, M.R. Flórez, P. Grinberg, R.E. Sturgeon, Simultaneous determination of co, Fe, Ni and Pb in carbon nanotubes by means of solid sampling high-resolution continuum source graphite furnace atomic absorption spectrometry, *J. Anal. At. Spectrom.* 28 (2013) 657–665.
- [9] F. Rovasi Adolfo, P. Cícero do Nascimento, L. Brudi, D. Bohrer, L. Machado de Carvalho, Simultaneous determination of Ba, Co, Fe, and Ni in nuts by high-resolution continuum source atomic absorption spectrometry after extraction induced by solid-oil-water emulsion breaking, *Food Chem.* 345 (2021) 128766.
- [10] I.N. Pasiyas, N.I. Rousis, A.K. Psoma, N.S. Thomaidis, Simultaneous or sequential multi-element graphite furnace atomic absorption spectrometry techniques: advances within the last 20 years, *At. Spectrosc.* 42 (6) (2021), <https://doi.org/10.46770/AS.202.707>.
- [11] M. Resano, L. Rello, M. Flórez, M.A. Belarra, On the possibilities of high-resolution continuum source graphite furnace atomic absorption spectrometry for the simultaneous or sequential monitoring of multiple atomic lines, *Spectrochim. Acta part B, At. Spectrosc.* 66 (2011) 321–328.
- [12] M. Resano, M.R. Flórez, E. García-Ruiz, High-resolution continuum source atomic absorption spectrometry for the simultaneous or sequential monitoring of multiple lines. A critical review of current possibilities, *Spectrochim. Acta part B, At. Spectrosc.* 88 (2013) 85–97.
- [13] A.C.M. Aleluia, F.A. de Santana, G.C. Brandao, S.L.C. Ferreira, Sequential determination of cadmium and lead in organic pharmaceutical formulations using high-resolution continuum source graphite furnace atomic absorption spectrometry, *Microchem. J.* 130 (2017) 157–161.
- [14] J.S. Almeida, O.C.C.O. Souza, L.S.G. Teixeira, Determination of Pb, Cu and Fe in ethanol fuel samples by high-resolution continuum source electrothermal atomic absorption spectrometry by exploring a combination of sequential and simultaneous strategies, *Microchem. J.* 137 (2018) 22–26.
- [15] G. Schlemmer, B. Radziuk, B. Verlag, O.G. Schlemmer, O.B. Radziuk, *Analytical Graphite Furnace Atomic Absorption Spectrometry a Laboratory Guide*, Birkhäuser Verlag, 1999.
- [16] B. Gómez-Nieto, M.J. Gismera, M.T. Sevilla, J.R. Procopio, Fast sequential multi-element determination of major and minor elements in environmental samples and drinking waters by high-resolution continuum source flame atomic absorption spectrometry, *Anal. Chim. Acta* 854 (2015) 13–19.
- [17] U. Heitmann, B. Welz, D.L.G. Borges, F.G. Lepri, Feasibility of peak volume, side pixel and multiple peak registration in high-resolution continuum source atomic absorption spectrometry, *Spectrochim. Acta part B At. Spectrosc.* 62 (2007) 1222–1230.
- [18] L. Fernández-López, B. Gómez-Nieto, M.J. Gismera, M.T. Sevilla, J.R. Procopio, Direct determination of copper and zinc in alcoholic and non-alcoholic drinks using high-resolution continuum source flame atomic absorption spectrometry and internal standardization, *Spectrochim. Acta part B, At. Spectrosc.* 147 (2018) 21–27.
- [19] S. Hesse, T. Ristau, J.W. Einax, Chemical vapor generation by coupling high-pressure liquid flow injection to high-resolution continuum source hydride

- generation atomic absorption spectrometry for determination of arsenic, *Microchem. J.* 123 (2015) 42–50.
- [20] M.A. Bechlin, F.M. Fortunato, R.M. da Silva, E.C. Ferreira, J.A. Gomes Neto, A simple and fast method for assessment of the nitrogen–phosphorus–potassium rating of fertilizers using high-resolution continuum source atomic and molecular absorption spectrometry, *Spectrochim. Acta part B At. Spectrosc.* 101 (2014) 240–244.
- [21] B. Welz, L.M.G. dos Santos, R.G.O. Araujo, S.C. do Jacob, M.G.R. Vale, M. Okrus, H. Becker-Ross, Unusual calibration curves observed for iron using high-resolution continuum source graphite furnace atomic absorption spectrometry, *Spectrochim. Acta part B At. Spectrosc.* 65 (2010) 258–262.
- [22] O. Zvěřina, J. Kuta, P. Coufalík, P. Kosečková, J. Komárek, Simultaneous determination of cadmium and iron in different kinds of cereal flakes using high-resolution continuum source atomic absorption spectrometry, *Food Chem.* 298 (2019) 125084.
- [23] L.M.G. dos Santos, B. Welz, R.G.O. Araujo, S. do C. Jacob, M.G.R. Vale, A. Martens, I.B. Gonzaga Martens, H. Becker-Ross, Simultaneous determination of Cd and Fe in beans and soil of different regions of Brazil using high-resolution continuum source graphite furnace atomic absorption spectrometry and direct solid sampling, *J. Agric. Food Chem.* 57 (2009) 10089–10094.
- [24] M. Resano, E. García-Ruiz, High-resolution continuum source graphite furnace atomic absorption spectrometry: is it as good as it sounds? A critical review, *Anal. Bioanal. Chem.* 399 (2011) 323–330, <https://doi.org/10.1007/s00216-010-4105-x>.
- [25] D.N. Wichems, R.E. Fields, J.M. Harnly, Characterization of hyperbolic calibration curves for continuum source atomic absorption spectrometry with array detection, *J. Anal. At. Spectrom.* 13 (1998) 1277–1284.
- [26] B. Welz, H. Becker-Ross, S. Florek, U. Heitmann, High-Resolution Continuum Source AAS: The Better Way to Do Atomic Absorption Spectrometry, John Wiley & Sons, Weinheim; [Great Britain], 2005.
- [27] Z. Kowalewska, J. Pilarczyk, L. Gościński, Spectral aspects of the determination of Si in organic and aqueous solutions using high-resolution continuum source or line source flame atomic absorption spectrometry, *Spectrochim. Acta part B At. Spectrosc.* 120 (2016) 45–56.
- [28] P. Kalač, Chemical composition and nutritional value of European species of wild growing mushrooms: a review, *Food Chem.* 113 (2009) 9–16.
- [29] F.G. Lepri, M.B. Dessuy, M.G.R. Vale, D.L.G. Borges, B. Welz, U. Heitmann, Investigation of chemical modifiers for phosphorus in a graphite furnace using high-resolution continuum source atomic absorption spectrometry, *Spectrochim. Acta part B At. Spectrosc.* 61 (2006) 934–944.
- [30] L.C. Pomaroli, M.A.M.S. da Veiga, M. Resano, F.V. Nakadi, Understanding polyatomic interference in the determination of phosphorus via PO molecules using high-resolution continuum source graphite furnace molecular absorption spectrometry with direct solid analysis, *J. Anal. At. Spectrom.* 35 (2020) 2305–2314.
- [31] M. Resano, J. Briceño, M.A. Belarra, Direct determination of phosphorus in biological samples using a solid sampling-high resolution-continuum source electrothermal spectrometer: comparison of atomic and molecular absorption spectrometry, *J. Anal. At. Spectrom.* 24 (2009) 1343.
- [32] R.C. de Campos, C.L.T. Correia, F. Vieira, T.D. Saint’Pierre, A.C. Oliveira, R. Gonçalves, Direct determination of P in biodiesel by high-resolution continuum source graphite furnace atomic absorption spectrometry, *Spectrochim. Acta part B, At. Spectrosc.* 66 (2011) 352–355.
- [33] A. Poble, S. Andrade, M. Scagliola, C. Vodopivec, A. Curtosi, A. Pucci, J. Marcovecchio, The use of epilithic Antarctic lichens (*Usnea aurantiacoatra* and *U. Antarctica*) to determine deposition patterns of heavy metals in the Shetland Islands, Antarctica, *Sci. Total Environ.* 207 (1997) 187–194.
- [34] M. Olech, Preliminary observations on the content of heavy metals in thalli of *Usnea antarctica* Du Rietz (Lichenes) in the vicinity of the H Arctowski, Polish Antarctic Station, *Polish Polar Reports* 12 (1991) 129–131.
- [35] H.S. Lim, M.J. Han, D.C. Seo, J.H. Kim, J.I. Lee, H. Park, J.-S. Hur, Y.H. Cheong, J. S. Heo, H.I. Yoon, J.-S. Cho, Heavy metal concentrations in the fruticose lichen *usnea aurantiacoatra* from King George Island, South Shetland Islands, West Antarctica, *Hanguk Ungyong Saengmyong Hwahakhoe Chi* 52 (2009) 503–508.
- [36] G. Palfner, J. Binimelis-Salazar, S.T. Alarcón, G. Torres-Mellado, G. Gallegos, F. Pea-Cortés, A. Casanova-Katny, Do new records of macrofungi indicate warming of their habitats in terrestrial Antarctic ecosystems? *Czech Polar Rep.* 10 (2020) 281–296.
- [37] P.D. Bridge, B.M. Spooner, Non-lichenized Antarctic fungi: transient visitors or members of a cryptic ecosystem? *Fungal Ecol.* 5 (2012) 381–394.
- [38] J. Singh, R.P. Singh, R. Khare, Influence of climate change on Antarctic flora, *Polar Sci.* 18 (2018) 94–101.
- [39] J. Tapia, M. Molina-Montenegro, C. Sandoval, N. Rivas, J. Espinoza, S. Basualto, P. Fierro, L. Vargas-Chacoff, Human activity in Antarctica: effects on metallic trace elements (MTEs) in plants and soils, *Plants* 10 (2021), <https://doi.org/10.3390/plants10122593>.
- [40] I.R. dos Santos, E.V. Silva-Filho, C. Schaefer, S. Maria Sella, C.A. Silva, V. Gomes, M.J.A.C.R. de Passos, P. Van Ngan, Baseline mercury and zinc concentrations in terrestrial and coastal organisms of Admiralty Bay, Antarctica, *Environ. Pollut.* 140 (2006) 304–311.
- [41] A.R. Reindl, L. Wolska, A.I. Piotrowicz-Cieślak, D. Saniewska, J. Bołatek, M. Saniewski, The impact of global climate changes on trace and rare earth elements mobilization in emerging periglacial terrains: insights from western shore of Admiralty Bay (King George Island, Antarctic), *Sci. Total Environ.* 926 (2024) 171540.
- [42] O. Zvěřina, K. Láska, R. Červenka, J. Kuta, P. Coufalík, J. Komárek, Analysis of mercury and other heavy metals accumulated in lichen *Usnea antarctica* from James Ross island, Antarctica, *Environ. Monit. Assess.* 186 (2014) 9089–9100.
- [43] S. Bhakta, T.K. Rout, D. Karmakar, C. Pawar, P.K. Padhy, Trace elements and their potential risk assessment on polar ecosystem of Larsemann Hills, East Antarctica, *Polar Sci.* 31 (2022) 100788.
- [44] R. Bargagli, J.C. Sanchez-Hernandez, L. Martella, F. Monaci, Mercury, cadmium and lead accumulation in Antarctic mosses growing along nutrient and moisture gradients, *Polar Biol.* 19 (1998) 316–322.
- [45] B. Wojtuń, K. Kolon, A. Samecka-Cymerman, M. Jasion, A.J. Kempers, A survey of metal concentrations in higher plants, mosses, and lichens collected on King George Island in 1988, *Polar Biol.* 36 (2013) 913–918.
- [46] I. Zelano, M. Malandrino, A. Giacomino, S. Buoso, E. Conca, Y. Sivry, M. Benedetti, O. Abollino, Element variability in lacustrine systems of Terra Nova Bay (Antarctica) and concentration evolution in surface waters, *Chemosphere* 180 (2017) 343–355.
- [47] R. Bargagli, The elemental composition of vegetation and the possible incidence of soil contamination of samples, *Sci. Total Environ.* 176 (1995) 121–128.
- [48] L. Gandois, Y. Agnan, S. Leblond, N. Séjalon-Delmas, G. Le Roux, A. Probst, Use of geochemical signatures, including rare earth elements, in mosses and lichens to assess spatial integration and the influence of forest environment, *Atmos. Environ.* 95 (2014) 96–104.
- [49] M. Aničić Urošević, G. Vuković, P. Vasić, T. Jakšić, D. Nikolić, S. Škrivanj, A. Popović, Environmental implication indices from elemental characterisations of collocated topsoil and moss samples, *Ecol. Indic.* 90 (2018) 529–539.
- [50] A.A. Yaroshovsky, Abundances of chemical elements in the Earth’s crust, *Geochem. Int.* 44 (2006) 48–55.
- [51] C. Reimann, P. de Caritat, Intrinsic flaws of element enrichment factors (EFs) in environmental geochemistry, *Environ. Sci. Technol.* 34 (2000) 5084–5091.



Contents lists available at ScienceDirect

## Spectrochimica Acta Part B: Atomic Spectroscopy

journal homepage: [www.elsevier.com/locate/sab](http://www.elsevier.com/locate/sab)

## Fast and simultaneous determination of zinc and iron using HR-CS GF-AAS in vegetables and plant material

Ondřej Zvěřina<sup>a,\*</sup>, Monika Vychytilová<sup>a</sup>, Jaqueline Rieger<sup>b</sup>, Walter Goessler<sup>b</sup><sup>a</sup> Masaryk University, Department of Public Health, Kamenice 5, 625 00 Brno, Czechia<sup>b</sup> University of Graz, Institute of Chemistry, Universitaetsplatz 1, 8010 Graz, Austria

## ARTICLE INFO

## Keywords:

High-resolution continuum source graphite furnace atomic absorption spectrometry  
Iron  
Zinc  
Simultaneous determination

## ABSTRACT

Due to the high nutritional importance of zinc and iron, accurate methods for their determination in foodstuffs are required. Here, we present a routine-ready method for their co-determination by means of high-resolution continuum source graphite-furnace atomic absorption spectrometry. As the technique allows for monitoring a narrow spectral interval, adjacent secondary lines of Zn (307.588 nm) and Fe (307.572 nm) can be measured simultaneously in a single firing. The analysis is therefore fast (under 2 min) and its sensitivity corresponds to common concentrations of the elements in foodstuffs. The accuracy of the method was verified by means of reference materials and also by comparison with an independent technique. Analysis of a large set of vegetable samples proved the applicability of the method in a routine laboratory setting. The vegetables for analysis were obtained from both markets and local gardeners. The results indicate higher contents of zinc and iron in homegrown vegetables compared to store-bought ones.

## 1. Introduction

As the most often deficient elements in human diet, iron and zinc have stayed in the spotlight of dietitians. Their content in the foodstuffs is an important nutritional parameter and thus fast and accurate methods for their determination are required.

In most foodstuffs, both iron and zinc occur at the levels ranging from milligrams to tens of milligrams per kilogram. They are usually determined after wet digestion of the solid samples with atomic spectrometric-based methods such as flame or graphite furnace atomic absorption spectrometry (F-AAS and GF-AAS), inductively coupled plasma with optical emission (ICP-OES) or mass spectrometry (ICP-MS). An alternative approach is direct solid sample analysis, often combined with GF-AAS (SS-GF AAS).

When it comes to determination of Fe and Zn, traditional GF-AAS is not the first-choice method. Detection limits for both elements are in the sub- $\mu\text{g L}^{-1}$  range, which actually hinders the analysis, as these elements are critical with regard to contamination from solvents, containers and also laboratory air [1]. The fluctuation of the blank is therefore the main limiting factor [1,2]. Using alternate wavelength is a common approach

to decrease this oversensitivity. A problem in this regard is with Zn, which has only one alternate spectral line of a very low sensitivity. However, the introduction of commercially available high-resolution continuum source (HR-CS) spectrometers made GF-AAS much more suitable for measuring high concentrations [3,4]. As the emission of Xe-lamp is intensive over the spectrum, sensitivity of secondary lines is only affected by their absorption and thus, they offer improved analytical usability [5].

Moreover, as the detection window in commercially available HR-CS instruments covers a spectral range of 0.2–1 nm, two (or even more) spectral lines can be measured simultaneously. This opens the possibility to multielemental analysis which doubles the efficiency in terms of running time and costs [6,7]. Although the number of HR-CS instruments in laboratories is increasing, the advantages that this technique has brought are not always exploited.

Here, we present a routine-ready method for simultaneous determination of Zn and Fe using HR-CS GF-AAS. Due to use of less-sensitive spectral lines, its linear range is suitable for direct analysis of digested foodstuffs. The method is fast and simple, does not require any chemical modifier and can be easily adopted in any lab.

\* Corresponding author.

E-mail address: [zverina@med.muni.cz](mailto:zverina@med.muni.cz) (O. Zvěřina).<https://doi.org/10.1016/j.sab.2023.106616>

Received 21 October 2022; Received in revised form 9 January 2023; Accepted 10 January 2023

Available online 13 January 2023

0584-8547/© 2023 Elsevier B.V. All rights reserved.

**Table 1**

Optimized temperature program for simultaneous determination of Zn and Fe using HR-CS GF-AAS.

Step	Temperature (°C)	Ramp (°C/s)	Hold (s)	Argon flow (L min <sup>-1</sup> )
Drying	120	10	12	2
Pyrolysis	500	100	10	2
Gas adaptation	500	0	5	–
Zn atomization	1550	1500	4	–
Fe atomization	2500	1500	4	–
Cleaning	2500	0	3	4

## 2. Experimental

### 2.1. Instrumentation

A high-resolution continuum source spectrometer ContrAA 800G (Analytik Jena, Germany) equipped with a graphite furnace with PIN-platform tubes was used for the analyses. The source of a continuum light is a Xe short-arc lamp combined with a high-resolution double-Echelle monochromator and charge-coupled device detector.

As a comparative technique, ICP-MS was used (Agilent 7900, Agilent Technologies). While both methods are well established for trace element determination, ICP-MS offers several advantages over GF-AAS, such as greater sensitivity and dynamic range and reduced matrix interferences. However, the instrumentation and running costs of ICP-MS are substantially higher.

### 2.2. Samples and their treatment

Samples of vegetables ( $n = 106$ ) were obtained from both local markets and also from local gardeners and mushroom pickers. In a laboratory, all the samples were homogenized using A-10 laboratory mill (IKA Germany). About 2 g of fresh material (weighed to 0.1 mg) were then mixed with 5 mL of HNO<sub>3</sub> and 1 mL of H<sub>2</sub>O<sub>2</sub> (of analpure and p.a. + purity, respectively, both obtained from Analytika, Czech republic) and digested by means of microwave assisted acid digestion using Multiwave Go plus digestion system (Anton Paar, Austria). The acid digests were then diluted up to 15 mL with ultrapure water (with specific resistivity of 18.2 MΩ cm<sup>-1</sup>).

Moreover, an additional set of 20 digests of various vegetables samples (carrots, lettuces, mushrooms, and potatoes) was measured

with both HR-CS GF-AAS method and ICP-MS for quality control. Whilst using the developed method, the digests were measured directly, for ICP-MS analysis the solutions were diluted ten times.

To check the trueness of the method, a set of 3 reference materials was processed the same way as the real samples and the results were compared with the certified concentrations. The reference materials included: Spinach Leaves (NIST 1570a), Green algae (Metranal 8), and Lichen (BCR-482). The weights of 250 mg of reference materials (roughly corresponding to 2 g of fresh material) were digested in triplicates and brought to a final volume of 15 mL.

### 2.3. A method for co-determination of Fe and Zn

Using a proposed method, both Fe and Zn were simultaneously determined using conventional HR-CS GF-AAS in a single firing. As the concentration of the elements in typical foodstuff digests is relatively high (ranging from hundreds of μg L<sup>-1</sup> to units of mg/L), secondary lines at 307 nm were selected. The intensity of selected lines is relatively low, but also the background noise is negligible in the given spectral region.

The temperature program (in Table 1) was optimized to be as fast as possible while maintaining optimal conditions for atomization of both elements due to two-stage atomization (see chapter Temperature program optimization). The duration of the temperature program is 88 s. Entire procedure including sample injection and furnace cooling takes 2 min. Each sample was measured three times and the median value was used.

Obtained peaks (see Fig. 1) were nicely shaped and well distinguished from the background. The peaks are separated not only spatially (16 pm is enough for a clear separation in HR-CS AAS) but also in time.

## 3. Results and discussion

### 3.1. Line selection: two possible combinations

In contrast to Fe, which has >500 absorption lines, Zn has only two useful analytical lines. Both those lines have adjacent Fe lines that fit into the narrow detection window of the instrument. So, the possible combinations are:

- primary resonance line of Zn at 213.857 nm (100% sensitivity) & secondary line of Fe at 213.970 nm, with a relative sensitivity of 0.83% (compared to the most intensive absorption line of the element – in case of Fe at 248.327 nm)

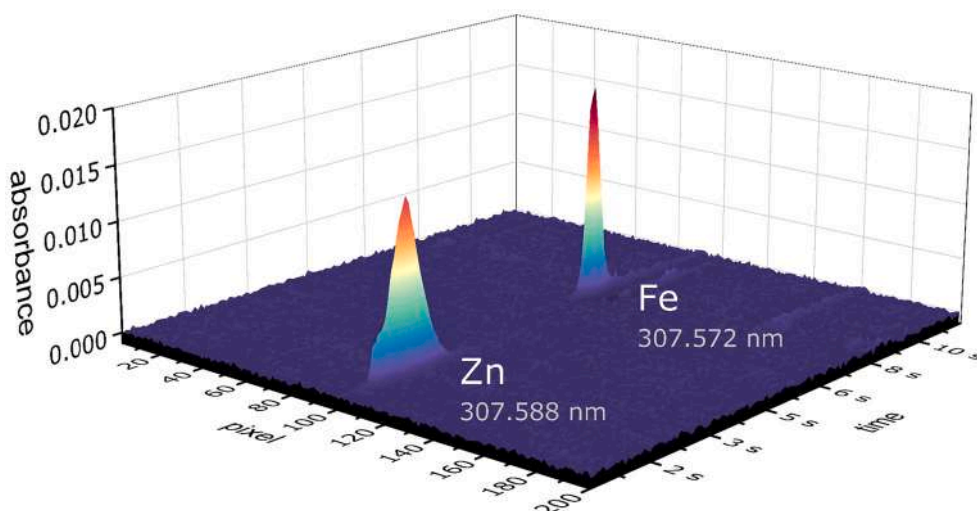


**Fig. 1.** A time- and wavelength-resolved absorption spectrum (analysis of a lettuce digest containing ~1 mg/L Zn and ~3 mg/L Fe).

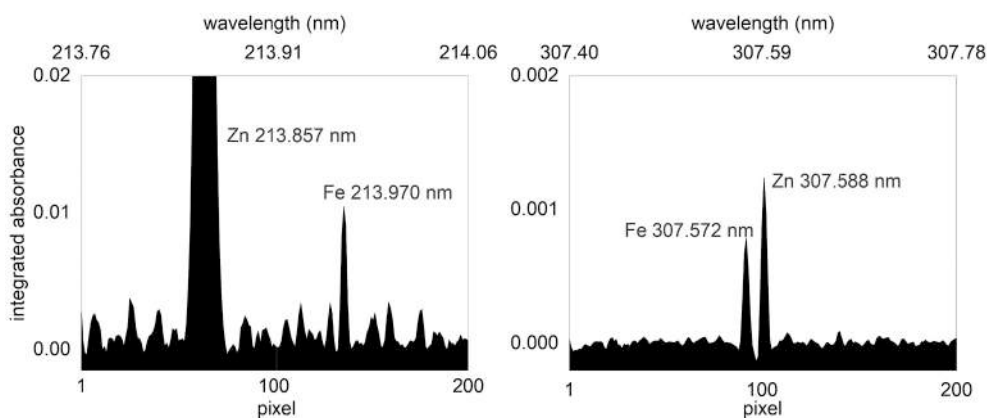


Fig. 2. Absorption spectrum of the same sample (digest of lettuce) recorded at spectral region of a primary Zn line at 213 nm (left) and a secondary line at 307 nm (right).

- secondary line of Zn at 307.588 nm, with 0.02% relative sensitivity & secondary line of Fe at 307.572 nm, with 0.043% relative sensitivity

The experiments have shown that the latter combination of less sensitive lines is far more suitable for their simultaneous determination in the vegetable samples. Three reasons led to the choice:

First, Because of the extreme sensitivity of the Zn primary line, the signal has to be attenuated for measuring concentrations higher than a few  $\mu\text{g L}^{-1}$ . This can be done by reading the signal at the line wings [8]. However, presence of the extremely strong Zn line affects the baseline position, which in turn affects reading of the relatively weak Fe line.

Second, the background noise observed in the spectral region of 307 nm was much lower compared to that at 213 nm (Fig. 2), improving the signal-to-noise ratio. Being expressed as the standard deviation of the signal recorded at pixels not involved in analytes measurement, the noise was about twenty-times lower. The NO absorption bands (arising from  $\text{HNO}_3$  used for the digestion) are one of the main culprits of deteriorating the background baseline at 213 nm [3,9].

Third, the primary Zn line has a direct overlap with another Fe line (213.859 nm, 0.17% sensitivity), which would have to be corrected by the background correction system or omitted from signal integration as Fe atomizes later than Zn. However, as with possible correction of NO bands, this would make the method less robust.

For the reasons mentioned above, analytical lines at a region of 307 nm are preferred.

### 3.2. Temperature program optimization

Temperature program, in particular the pyrolysis and atomization temperature, has to reflect the thermal behavior of the analyte. A key factor in optimizing the program for the two elements selected was that zinc is a much more volatile element than iron. This difference in volatility allowed the atomization to be split into two separate steps, and thus, achieving optimal atomization conditions for both elements. Where possible, splitting the atomization into separated steps for each element is preferred because it yields the best possible performance for the multi-elemental methods [7]. In addition, this allows for better temporal separation of the signals of individual elements and integration of only the relevant time region of the recorded spectrum (see Reading the signal chapter).

For Zn, the pyrolysis temperature of 500 °C was set as no significant background absorption was observed during the analysis of any of the samples investigated. Hence, there was also no need to use a matrix modifier, which allowed for a faster analysis. Atomization at temperatures around 1350 °C provided the highest signal, however, led to a formation of double peaks, which may compromise reproducibility and repeatability of the measurement. Atomization at higher temperature

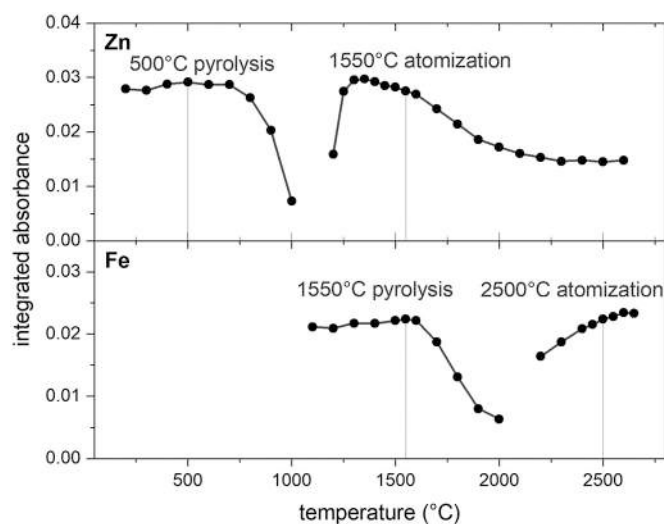


Fig. 3. Pyrolysis and atomization curves for Zn and Fe.

provided nicely shaped peaks with a better repeatability. Improving a signal-to-noise ratio by raising the atomization temperature 100–200 °C higher than the maximum is generally recommended for volatile elements [10]. Therefore, the transient signal was the reason for selecting a temperature of 1550 °C.

As can be seen in Fig. 3, 1550 °C as an Zn atomization temperature was in fact just suitable pyrolysis temperature for analysis of Fe. During the atomization, Fe pronounced symmetrical peaks at all the investigated temperatures. Therefore, the atomization temperature of 2500 °C was chosen as a compromise between sufficient sensitivity and saving the graphite tube life-time.

The resulting time- and wavelength-resolved spectrum can be seen in Fig. 1.

### 3.3. Reading the signal

Signal integration was limited to 0–3.5 s for Zn and 5–8 s for Fe. This setting reduces the integration of non-useful noise before and after the analytical signal and thus improves the signal-to-noise ratio.

In this way, the two lines are not only separated spatially (different wavelengths), but also temporally (different time intervals). As a result, there is no overlap of the lines even in the case of a significant excess of one of the elements. Selectivity was checked by measuring 1000  $\mu\text{g L}^{-1}$  solutions of each element in the presence of 10- and 100-fold excess of the other. In neither case was the measurement affected.

**Table 2**  
Figures of merit.

Parameter	Zn	Fe
LOD	0.02 mg/L	0.05 mg/L
LOQ	0.06 mg/L	0.2 mg/L
working range	0.06–5 mg/L	0.2–10 mg/L
R-squared	0.9999	0.9997
repeatability (intra-day, $n = 5$ )*	3.1%	4.5%
reproducibility (inter-day, $n = 5$ )*	9.0%	8.9%

\* A precision expressed as a relative standard deviation (RSD) of replicated measurement of a digest of NIST 1570a (repeatability) and the RSD of measurements conducted in five consecutive days (reproducibility).

### 3.4. Characteristic concentration: the effect of the number of pixels

In HR-CS spectrometry, the sensitivity depends also on the number of pixels involved in the signal integration. According to the number of used pixels (central pixel [CP] only, CP  $\pm$  1, CP  $\pm$  2, and, CP  $\pm$  3 pixels), the characteristic concentrations were as follows: for Zn, 400, 150, 125, and 125  $\mu\text{g L}^{-1}$  and, for Fe, 1700, 650, 500, and, 500  $\mu\text{g L}^{-1}$ , respectively. It follows that the integration of  $>5$  pixels (CP  $\pm$  2) did not improve the characteristic concentration as the range already covered the entire profile of the lines. Therefore, reading of 5 pixels, i.e. CP  $\pm$  2, was selected to obtain the highest possible signal. With this setting, the characteristic concentration was 125  $\mu\text{g L}^{-1}$  for Zn and 500 for Fe  $\mu\text{g L}^{-1}$ .

### 3.5. Comparison with similar methods

Compared to the conventional GF-AAS measurement, the proposed method offers several advantages:

- time effective (twice against the measuring element by element),
- cost effective (saving cuvette life, argon, electricity),
- less prone to contamination from ambient air (fluctuation of blank hinders measurement of Zn and Fe at primary lines)

To our best knowledge, there is currently only one paper on simultaneous determination of Zn and Fe using HR-CS GFAAS. For analysis of samples of dried blood spots using solid sampling, the authors used a compromise temperature program with a single atomization temperature of 2400 °C [3]. During the optimization of the method, the authors examined only the temperature range from 1800 °C. Thus, their range did not cover the maximum absorbance and showed only a descending part of the curve. From the atomization curves in Fig. 3 it is obvious that use of a single atomization step at the temperature ideal for Fe leads to a reduction in Zn signal by about 50% (mainly due to diffusion effect).

The other authors measured Fe and Zn in water sequentially [9]. Sequential approach, in contrast to the simultaneous measurement, involves realignment of the monochromator between the first and second atomization step. This approach allowed authors to measure both elements using their primary lines, which was necessary given the mission of the study. However, in our experience, realignment of the monochromator during the atomization process may not be that straightforward and control software is not well prepared for such operation and thus it is not suitable for routine use.

**Table 3**  
Determined levels of Zn and Fe in reference materials (values in  $\text{mg kg}^{-1} \pm$  standard deviation ( $n = 3$ ), corrected to a dry mass at 105 °C).

Reference material	Zn			Fe		
	Found	Certified	Trueness <sup>a</sup>	Found	Certified	Trueness <sup>a</sup>
NIST 1570a Spinach leaves	85.1 $\pm$ 5.2	82.3 $\pm$ 3.9	103%	259 $\pm$ 17	–	–
Metranal 8 Green algae	35.1 $\pm$ 0.5	38 $\pm$ 3	92%	287 $\pm$ 10	290 $\pm$ 20	99%
BCR-482 Lichen	102 $\pm$ 9	100.6 $\pm$ 2.2	101%	751 $\pm$ 16	804 $\pm$ 160 <sup>b</sup>	93%

<sup>a</sup> Expressed as a ratio between the mean measured content and mean reference value \*100.

<sup>b</sup> Indicative value.

**Table 4**  
Contents of zinc and iron in vegetables and mushrooms ( $\text{mg kg}^{-1} \pm$  standard deviation).

Samples	Zn	Fe
Carrots (homegrown, $n = 30$ )	2.9 $\pm$ 1.1	2.9 $\pm$ 1.5
Carrots (market, $n = 18$ )	1.8 $\pm$ 0.5	2.1 $\pm$ 0.9
Lettuce (homegrown, $n = 37$ )	3.8 $\pm$ 1.7	6.9 $\pm$ 3.2
Lettuce (market, $n = 15$ )	2.8 $\pm$ 1.2	6.7 $\pm$ 2.5
Mushrooms (wild, $n = 6$ )	12.1 $\pm$ 4.3	5.3 $\pm$ 2.8

### 3.6. Validation: figures of merit, trueness checking

Performance of the method (Table 2) is given by the use of secondary lines and its purpose – to be used for routine analysis of food.

Compared to the nominal sensitivity of GF-AAS, limits of detection and quantification (LOD and LOQ) for both Fe and Zn are substantially reduced. This reduction in sensitivity reflects the low intensity of the selected absorption lines (0.02% for Zn and 0.043% for Fe). The resulting working range approximately corresponds to that of F-AAS (including HR-CS F-AAS), which typically spans from tenths to single units of ppm for both elements [11–13].

At first glance, concentrations at ppm levels may seem relatively high for GF-AAS as the method traditionally used for trace analysis. However, such concentrations are commonly measured in multi-elemental determinations, where secondary spectral lines are widely used [7]. Thus, HR-CS GF-AAS is nowadays commonly used even for determinations that have traditionally been performed by F-AAS. Similarly, detection limits ranging from 1 to 2  $\text{mg Fe kg}^{-1}$  (dry weight) were reported for direct solid sample analysis of plant material (using HR-CS SS-GF AAS), when Fe was measured using its secondary line in a simultaneous determination [14,15].

The working range of the method (Table 2) matches the actual elements' concentration in typical digests of food. Relatively narrow calibration ranges (usually 2–3 orders of magnitude) are usual in AAS. For comparison, the working ranges of ICP-based techniques are substantially wider, reaching from 6 orders of magnitude for ICP-OES to up to 9 orders of magnitude for ICP-MS [16]. However, HR-CS AAS has brought some capabilities for extending the limited dynamic range. For example, in the case of need for measuring even higher concentrations, the range may be further extended by measuring the signal at line wings [8], or by injecting a reduced volume of a sample.

Contents of Zn and Fe determined in reference materials corresponded with declared values (Table 3). No statistically significant differences were observed using Student's *t*-test at 95% confidence level. The trueness ranged between 92 and 103%. The matrices of the reference materials used included spinach, lichen, and algae. (See Table 4.)

To ensure that even real-sample matrices do not affect the measurement by interferences, the results obtained for a set of vegetables (carrots, lettuces, mushrooms, potatoes, altogether  $n = 20$ ) were compared to those obtained by ICP-MS as an independent technique. The results agreed closely with correlation coefficients of  $r > 0.99$  and no significant difference between the two methods was observed using paired *t*-test.

The results were plotted using Bland-Altman plot, which is a convenient approach for comparison of methods. In contrast to basic

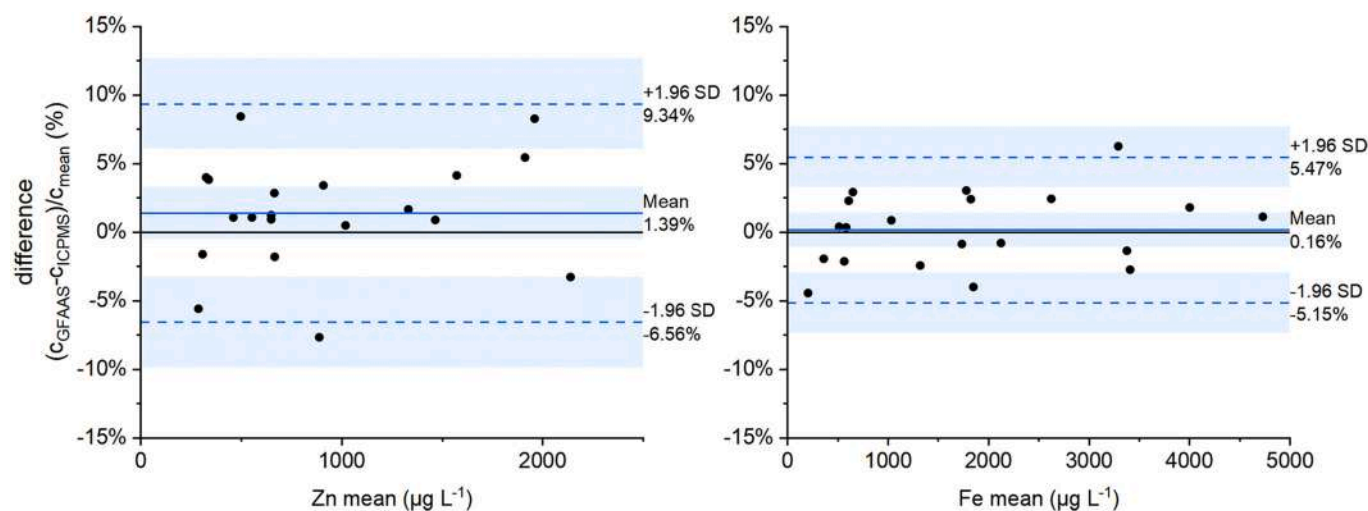


Fig. 4. A Bland-Altman comparison of the results obtained by HR-CS GF-AAS and ICP-MS. The difference between methods (y-axis) is plotted against the average value obtained using both methods (x-axis). The marked lines approximately define 95% confidence intervals as mean  $\pm$  1.96 standard deviation (SD).

comparison using correlation coefficient, it is not influenced by the range of the values and readily detects instrument bias [17]. As can be seen in Fig. 4, the values obtained by both techniques agreed sufficiently closely. The method biases (1.4 and 0.2% for Zn and Fe, respectively) were very small. Even though the precision is somewhat lower in the case of Zn, most of the results still fall between confidence interval  $\pm$  1.96\*standard deviation.

### 3.7. Zn and Fe in vegetable and mushroom samples

We used the method for a routine analysis of vegetables (carrots, lettuce) and mushrooms (including *Chanterellus*, *Boletus*, and *Amanita rubescens*), altogether 106 samples. The samples were obtained from local gardeners and mushroom pickers in Czech cities Brno and Letohrad and also from local markets.

As for the vegetables, the lettuce samples were significantly richer in both elements compared to carrots. Mean levels of elements were consistently higher for homegrown vegetables, however, the differences were statistically significant only for carrots (*t*-test, significance level 0.05).

## 4. Conclusions

The advantages that HR-CS has brought to the GF-AAS include multi-element analysis and also the ability to handle higher concentrations. Here, the two advantages are combined in a method useful for co-measuring iron and zinc at  $\text{mg L}^{-1}$  levels, for example in vegetables and other food samples. The sensitivity is similar to flame AAS, however, the method provides the benefits of graphite furnace such as low sample consumption (20  $\mu\text{L}$  for the analysis), ease of automation and operation and a possibility of introducing samples with more complex matrices.

### CRedit authorship contribution statement

**Ondřej Zvěřina:** Conceptualization, Methodology, Investigation, Writing – original draft. **Monika Vychytilová:** Investigation, Resources. **Jaqueline Rieger:** Investigation, Validation. **Walter Goessler:** Methodology, Writing – review & editing, Supervision.

### Declaration of Competing Interest

The authors declare that they have no known competing financial interests or personal relationships that could have appeared to influence the work reported in this paper.

### Data availability

Data will be made available on request.

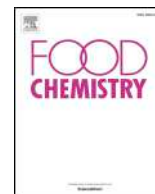
### Acknowledgement

Authors thank the Ministry of Education, Youth and Sports for supporting this research (project 8J21AT006) and also Masaryk University (projects MUNI/C/0063/2022 and MUNI/A/1366/2022).

### References

- [1] G. Schlemmer, M. Petek, Optimization of a class 100 clean room cabinet for electrothermal atomization AAS, *At. Spectrosc.* 21 (2000) 1–4.
- [2] Z. Polgári, Z. Ajtony, P. Kregsamer, C. Strelí, V.G. Mihucz, A. Réti, B. Budai, J. Kralovszky, N. Szoboszlai, G. Záray, Microanalytical method development for Fe, Cu and Zn determination in colorectal cancer cells, *Talanta*. 85 (2011) 1959–1965.
- [3] A.L. Vieira, E.C. Ferreira, S.R. Oliveira, F. Barbosa, J.A.G. Neto, Simultaneous determination of Fe and Zn in dried blood spot by HR-CS GF AAS using solid sampling, *Microchem. J.* 160 (2021), 105637.
- [4] B. Welz, L.M.G. dos Santos, R.G.O. Araujo, S.C. do Jacob, M.G.R. Vale, M. Okrus, H. Becker-Ross, Unusual calibration curves observed for iron using high-resolution continuum source graphite furnace atomic absorption spectrometry, *Spectrochim. Acta Part B At. Spectrosc.* 65 (2010) 258–262.
- [5] G. Ring, J. O'Mullane, A. O'Riordan, A. Furey, Trace metal determination as it relates to metallosis of orthopaedic implants: evolution and current status, *Clin. Biochem.* 49 (2016) 617–635.
- [6] S.L.C. Ferreira, M.A. Bezerra, A.S. Santos, W.N.L. dos Santos, C.G. Novaes, O.M. C. de Oliveira, M.L. Oliveira, R.L. Garcia, Atomic absorption spectrometry – a multi element technique, *Trends Anal. Chem.* 100 (2018) 1–6.
- [7] I.N. Pasiás, N.I. Rousis, A.K. Psoma, N.S. Thomaidis, Simultaneous or sequential multi-element graphite furnace atomic absorption spectrometry techniques: advances within the last 20 years, *At. Spectrosc.* (2021), <https://doi.org/10.46770/AS.2021.707>.
- [8] O. Zvěřina, P. Coufalík, J. Šimůnek, P. Kachlík, R. Chlupová, J. Pavelková, Inorganic pollutants in the indoor environment of the Moravian library: assessment of Cd, Pb, Cu, and Zn in total suspended particles and dust using HR-CS GF-AAS, *Environ. Monit. Assess.* 192 (2020) 771.
- [9] M. Krawczyk, M. Jeszka-Skowron, H. Matusiewicz, Sequential multi-element determination of iron and zinc in water samples by high-resolution continuum source graphite furnace atomic absorption spectrometry after column solid-phase extraction onto multiwalled carbon nanotubes, *Microchem. J.* 117 (2014) 138–143.
- [10] B. Welz, M.G.R. Vale, Atomic absorption spectrometry and related techniques, in: G. Nelu, R. Sonia (Eds.), *Ewing's Analytical Instrumentation Handbook*, Fourth Edition, 2018.
- [11] S.N.P. Souza, C.C. Nascentes, L.M. Costa, Validation of a microwave-assisted digestion procedure of pâté samples using diluted  $\text{HNO}_3$  for Fe and Zn determination by FS FAAS, *Anal. Methods* 5 (2013) 6411–6415.
- [12] O. Acar, A. Tunçeli, A.R. Türker, Comparison of wet and microwave digestion methods for the determination of copper, Iron and Zinc in some food samples by FAAS, *Food Anal. Methods* 9 (2016) 3201–3208.

- [13] E. Zambrzycka-Szelewa, E. Nalewajko-Sieliwoniuk, M. Zaremba, A. Bajguz, B. Godlewska-Żyłkiewicz, The mineral profile of polish beers by fast sequential multielement HR CS FAAS analysis and its correlation with Total phenolic content and antioxidant activity by Chemometric methods, *Molecules*. 25 (2020), <https://doi.org/10.3390/molecules25153402>.
- [14] M. Pozzatti, F.V. Nakadi, M.G.R. Vale, B. Welz, Simultaneous determination of nickel and iron in vegetables of Solanaceae family using high-resolution continuum source graphite furnace atomic absorption spectrometry and direct solid sample analysis, *Microchem. J.* 133 (2017) 162–167.
- [15] F.R. Adolfo, P.C. do Nascimento, G.C. Leal, D. Bohrer, C. Viana, L.M. de Carvalho, Simultaneous determination of Fe and Ni in guarana (*Paullinia cupana* Kunth) by HR-CS GF AAS: comparison of direct solid analysis and wet acid digestion procedures, *J. Food Compos. Anal.* 88 (2020), 103459.
- [16] S. Suzanne Nielsen, *Food Analysis*, Springer International Publishing, 2017.
- [17] C. Sobin, N. Parisi, T. Schaub, E. de la Riva, A bland-Altman comparison of the Lead care® system and inductively coupled plasma mass spectrometry for detecting low-level lead in child whole blood samples, *J. Med. Toxicol.* 7 (2011) 24–32.



## Analytical Methods

# Simultaneous determination of cadmium and iron in different kinds of cereal flakes using high-resolution continuum source atomic absorption spectrometry



Ondřej Zvěřina<sup>a,\*</sup>, Jan Kuta<sup>b</sup>, Pavel Coufalík<sup>c</sup>, Pavlína Kosečková<sup>a</sup>, Josef Komárek<sup>d</sup>

<sup>a</sup> Department of Public Health, Faculty of Medicine, Masaryk University, Kamenice 5, 625 00 Brno, Czech Republic

<sup>b</sup> Research Centre for Toxic Compounds in the Environment (RECETOX), Faculty of Science, Masaryk University, Kamenice 5, 625 00 Brno, Czech Republic

<sup>c</sup> Institute of Analytical Chemistry of the Czech Academy of Sciences, Veveří 97, 602 00 Brno, Czech Republic

<sup>d</sup> Department of Chemistry, Faculty of Science, Masaryk University, Kotlářská 2, 611 37 Brno, Czech Republic

## ARTICLE INFO

## Keywords:

Cereals  
Cadmium  
Iron  
Simultaneous determination  
HR CS GFAAS

## ABSTRACT

A method for simultaneous determination of cadmium and iron in cereal flakes using high-resolution continuum source graphite furnace atomic absorption spectrometry is presented.

Sample digest is introduced into the graphite furnace together with Pd/Mg(NO<sub>3</sub>)<sub>2</sub> modifier. The primary absorption line of cadmium and adjacent secondary line of iron are used for the determination. Atomization is performed as a two-step process in order to meet ideal conditions for both elements. Interference produced by molecular absorption of PO molecular bands is suppressed by correction model using least squares background correction.

Using the proposed method, levels of cadmium and iron were determined in different kinds of cereal flakes, where both elements are of great interest. Working range (0.01–2 μg L<sup>-1</sup> for Cd and 10–500 μg L<sup>-1</sup> for Fe) was suitable for the determination of analytes in samples.

The method is fast, robust, and may be routinely used routinely in the analysis of foodstuffs.

## 1. Introduction

Atomic absorption spectrometry with a graphite furnace (GF AAS) has been one of the most commonly used techniques for trace element determination. In its traditional concept as a line-source AAS technique, the method is most often used for single element analysis. More recently, since the expansion of commercially available high-resolution continuum source (HR CS) spectrometers since 2003 (2007 in the case of the furnace-atomization technique), multielemental analysis has become convenient and reliable even in typical AAS laboratories. The determination of several elements in a single run can significantly shorten the analysis time and even reduce its cost. Nonetheless, several conditions must be fulfilled for such measurement and its optimization may not be straightforward.

Multielemental analysis in HR CS GFAAS is made possible thanks to the combination of a continuum-source short-arc xenon lamp and echelle monochromator with a CCD detector, which allows monitoring not only of the analytical line itself, but also of its spectral neighborhood. Any other line in this spectral interval may also be monitored.

The main factor limiting simultaneous analysis, however, is the narrow range of the monitored wavelength, which is about 0.2–0.3 nm in the UV region and where most useful analytical lines are located. The fundamental principles of multielemental analysis in HR CS AAS have already been summed up in a review by Resano, Flórez, and García-Ruiz (2013). Despite limitations arising from the principles of the method, a number of multielemental determinations have been published in the last decade (Ferreira et al., 2018).

In this paper, we present a method for the simultaneous determination of cadmium (Cd) and iron (Fe) in samples of cereal flakes. In fact, dos Santos, Araujo et al. (2009) and dos Santos, Welz et al. (2009) demonstrated the first multielemental use of HR CS GFAAS also in the simultaneous determination of cadmium and iron, employing a prototype spectrometer equipped with solid sampling. The approach was later adapted by Leao, Junior, Brandao, and Ferreira (2016), who extended the method to include the determination of tin. The aim of this work was to develop an easy-to-use analytical method for the simultaneous determination of Cd and Fe in cereal-based foodstuffs, based on the traditional microwave-assisted wet digestion of samples

\* Corresponding author.

E-mail address: [zverina@med.muni.cz](mailto:zverina@med.muni.cz) (O. Zvěřina).

<https://doi.org/10.1016/j.foodchem.2019.125084>

Received 31 January 2019; Received in revised form 12 June 2019; Accepted 25 June 2019

Available online 26 June 2019

0308-8146/ © 2019 Elsevier Ltd. All rights reserved.

and a commercially available HR CS GFAAS spectrometer.

Both Cd and Fe are very important elements for human health, though in two completely different ways. Fe is an essential element for human life. It is required to make the protein haemoglobin in red blood cells, whose principal function is to transport oxygen from the lungs to the body's cells. The decreased level of haemoglobin in erythrocytes caused by Fe-deficiency anaemia is a worldwide public health problem (Lopez, Cacoub, Macdougall, & Peyrin-Biroulet, 2016). Despite cereals' limited ability to accumulate Fe from soil, together with presence of antinutritional factors (mainly phytate) which hinder its absorption, cereal-based foods present an important dietary source of Fe as they are widely consumed staple foods in many countries (Shahzad, Rouached, & Rakha, 2014; WHO, 1999; EFSA, 2015).

In contrast, Cd is an element offering no beneficial effects on human health. The regular intake of Cd leads to its accumulation and increases the risk of kidney disease, osteoporosis, and developing cancer (Alexander et al., 2009; International Agency for Research on Cancer Monographs, 1993). In the human diet, most Cd comes from agricultural products, as plants accumulate Cd from soils, which may be contaminated by Cd-containing fertilizers or sewage sludge (Alexander et al., 2009). Cereals (especially whole grains) are among the main contributors of dietary Cd intake, primarily because of their high consumption. Different cereal varieties vary in Cd accumulation potential, and therefore, numerous breeding programs aim at reducing the risk related to Cd in human diet (Vergine et al., 2017). In the case of lower body Fe stores, the uptake of Cd from the diet is further enhanced (European Food Safety Authority Scientific Opinion, 2012; Wennberg, Lundh, Nilsson Sommar, & Bergdahl, 2017). For these reasons, the Scientific Panel on Contaminants in the Food Chain (CONTAM) set maximum limits for Cd contents in these foodstuffs (0.10 mg per kilogram of cereal grains excluding wheat and rice, and 0.20 mg per kilogram of wheat and rice grains, wheat bran and wheat germ for direct consumption, and soy beans) (European Food Safety Authority Scientific Opinion, 2012).

In addition to the main objective of developing a reliable method for Cd and Fe determination, a secondary aim was to assess the levels of the two studied metals in different kinds of cereal flakes commonly traded on the Czech market.

## 2. Experimental

### 2.1. Samples and sample treatment

In total, 25 packs of various cereal flakes were purchased in local stores. The flakes were of 10 different kinds commonly available in the Czech Republic (coarse and fine oat flakes, spelt, wheat, rye, millet, buckwheat, rice, barley, and amaranth flakes). The products originated mainly from European Union countries, but also from Ukraine, India and China.

About twenty grams of each sample were homogenized using a Pulverisette 7 planetary ball mill (Fritsch GmbH, Germany) for 5 min at 450 RPM. The homogenized material was mineralized using the MLS-1200 Mega microwave digestion system (Milestone, Italy). Three 250-mg aliquots of each sample were mixed with 2.5 mL of nitric acid and 0.5 mL of hydrogen peroxide and digested. The obtained solutions were diluted to a final volume of 25 mL. In the case of the presence of undissolved silicates, the solutions were also filtered.

In addition, sets of six procedural blanks and six mineralizates of BCR-191 Brown bread certified reference material (IRMM, Geel, Belgium) were prepared for quality assurance purposes.

In order to evaluate the influence of HNO<sub>3</sub> concentration on the signal, the residual acidity of digests was determined. Aliquots of digests were titrated with a standardized solution of sodium hydroxide

and phenolphthalein as an indicator.

### 2.2. HR CS GFAAS instrumentation

All measurements were carried out using a ContrAA 800 G high-resolution continuum source atomic absorption spectrometer (Analytik Jena, Germany). The spectrometer is equipped with a Xenon short arc lamp as a continuum source and a high-resolution echelle double monochromator combined with a CCD array detector. The model used was equipped with a transversely heated graphite tube atomizer and an MPE 60 autosampler.

### 2.3. Analytical lines selection

The primary line of Cd at 228.802 nm and a secondary line of Fe at 228.725 nm of relative sensitivity 0.91% were selected. These lines are located in sufficient proximity and their intensities correspond well with the demands of analysis in terms of required sensitivity. The absorption at both lines was measured using three pixels (the central pixel and the adjacent ones).

### 2.4. Analytical procedure

For the determination of Cd and Fe in the samples, a 20 µl of digest was introduced into the graphite tube together with 5 µl of Pd/Mg (NO<sub>3</sub>)<sub>2</sub> modifier. The determination was performed using the 228.802 nm line for Cd and the 228.726 nm line for Fe, these measured simultaneously. The optimized heating program containing the atomization steps is shown in Table 1. The total time of analysis was 152 s (without sample introduction and cooling). The obtained spectra were corrected for interference from PO bands (see chapter Handling interference).

A set of 10 samples were analyzed by means of ICP-MS at the Centre for Toxic Compounds in the Environment RECETOX (Brno, Czech Republic). An Agilent 7700x ICP-MS instrument (Agilent Technologies, Japan) was used for the comparative determination of Cd and Fe in digested samples. Measurement was carried out in He collision mode to suppress potential spectral interferences. Quantification was performed on <sup>57</sup>Fe and <sup>111</sup>Cd isotopes with correction on <sup>72</sup>Ge and <sup>115</sup>In internal standards.

## 3. Results and discussion

### 3.1. Optimization of temperature program

As Cd and Fe differ significantly in their volatility, the temperature programme has to reflect their thermal behaviour carefully. A sample of oat flake digest with suitable signals for the determined elements was used to develop and optimize the method. A modifier containing 1 g L<sup>-1</sup> Pd and 0.6 g L<sup>-1</sup> Mg(NO<sub>3</sub>)<sub>2</sub> was used for the stabilization of analytes. Fig. 1 shows the pyrolysis and atomization curves for Cd and

**Table 1**  
Temperature program for the simultaneous determination of Cd and Fe.

Step	Temp (°C)	Ramp (°C/s)	Hold (s)	Ar flow (l/min)
Drying 1	80	6	20	2
Drying 2	90	3	15	2
Drying 3	110	5	10	2
Pyrolysis 1	350	50	20	2
Pyrolysis 2	700	300	10	2
Cd atomization	1250	1500	4	0
Fe atomization	2325	2500	5	0
Clean	2550	150	3	2

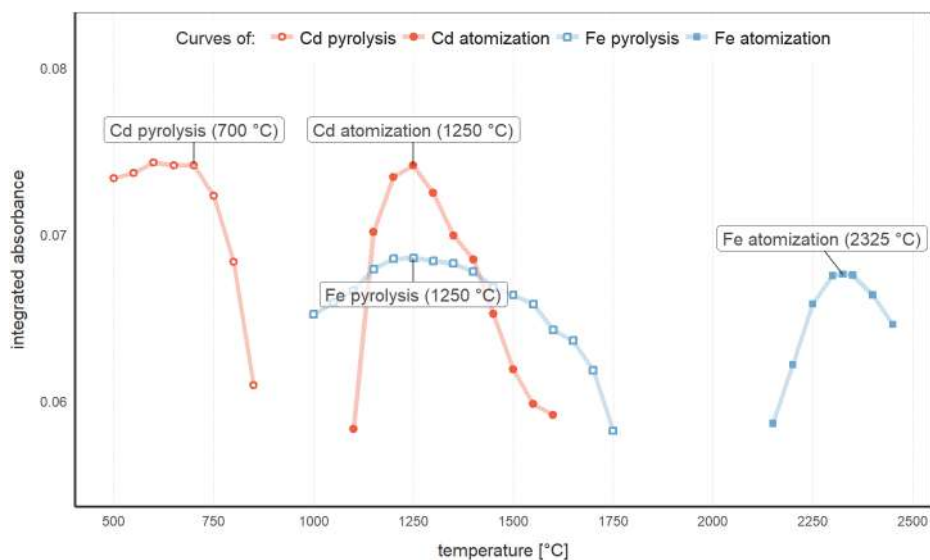


Fig. 1. Atomization and pyrolysis curves for Cd and Fe, obtained by measuring a solution prepared by the acid digestion of oat flakes, and in the presence of Pd/Mg(NO<sub>3</sub>)<sub>2</sub> modifier.

Fe obtained by injecting 20 µl of oat flake digest together with 5 µl of Pd/Mg(NO<sub>3</sub>)<sub>2</sub> modifier. The presence of modifier allowed a pyrolysis temperature of 700 °C without any vaporization loss of Cd. The highest signal for Cd was obtained with an atomization temperature of 1250 °C, which was shown to be a suitable temperature for Fe pyrolysis.

By dividing atomization into two steps, a significant improvement in terms of signal intensity and the spatial separation of analytical signals from interference was achieved. Although the analysis can be performed using only one atomization at the Fe atomization temperature of 2325 °C, a 60% increase in the Cd signal was observed when it was measured in optimal conditions, i.e., in a special atomization step at 1250 °C.

In literature, examples of methods based on both single- and multi-step atomizations can be found. The first approach was taken by Leao et al. (2016), who determined Cd, Sn, and Fe in digests of canned foods. A two-step atomization approach was employed in the analysis of grain products, beans, and soil by dos Santos, Araujo et al. (2009) and dos Santos, Welz et al. (2009), who used a prototype high-resolution spectrometer with solid sampling. Using the same prototype, Vignola, Borges, Curtius, Welz, and Becker-Ross (2010) observed an improvement in the Cd signal similar to that reported in this study, during the analysis of sewage sludge employing two atomization steps.

### 3.2. Handling interference

In addition to improving Cd sensitivity, the two-step atomization approach also allowed the better spatial separation of useful analytical signals from interference produced mostly by the molecular absorption of PO bands. As PO molecules are formed at high temperatures, they do not occur during Cd atomization at 1250 °C. Although it was shown that Pd-based modifier suppresses the formation of PO molecules in favor of atomic phosphorus (Heitmann, Becker-Ross, Florek, Huang, & Okrus, 2006; Lepri et al., 2006; Resano, Briceño, & Belarra, 2009), still, a small level of interference was observed during the second atomization step, this overlapping spectrally with the Fe line. The contribution of PO molecular absorption to the signal varied from sample to sample, but generally accounted for less than 10%. Thanks to the possibilities of least-squares background correction (LSBC), the reference spectrum of PO could be subtracted proportionally from the signal. For this purpose, the reference spectrum of a solution containing 50 µg NaH<sub>2</sub>PO<sub>4</sub> was recorded and further subtracted from the signal using LSBC (see Fig. 2).

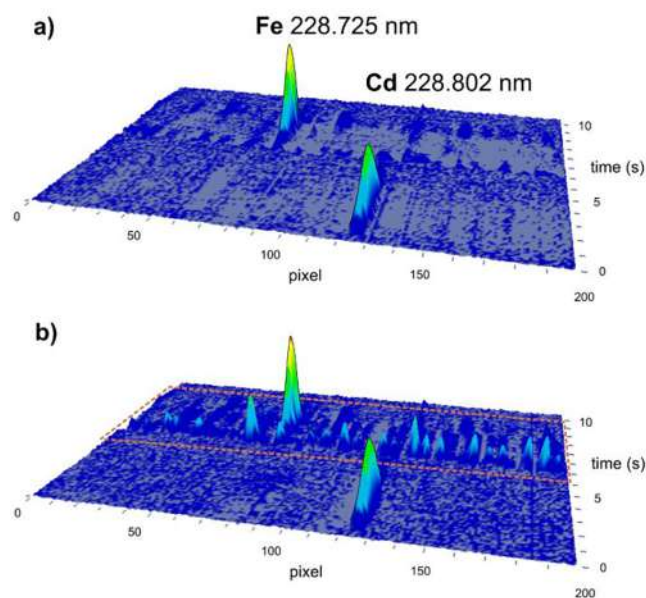


Fig. 2. Spectrum obtained during real sample analysis after (a) and before (b) the masking of interference by background correction.

### 3.3. Calibration

The calibration was carried out against HNO<sub>3</sub>-acidified aqueous standards with a concentration range of 0.05–2 µg L<sup>-1</sup> Cd and 25–500 µg L<sup>-1</sup> Fe.

Although the HNO<sub>3</sub> herein used for mineralization causes only mild cuvette corrosion in comparison with highly corrosive acids such as HClO<sub>4</sub> or HCl (Rohr, Ortner, Schlemmer, Weinbruch, & Welz, 1999), it is desirable to know its concentration as it forms the main matrix component of the analysed solutions. The concentration of HNO<sub>3</sub> in both reagent and procedural blanks was 1.43 ± 0.01 mol L<sup>-1</sup>. Residual acidities in sample digests were 1.18 ± 0.03 mol L<sup>-1</sup>, which means a reduction in the initial acidity by about 20%. Thus, calibration standards were acidified to a similar extent as samples (1 mol L<sup>-1</sup>). Experiments showed, however, that the slopes of the calibration curves did not differ significantly when using calibration solutions in 0.1-, 1-, and 2 mol L<sup>-1</sup> HNO<sub>3</sub>.

**Table 2**  
Method performance parameters.

Parameter	Cd	Fe
LOD	0.01 $\mu\text{g L}^{-1}$	0.01 $\text{mg L}^{-1}$
LOD procedural	0.02 $\mu\text{g L}^{-1}$	0.01 $\text{mg L}^{-1}$
LOD for solid sample <sup>a</sup>	2 $\mu\text{g kg}^{-1}$	1.4 $\text{mg kg}^{-1}$
LOQ	0.03 $\mu\text{g L}^{-1}$	0.04 $\text{mg L}^{-1}$
LOQ procedural	0.06 $\mu\text{g L}^{-1}$	0.05 $\text{mg L}^{-1}$
LOQ for solid sample <sup>a</sup>	6 $\mu\text{g kg}^{-1}$	4.6 $\text{mg kg}^{-1}$
Spike Recovery <sup>b</sup>	97–106%	93–104%
BCR-191 found <sup>c</sup>	27.6 $\pm$ 1.0 $\mu\text{g kg}^{-1}$	38.2 $\pm$ 1.5 $\text{mg kg}^{-1}$
BCR-191 certified	28.4 $\pm$ 1.4 $\mu\text{g kg}^{-1}$	40.7 $\pm$ 2.3 $\text{mg kg}^{-1}$

<sup>a</sup> Limits expressed as mass of analyte per mass of sample considering a 0.25 g sample contained in a volume of 25 mL, i.e. dilution factor = 100.

<sup>b</sup> Spike recovery was determined for six real sample solutions spiked with 0.25  $\mu\text{g/l}$  Cd and 250  $\mu\text{g/l}$  Fe, respectively.

<sup>c</sup> Values for certified material are expressed as mean  $\pm$  standard deviation, obtained by measuring six digests.

### 3.4. Validation studies

The figures of analytical merit are summarized in Table 2.

The limits of detection (LOD) and quantification (LOQ) were calculated as  $3s/m$  and  $10s/m$ , respectively, where  $s$  is the standard deviation of the signal obtained by repeated analysis of the blank solution and  $m$  is the slope of the calibration graph. To cover the whole operation with real samples – digestion, dilution, etc., the procedural LOD and LOQ were calculated with  $s$  obtained from the analyses of six digestion blanks.

The accuracy of the method was tested by means of the analysis of the certified reference material BCR-191 Brown Bread in six replicates. Trueness, expressed as method bias, was  $-2.8\%$  for Cd and  $-6.1\%$  for Fe. Method precision, calculated as the relative standard deviation of concentrations determined in six digests, was  $3.5\%$  for Cd and  $4.0\%$  for Fe.

The accuracy of real sample analysis was further investigated by comparing the presented method with a different analytical technique. Fig. 3 presents a comparison of the results obtained by the presented HR CS GFAAS method and ICP-MS measurement. There was no significant deviation between the two methods according to the regression line slopes, which were close to 1 with negligible intercepts.

### 3.5. Real sample testing: Cd and Fe in cereal flakes

In total, 25 samples of cereal flakes were processed and analyzed using the presented method. Samples were brought into solution by

**Table 3**  
Contents of Cd and Fe in cereal flakes.

cereals	n	cadmium		iron	
		Range ( $\mu\text{g.kg}^{-1}$ )	Median ( $\mu\text{g.kg}^{-1}$ )	Range ( $\text{mg.kg}^{-1}$ )	Median ( $\text{mg.kg}^{-1}$ )
oat flakes (coarse)	6	16.0–53.0	45.3	34.8–53.1	48.3
oat flakes (fine)	4	16.0–150	39.8	32.8–58.2	34.3
spelt flakes	2	24.4–44.8	34.6	33.8–35.4	34.6
wheat flakes	2	19.6–21.9	24.2	19.2–31.3	25.2
rye flakes	2	5.6–15.4	10.5	23.0–23.5	23.3
millet flakes	2	6.3–7.4	6.9	7.3–20.3	13.8
buckwheat flakes	3	13.7–20.9	17.2	17.3–24.3	23.7
rice flakes	1	–	33.4	–	5.6
barley flakes	2	7.9–12.6	10.3	15.0–23.6	19.3
amaranth flakes	1	–	16.4	–	66.2

conventional microwave-assisted digestion with a dilution factor of 1:100. The achieved detection limits (Table 2) corresponded to the use of the sensitive primary Cd line and a secondary Fe line with only 0.91% relative sensitivity. The working range that resulted from these parameters was shown to be appropriate for selected samples of cereal flakes and presumably also for other kinds of foodstuffs with similar levels and ratios of the elements (including, for example, fish muscle). The repeatability of the measurement, expressed as the relative standard deviation for five consecutive sample analyses, was  $< 5\%$  for both elements in most cases.

The results are summarized in Table 3. With regard to Cd content, one sample of fine oat flakes with a Cd content of  $0.150 \text{ mg.kg}^{-1}$  exceeded the maximum level set at  $0.1 \text{ mg.kg}^{-1}$  (European Commission Regulation (EC) No. 1881/2006 (as amended)). Regarding Fe, coarse cereals are generally considered to be a rich source (Kaur, Jha, Sabikhi, & Singh, 2014). Samples varied greatly in their contents of Fe, with amaranth flakes being the richest source of Fe ( $66.2 \text{ mg.kg}^{-1}$ ) and rice flakes being the least rich source ( $4.8 \text{ mg.kg}^{-1}$ ).

Oat flakes, which are especially popular in the Czech Republic, contained  $32.8\text{--}58.2 \text{ mg.kg}^{-1}$  Fe. Although other cereals such as wheat and rice are consumed in higher quantities, oats are usually eaten as a whole grain cereal in porridge and also included in a variety of baked foods and muesli (Kaur et al., 2014; Rasane, Jha, Sabikhi, Kumar, & Unnikrishnan, 2015). This fact makes oats a more reasonable Fe source, since a significant proportion of the Fe located in the seedy parts other than endosperm is usually lost during milling (Shahzad et al., 2014). However, it should be stressed that, for the same reason, whole grains contain more Cd than milled and processed material (Alexander et al., 2009; Cubadda, Raggi, Zanasi, & Carcea, 2003).

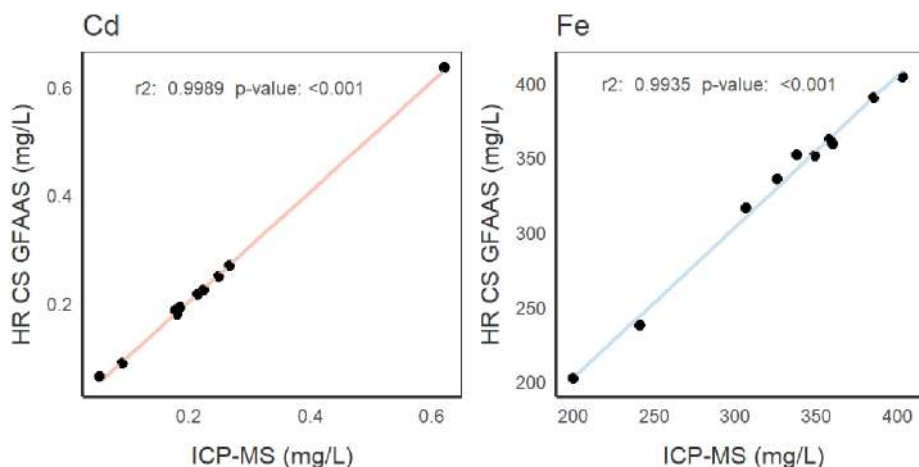


**Fig. 3.** Comparison of Cd and Fe concentrations in 10 randomly selected digests obtained by ICP-MS and the proposed HR CS GFAAS method (the curves' slopes are 1.0146 and 1.0134, respectively).

### 3.6. Conclusions: method overview

The presented method for the simultaneous determination of Cd and Fe was proven to work well during routine usage. In this approach, the two elements are determined in a single run. Pd/Mg(NO<sub>3</sub>)<sub>2</sub> modifier is used for its thermal stabilization. The method is fast, simple, and does not require the use of any permanent modifier.

The accuracy of the method was verified by means of the analysis of certified reference material. The achieved sensitivity enabled the determination of Cd and Fe in all tested samples. Results were in excellent agreement with the comparative analysis of samples using ICP-MS.

The analysis of the two studied elements in one firing is faster and more economical than separate analyses. The method may be widely applicable in laboratories equipped with HR CS GFAAS spectrometers due to its simplicity and robustness and to the fact that both Cd and Fe are often of particular interest.

### Acknowledgements

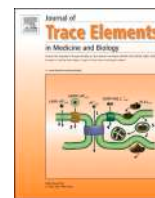
This work was financially supported by Masaryk University (projects MUNI/A/1288/2017, MUNI/A/1278/2018, and by funds from the Faculty of Medicine MU to junior researcher Ondřej Zvěřina) and the RECETOX research infrastructure (LM2015051 and CZ.02.1.01/0.0/0.0/16\_013/0001761). The involvement of Pavel Coufalík was supported by the Institute of Analytical Chemistry of the CAS under the Institutional Research Plan RVO: 68081715.

### Declaration of Competing Interest

The authors declare no competing financial interest.

### References

- Alexander, J., Benford, D., Cockburn, A., Cravedi, J., Dogliotti, E., Di Domenico, A., ... Verger, P. (2009). Scientific Opinion of the Panel on Contaminants in the Food Chain on a request from the European Commission on cadmium in food. *The EFSA Journal*, 9(8), 1–139. <https://doi.org/10.2903/j.efsa.2009.980>.
- Cubadda, F., Raggi, A., Zanasi, F., & Carcea, M. (2003). From durum wheat to pasta: Effect of technological processing on the levels of arsenic, cadmium, lead and nickel—a pilot study. *Food Additives and Contaminants*, 20(4), 353–360. <https://doi.org/10.1080/0265203031000121996>.
- Dos Santos, L. M. G., Araujo, R. G. O., Welz, B., Do, S., Jacob, C., Goreti, M., ... Becker-Ross, H. (2009). Simultaneous determination of Cd and Fe in grain products using direct solid sampling and high-resolution continuum source electrothermal atomic absorption spectrometry. *Talanta*, 78, 577–583. <https://doi.org/10.1016/j.talanta.2008.12.006>.
- Dos Santos, L. M. G., Welz, B., Araujo, R. G. O., Jacob, S. do C., Vale, M. G. R., Martens, A., ... Becker-Ross, H. (2009). Simultaneous determination of Cd and Fe in beans and soil of different regions of Brazil using high-resolution continuum source graphite furnace atomic absorption spectrometry and direct solid sampling. *Journal of Agricultural and Food Chemistry*, 57(21), 10089–10094. <https://doi.org/10.1021/jf9024773>.
- European Food Safety Authority Scientific Opinion (2012). SCIENTIFIC REPORT OF EFSA Cadmium dietary exposure in the European population 1. *EFSA Journal*, 10(1), 1–37. <https://doi.org/10.2903/j.efsa.2012.2551>.
- EFSA Panel on Dietetic Products, Nutrition and Allergies (NDA) (2015). Scientific opinion on dietary reference values for iron. *EFSA Journal*, 13(10), 4254. <https://doi.org/10.2903/j.efsa.2015.4254>.
- Ferreira, S. L. C., Bezerra, M. A., Santos, A. S., dos Santos, W. N. L., Novaes, C. G., de Oliveira, O. M. C., ... Garcia, R. L. (2018). Atomic absorption spectrometry – A multi element technique. *TrAC Trends in Analytical Chemistry*, 100, 1–6. <https://doi.org/10.1016/J.TRAC.2017.12.012>.
- Heitmann, U., Becker-Ross, H., Florek, S., Huang, M. D., & Okrusch, M. (2006). Determination of non-metals via molecular absorption using high-resolution continuum source absorption spectrometry and graphite furnace atomization. *Journal of Analytical Atomic Spectrometry*, 21(11), 1314. <https://doi.org/10.1039/b607384k>.
- International Agency for Research on Cancer Monographs. (1993). Cadmium and cadmium compounds. Lyon. Retrieved from <https://monographs.iarc.fr/wp-content/uploads/2018/06/mono100C-8.pdf>.
- Kaur, K. D., Jha, A., Sabikhi, L., & Singh, A. K. (2014). Significance of coarse cereals in health and nutrition: A review. *Journal of Food Science and Technology*, 51(8), 1429–1441. <https://doi.org/10.1007/s13197-011-0612-9>.
- Leao, D. J., Junior, M. M. S., Brandao, G. C., & Ferreira, S. L. C. (2016). Simultaneous determination of cadmium, iron and tin in canned foods using high-resolution continuum source graphite furnace atomic absorption spectrometry. *Talanta*, 153, 45–50. <https://doi.org/10.1016/j.talanta.2016.02.023>.
- Lepri, F. G., Dessuy, M. B., Goreti, M., Vale, R., Borges, D. L. G., Welz, B., & Heitmann, U. (2006). Investigation of chemical modifiers for phosphorus in a graphite furnace using high-resolution continuum source atomic absorption spectrometry. <https://doi.org/10.1016/j.sab.2006.08.001>.
- Lopez, A., Cacoub, P., Macdougall, I. C., & Peyrin-Biroulet, L. (2016). Iron deficiency anaemia. *The Lancet*, 387(10021), 907–916. [https://doi.org/10.1016/S0140-6736\(15\)60865-0](https://doi.org/10.1016/S0140-6736(15)60865-0).
- Rasane, P., Jha, A., Sabikhi, L., Kumar, A., & Unnikrishnan, V. S. (2015). Nutritional advantages of oats and opportunities for its processing as value added foods – A review. *Journal of Food Science and Technology*, 52(2), 662–675. <https://doi.org/10.1007/s13197-013-1072-1>.
- Resano, M., Briceño, J., & Belarra, M. A. (2009). Direct determination of phosphorus in biological samples using a solid sampling-high resolution-continuum source electrothermal spectrometer: Comparison of atomic and molecular absorption spectrometry. <https://doi.org/10.1039/b907937h>.
- Resano, M., Flórez, M. R., & García-Ruiz, E. (2013). High-resolution continuum source atomic absorption spectrometry for the simultaneous or sequential monitoring of multiple lines. A critical review of current possibilities. *Spectrochimica Acta Part B: Atomic Spectroscopy*, 88, 85–97. <https://doi.org/10.1016/j.sab.2013.06.004>.
- Rohr, U., Ortner, H., Schlemmer, G., Weinbruch, S., & Welz, B. (1999). Corrosion of transversely heated graphite tubes by mineral acids. *Spectrochimica Acta Part B: Atomic Spectroscopy*, 54(5), 699–718. [https://doi.org/10.1016/S0584-8547\(98\)00254-7](https://doi.org/10.1016/S0584-8547(98)00254-7).
- Shahzad, Z., Rouached, H., & Rakha, A. (2014). Combating mineral malnutrition through iron and zinc biofortification of cereals. *Comprehensive Reviews in Food Science and Food Safety*, 13(3), 329–346. <https://doi.org/10.1111/1541-4337.12063>.
- Vergine, M., Aprile, A., Sabella, E., Genga, A., Siciliano, M., Rampino, P., ... De Bellis, L. (2017). Cadmium concentration in grains of durum wheat (*Triticum turgidum* L. subsp. durum). *Journal of Agricultural and Food Chemistry*, 65, 42. <https://doi.org/10.1021/acs.jafc.7b01946>.
- Vignola, F., Borges, D. L. G., Curtius, A. J., Welz, B., & Becker-Ross, H. (2010). Simultaneous determination of Cd and Fe in sewage sludge by high-resolution continuum source electrothermal atomic absorption spectrometry with slurry sampling. *Microchemical Journal*, 95(2), 333–336. <https://doi.org/10.1016/J.MICROC.2010.01.014>.
- Wennberg, M., Lundh, T., Nilsson Sommar, J., & Bergdahl, I. A. (2017). Time trends and exposure determinants of lead and cadmium in the adult population of northern Sweden 1990–2014. *Environmental Research*, 159, 111–117. <https://doi.org/10.1016/j.envres.2017.07.029>.
- WHO. (1999). Prevention and Control of Iron Deficiency Anaemia in Women and Children. Retrieved from [https://www.who.int/nutrition/publications/micronutrients/anaemia\\_iron\\_deficiency/UNICEF\\_WHO\\_ida\\_consultation\\_report.pdf?ua=1](https://www.who.int/nutrition/publications/micronutrients/anaemia_iron_deficiency/UNICEF_WHO_ida_consultation_report.pdf?ua=1).



## A simple dilute-and-shoot procedure for the determination of platinum in human pleural effusions using HR-CS GF-AAS

Ondřej Zvěřina<sup>a,\*</sup>, Ondřej Venclíček<sup>b,1</sup>, Jan Kuta<sup>c</sup>, Pavel Coufalík<sup>d</sup>, Ingrid Hagarová<sup>e</sup>, Kristián Brat<sup>b</sup>

<sup>a</sup> Department of Public Health, Faculty of Medicine, Masaryk University, Kamenice 5, 625 00, Brno, Czech Republic

<sup>b</sup> Department of Respiratory Diseases, University Hospital Brno and Faculty of Medicine, Masaryk University, Jihlavská 20, 625 00, Brno, Czech Republic

<sup>c</sup> Research Centre for Toxic Compounds in the Environment (RECETOX), Faculty of Science, Masaryk University, Kamenice 5, 625 00, Brno, Czech Republic

<sup>d</sup> Institute of Analytical Chemistry of the Czech Academy of Sciences, Veveří 97, 602 00, Brno, Czech Republic

<sup>e</sup> Institute of Laboratory Research on Geomaterials, Faculty of Natural Sciences, Comenius University in Bratislava, Slovakia

### ARTICLE INFO

#### Keywords:

Lung cancer  
Platinum  
Pleural effusion  
HR-CS GF-AAS

### ABSTRACT

**Background:** High-resolution continuum source AAS is an emerging technique for the determination of trace elements in clinical analysis. We aimed to develop a method for the direct determination of platinum (Pt) in pleural effusions that could deepen the understanding of the dynamics of intrapleural Pt concentration during cytostatic therapy.

**Materials and methods:** Samples were collected by thoracic drainage from five patients with lung cancer undergoing platinum based chemotherapy. A simple dilute-and-shoot method for Pt determination in the pleural effusions was developed. Ashing of the sample in an oxygen flow in a graphite tube allowed for direct analysis without prior mineralization. The trueness of the method was verified using an independent technique (ICP-MS). As platinum derivatives are only active in its free form (not bound to proteins), Pt in samples was further divided into free and protein-bound forms by means of ultrafiltration.

**Results:** Using the proposed method, Pt contents (free and total) were determined in samples collected at different times after the intravenous application of the Pt derivative. The concentration of total Pt reached values of up to 5,000 µg/L and different patterns of its dynamics in intrapleural fluid were observed.

**Conclusions:** The developed method enables the fast and simple determination of Pt in biological fluids. It may be applied on a large scale to improve the understanding of Pt dynamics during cytostatic therapy, and also to determine the optimal timing of both thoracic drainage and administration of systemic chemotherapy.

### 1. Introduction

High-resolution continuum source atomic absorption spectrometry (HR-CS AAS) has brought significant improvements and new possibilities with respect to the determination of trace elements in biological materials. The importance of this accurate and sensitive analytical method is growing, especially in the case of the analysis of medical samples and microsamples. In this work, this method was adapted to determine the concentration of platinum (Pt) in pleural effusions from lung cancer patients.

Lung cancer is the most common form of cancer worldwide (with the exception of skin cancers) with high incidence and mortality. In 2018,

more than two million new cases were reported worldwide [1], claiming 1,761,007 lives [2]. In the Czech Republic, >6,500 new cases of lung cancer were reported in 2016 [3]. This project focused on lung cancer patients presenting with a significant pleural effusion that required thoracic drainage.

Pleural effusion is an accumulation of a pathological amount of fluid in the pleural cavity [4]. The quantity is not precisely defined, we consider pleural effusion to be any amount of fluid that is visible in the pleural cavity using a CT, X-ray or ultrasound of the chest. The occurrence of pleural effusion in patients with lung cancer ranges between 7 and 23 % [5]. Malignant pleural effusion most frequently occurs in patients with lung cancer of adenocarcinoma histology, followed by

\* Corresponding author at: Department of Public Health, Masaryk University, Kamenice 5, 625 00, Brno, Czech Republic.

E-mail address: [zverina@med.muni.cz](mailto:zverina@med.muni.cz) (O. Zvěřina).

<sup>1</sup> The authors contributed equally to this work.

patients with small-cell lung cancer [5]. Significant pleural effusion presents by dyspnoea and it is often necessary to manage it by thoracic drainage [6].

In such cases, it is possible to determine the concentrations of Pt derivatives in pleural effusion samples, collected from the chest drain at specific time points after the intravenous application of Pt-based cytostatic therapy.

Only a few papers addressed this topic previously, mostly reporting on the concentration of Pt in the pleural effusion after its intrapleural administration [7], or the concentration of Pt directly in the tumor tissue [8].

The clinical importance of the pleural dynamics of Pt concentration, particularly of its effective free fraction (i.e. protein-unbound), lies in the possibility of timing systemic chemotherapy within the management of pleural effusion. Both cisplatin (cis-DDP) and carboplatin (CBDCA) are irreversibly bound to proteins, however, the protein binding of CBDCA is lower [9]. The question is whether the concentration of free Pt in the pleural effusion may directly affect the metastases of the pleura (in the sense of local therapy) and whether it would be advantageous to leave a certain amount of pleural effusion, containing the active Pt (a volume tolerable by the patient), intentionally in situ to maintain the effect of Pt on the pleural metastases, rather than attempting to completely evacuate the pleural cavity.

The clinical aim of the investigation should therefore be to find the optimal timing of both thoracic drainage and the administration of systemic chemotherapy. Analysis of pleural effusion samples collected regularly during the platinum-based chemotherapy may provide clinically relevant information about the time course of Pt concentration. However, there is a limited number of patients in need of both chest drainage and platinum-based chemotherapy at the same time, therefore obtaining the samples itself is complicated.

Since the measurement of Pt concentrations in biological fluids may be not so straightforward, new methods of laboratory testing are desired. Graphite furnace atomic absorption spectrometry (GF-AAS) is among the methods traditionally used for the determination of Pt in clinical samples [10,11] together with inductively coupled plasma-mass spectrometry, adsorptive voltammetry, and neutron activation analysis [12,13]. A modern version of GF-AAS equipped with a high-resolution continuum source (HR-CS) instrument has brought numerous improvements to the technique [14–16] and HR-CS GF-AAS is now gradually being put into practice. For the analysis of clinical samples, the salient feature of the technique is background correction carried out mathematically using HR spectra, which allows the handling of higher nonspecific absorbance than classical approaches like deuterium or Zeeman background corrections [14]. This feature is particularly useful when analyzing complex biological matrices such as pleural effusions.

Our main goal was to develop a simple dilute-and-shoot method for the direct determination of Pt using HR-CS GF-AAS despite the fact that pleural effusions represent a complicated matrix containing substantial amounts of proteins. The second aim was to fractionate Pt contained in the pleural effusions into free and protein-bound forms by means of ultrafiltration using a 20 kDa cut-off.

To our best knowledge, HR-CS GF-AAS method for a direct determination of Pt in biological fluids without a prior sample mineralization has not yet been described in the literature. In addition, we explored the possibility of modulating signal intensity by using secondary spectral lines of Pt which also opens up an attractive opportunity of the simultaneous co-determination of iron in a single run.

## 2. Experimental

### 2.1. Experimental setup

The experimental scheme was designed to develop, test, and validate the analytical procedure for Pt determination using HR-CS GF-AAS. For the determination of total Pt content, diluted samples were dosed into

the graphite tube and ashed in the oxygen flow prior to atomization. Free Pt was determined after its ultrafiltration (the filtrate was directly dosed into the tube).

The trueness of Pt measurement was evaluated by an independent determination of Pt using inductively coupled plasma-mass spectrometry (ICP-MS).

Protein content in an aliquot of the sample was determined by means of the bicinchoninic acid method (BCA) followed by UV-vis detection.

### 2.2. HR-CS GF-AAS instrumentation

A ContrAA 800 G high-resolution continuum source atomic absorption spectrometer (Analytik Jena, Germany) was used for all performed measurements. The spectrometer is equipped with a transversely heated graphite furnace and a 300 W xenon short-arc lamp, operating in hot-spot mode, combined with a high-resolution echelle double monochromator and CCD array detector.

The determination of Pt in pleural effusions was performed on both the primary atomic line of 265.945 nm (using three pixel integration and also signal attenuation, i.e. the signal was read at the wings of the line – see Section 2.6. *Pt determination by HR-CS GF-AAS*) and the less sensitive secondary lines 306.471 nm and 292.979 nm for a possible reduction of excessive signals.

### 2.3. Reagents and standards

A solution of Triton X-100 surfactant (Merck, Germany) was used for the dilution of samples. Pt standard (Analytika Ltd., Czech Republic) and HNO<sub>3</sub> (Analpure, Analytika Ltd., Czech Republic) were used to prepare calibration solutions. BCA protein assay kit (Pierce, USA) was used to determine the total protein content in samples.

### 2.4. Samples of pleural effusion

In this research, samples were taken from patients with lung cancer. The study was approved by the Ethics Committee of the University Hospital Brno on November 13th, 2019; approval code/number: 02-131119. Pleural effusion samples were collected from three patients undergoing cisplatin-based and two patients undergoing carboplatin-based chemotherapy. The time intervals after the intravenous application of the platinum derivative were set at 1, 3, 6, 12 and 24 h after the infusion. In two cases, incomplete sets of samples were obtained due to technical difficulties (e.g., obturation of the chest tube). Samples (19 altogether) in polypropylene vials were immediately frozen and stored at –18 °C until analysis.

### 2.5. Preparation of analytical samples

Prior to analysis, the samples were thawed at laboratory temperature and filtered through 0.22 µm Spin-X centrifuge filter units.

In order to determine the total Pt contents, the samples were diluted with 0.01 % (v/v) Triton X-100 in the ratio of 1 + 3 and also 1 + 9.

Free Pt was determined after ultrafiltration of the pleural effusions using Centriscart I units (Supelco, MWCO 20 kDa). Samples in units were centrifuged using EBA 20 centrifuge (Hettich, Germany) at 1750×g for 90 min. The filtrate was then transferred into a new tube immediately after centrifugation.

A potential loss of the analyte due to adsorption to the ultrafiltration unit was assessed by a mass balance test. The test involved measuring Pt concentration in both permeate and retentate and comparing the combined Pt masses to that in the introduced sample.

### 2.6. Pt determination by HR-CS GF-AAS

The temperature program for Pt determination using HR-CS GF-AAS was optimized for the determination of Pt contents in pleural effusions

as well as in their ultrafiltrates. First, direct analysis of ultrafiltered samples, undiluted pleural effusions, and decomposed samples was performed. Subsequently, the samples were diluted with Triton X-100 solution in the ratio of 1 + 1, 1 + 2, 1 + 3 and 1 + 9. For the development of the atomization program, the Pt standard solution (acidified with HNO<sub>3</sub>) and the sample of pleural effusion diluted with Triton X-100 solution in the ratio of 1 + 9 were used.

Calibration was performed using both external calibration against aqueous solutions and also using standard additions to four samples of pleural effusions, including an ultrafiltered sample.

The signal was measured at the resonance line of Pt (265.945 nm) at the central pixel plus the adjacent ones (CP ± 1). To explore the possibilities of reducing signal intensity (e.g. for extension of the linear range) the signal was also measured on the wings of the atomic line (with weak attenuation, ±2 pixels), and also using selected secondary lines of Pt (306.471 nm and 292.979 nm).

Pt determination was performed using a temperature program that included oxygen ashing (Table 1). Atomization from a graphite platform was performed for a sample volume of 20 µL for all measurements.

The experimental limit of detection (LOD) and quantification (LOQ) were calculated as three and ten times the standard deviation, respectively, where standard deviation was obtained from ten measurements of an experimental blank (a control sample of pleural effusion with no detectable Pt concentration).

## 2.7. Comparative ICP-MS measurement

The reference determination of Pt contents was performed using an inductively coupled plasma mass spectrometer (7700x Agilent ICP-MS, Agilent Technologies Inc., Japan) at the Centre for Toxic Compounds in the Environment RECETOX (Brno, Czech Republic). Quantification was based on external calibration (<sup>194</sup>Pt and <sup>195</sup>Pt isotopes) with the correction of signal drift and non-spectral interferences on internal standards (<sup>185</sup>Re and <sup>209</sup>Bi). Samples were 100x diluted with 4 % HCl prior to analysis.

## 2.8. Determination of protein content

As proteins are the main component of the pleural effusion matrix, their content was determined in a set of 11 samples and their respective ultrafiltrates. The total protein contents were quantified using Pierce BCA Protein Assay kit (Thermo Scientific). The analysis was based on the reduction of Cu(II) to Cu(I) followed by selective detection of the cuprous cation using bicinchoninic acid. The absorption of the purple-colored reaction product was then detected by UV-vis at 562 nm using a Specord 50 plus UV-vis spectrophotometer (Analytik Jena,

**Table 1**  
Optimized temperature program for Pt determination using oxygen ashing in HR-CS GF-AAS.

no. #	step	temperature (°C)	ramp (°C/s)	hold (s)	gas
1	Drying 1	95	5	5	Ar (2 L/min)
2	Drying 2	110	5	5	Ar (2 L/min)
3	Pyrolysis	350	50	20	Ar (2 L/min)
4	Oxygen ashing	500	20	20	O <sub>2</sub> (2 L/min)
5	Pyrolysis (gas exchange)	500	0	10	Ar (2 L/min)
6	Pyrolysis	1300	300	20	Ar (2 L/min)
7	Gas adaptation	1300	0	5	–
8	Atomization	2350	1500	5	–
9	Cleaning	2500	500	4	Ar (2 L/min)

Germany).

## 2.9. Statistical analysis

Statistical calculations were performed and Figs. 2, 4 and 5 generated using R software [17]. Differences between the values obtained by AAS and ICP-MS measurements were compared using *t*-test as well as differences between aqueous and matrix-matched standard solutions prepared for calibration. Values of *P* < 0.05 were considered statistically significant.

## 3. Results

### 3.1. Analytical procedure involving oxygen ashing

A high content of organic matter in the pleural effusion represents a considerable complication in the atomization process. The protein content was 34 ± 6 g/L. Residues of such an organic-rich matrix in the atomizer, resulting from the dosing of undiluted pleural effusion, are obvious in Fig. 1. Of the tested dilution ratios of pleural effusion with Triton X-100 solution, the ratio of 1 + 9 proved to be suitable for measurement. Undiluted samples clog the atomizer rapidly, even when oxygen ashing is used. In addition, the dosing of a sample causes uneven spillage of the sample across the platform and reduces the reproducibility of the measurement. Even though ultrafiltration significantly reduced the protein content, samples for free-Pt determination still needed to be treated with oxygen ashing in order to prevent gradual clogging of the tube (see Fig. 1), as they still contained 1.7 ± 1.2 g/L – about half the protein content of the ten-times diluted effusions. The use of oxygen ashing during the pyrolysis step (Table 1) proved to be an effective technique for overcoming this problem and allowed the determination of Pt in all samples. Thus, samples of pleural effusions and their ultrafiltrates do not need to be mineralized prior to analysis.

The optimized temperature program for the atomizer (Table 1) included a gradual increase in the temperature of the drying step due to significant sample foaming. The temperature of oxygen ashing (carbon removal) was set to 500 °C due to the highly corrosive effects of oxygen above this temperature. The next pyrolysis step at 1300 °C served to remove inorganic salts from the sample matrix. Overall, the temperature program including oxygen ashing lasted 164 s.

### 3.2. Measurement using different Pt lines

The calibration lines obtained using the primary line (CP ± 1 and also using attenuation, i.e. the reading of the signal on the wings of the absorption profile) and secondary lines are presented in Fig. 2. Even when using the most sensitive line, 265.945 nm, the upper end of the working range reaches up to 1,000 µg/L, which is sufficient in most cases.

The correlation coefficients (*r*) were >0.999 for all the calibration curves, including the 5-point calibration ranging from 10 to 40 µg/L (which results in integrated absorbance of approx. 0.03), tested for the samples with very low Pt concentrations (not included in the figure).

In the case of high concentration samples, dilution is a preferred strategy, as a smaller amount of matrix is introduced into the atomizer. However, in some cases (e.g. of spectral interferences), it may be beneficial to use less-sensitive Pt lines. Similar sensitivities and calibration ranges for secondary lines were reported by Eskina et al. who applied HR-CS GF-AAS for determination of Pt in spent-automobile catalysts solutions [18].

It is worth special attention that the use of the Pt line 292.979 nm provides an attractive possibility to co-determine iron in the sample in one run (see the Section 3.3. Possibility of simultaneous Fe determination).

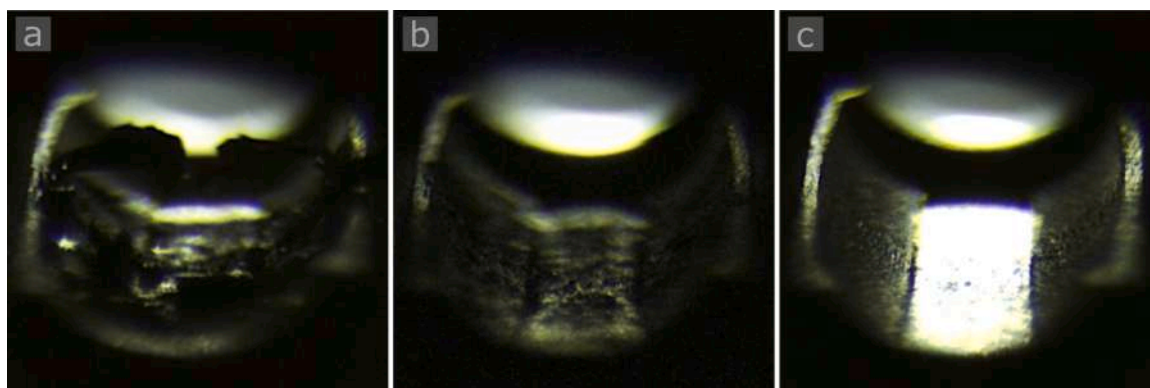


**Fig. 1.** Tube atomizer after 5 firings of diluted (1 + 3) pleural effusion without oxygen ashing (a), after 30 firings of ultrafiltrate of pleural effusion without oxygen ashing (b), and after 100 firings of diluted (1 + 3) pleural effusion with oxygen ashing (c).

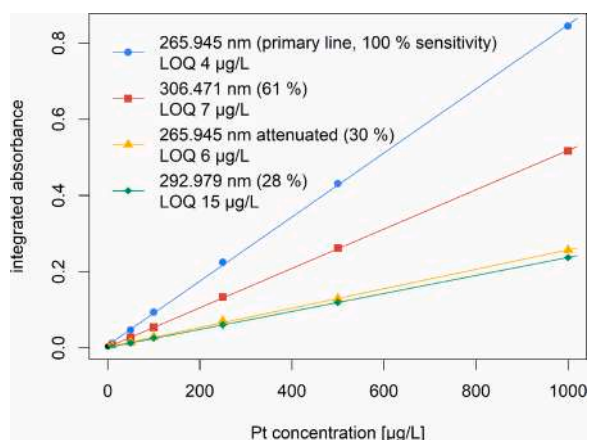


**Fig. 2.** Calibration using different Pt lines.

**3.3. Possibility of simultaneous Fe determination**

As can be seen in Fig. 3, there is a secondary iron (Fe) line visible in the vicinity of the Pt line 292.979 nm, which can be used for

simultaneous Fe determination. The sensitivity of the 292.901 nm Fe line is 0.56 % (related to the sensitivity of its primary line), which allows Fe determination in concentrations of approx mg/L, i.e. at its usual serum concentration.

**3.4. Aqueous vs. matrix-matched calibration**

To check the possible influence of the sample matrix on signal intensity, in addition to aqueous standards, sets of matrix-matched calibration solutions were also prepared from pleural effusions not exposed to Pt. The slopes of the calibration functions prepared in pleural effusions diluted in the ratios of 1 + 3 and 1 + 9, and also in ultrafiltrated sample were in agreement with the slope of the calibration curve determined using aqueous Pt standards (t-test 95 %, R-squared in all cases >0.9995). This allowed straightforward calibration with aqueous standards.

**3.5. Comparing HR-CS GF-AAS method with ICP-MS**

As there is no suitable certified reference material with a similar matrix and Pt content available, the trueness of the method was checked by comparing the obtained results with a reference measurement by ICP-MS.

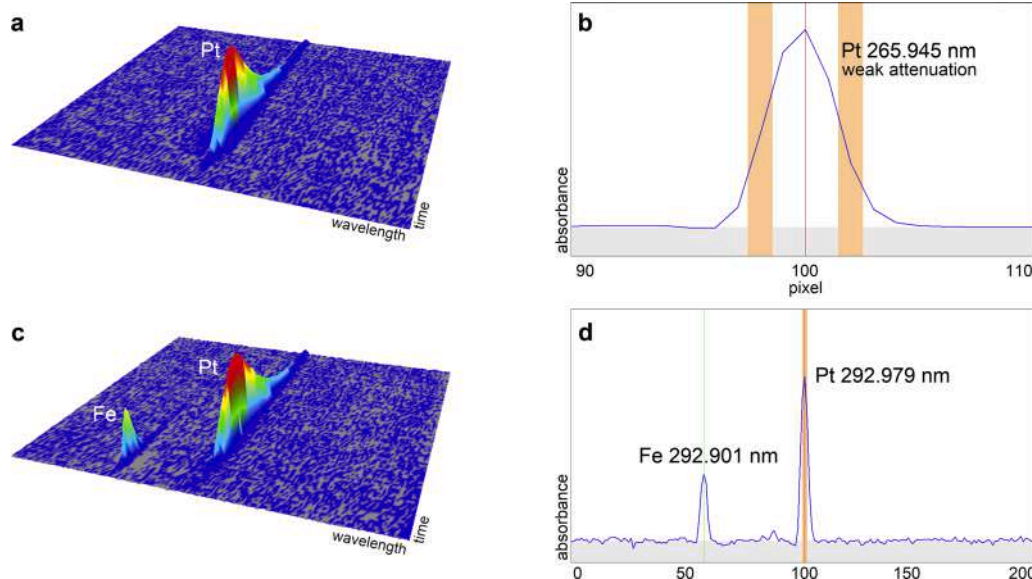


**Fig. 3.** Signals of diluted pleural effusion measurement: Pt at primary line 265.945 nm (a) and signal reading with weak attenuation (b), and Fe line 292.901 nm in vicinity of Pt line 292.979 nm (c, d).

A test set of pleural effusions and their ultrafiltrates (14 samples altogether with Pt concentration from 5 to 690  $\mu\text{g/L}$ ) was analyzed by both methods and no significant differences between the obtained results were observed (paired *t*-test,  $p = 0.9$ ). A visual comparison of the results of both the methods is given in Fig. 4.

#### 4. Discussion and conclusion

The aim of this work was to describe a new analytical method and its usability for analyses of Pt concentrations in high-protein-content biological samples (in our case pleural fluid). Using the proposed method, Pt concentrations were determined in a test set of 50 samples (comprising 25 samples of pleural fluids and 25 ultrafiltered aliquots).

##### 4.1. Sensitivity of the method

When measured at the primary Pt line (265.945 nm), LOD and LOQ were 1 and 4  $\mu\text{g/L}$ , respectively (Fig. 2). Sensitivity of the presented method in terms of LOQ is therefore slightly higher than that reported for classic line-source GF-AAS (e.g. 12  $\mu\text{g/L}$  in urine or 21  $\mu\text{g/L}$  in blood plasma [11,16]) and more than order of magnitude higher when compared to flame HR-CS AAS (180  $\mu\text{g/L}$  [16]).

##### 4.2. Determining the contents of free- and total Pt in pleural effusions

Total Pt contents reached values of up to 5,000  $\mu\text{g/L}$ , a value which, due to dilution, was still within the calibration range, even when measuring at the most sensitive Pt-line at 265.945 nm. For samples with a particularly high Pt content, the sensitivity can be reduced not only by dilution, but also by using secondary lines. In particular, the use of the 292.979 nm Pt line may be beneficial due to the possibility of the simultaneous co-determination of Fe, whilst the sensitivity of 28 % is still satisfactory for the determination of total Pt.

Protein-unbound Pt occurred at levels ranging from tens of  $\mu\text{g/L}$  to up to 2,500  $\mu\text{g/L}$ . The former concentrations were still easily measurable due to the fact that such filtered samples do not require to be further diluted, as the protein content is already reduced by the ultrafiltration. The latter had to be diluted or injected into the tube in a reduced volume in order to be measured using the primary Pt line.

According to the mass study test, there was no loss of Pt during ultrafiltration, as the sum of Pt masses in the filtrate and retentate was 96.1–103.9 % compared to the originally introduced sample ( $n = 6$ ).

##### 4.3. Clinical relevance of Pt determination in pleural effusions

From a clinical point of view, it is currently impossible to draw meaningful and reliable scientific conclusions concerning the analyzed samples from the five patients participating in this study. Therefore, we comment on this aspect only briefly.

In a healthy person, the pleural space contains only a small amount of fluid, this enabling physiological lung motion. The fluid is produced in the parietal pleura and reabsorbed by the parietal pleura lymphatics. The estimated pleural fluid turnover is about 0.15 mL/kg/h [19]. An effusion occurs in the case of an imbalance between the production and reabsorption of the pleural fluid, e.g., in cases of malignancy.

We observed two different patterns of pleural fluid Pt dynamics, these exhibiting considerable variability with respect to the results. Patients 1-3 exhibited the pattern of a gradual increase in total Pt concentration over the 24-h (or 12-h) sampling period. The concentration of free (protein-unbound) Pt in the pleural effusion peaked 6–12 h after the intravenous administration of the drug and then decreased. It appears that a larger proportion of Pt entered the pleural space bound to plasmatic proteins during production of the effusion by the parietal pleura.

In patients 1-3, who underwent cisplatin-based chemotherapy, the daily fluid production was rather limited, not exceeding a few hundreds of mL per day. In contrast, the results for patients 4 and 5, who underwent carboplatin-based chemotherapy, differed from the pattern observed for patients 1-3. In these patients, the platinum concentration peaked immediately after the intravenous administration of the drug and then followed a clear and steady downward trend, however, there is a difference even between CBDCA patients – patient 5 showed higher concentration of total Pt than patient 4, while a major proportion of the initial total Pt was constituted by free Pt, the fraction of protein-bound Pt subsequently increasing during the 24 h sampling period. We speculate that in this patient the pleural concentration of platinum directly followed the intravenous administration of the drug because of the extreme permeability of the parietal pleura. To support this thesis, we further evaluated the clinical data on this patient. The patient had a very severe metastatic cancer involving the pleura and an extensive daily production of pleural fluid of up to 2,500 mL per day. Only a few days after platinum chemotherapy treatment, the daily volumes of pleural fluid production decreased to a minimum and the chest drains could be removed. The patient responded well to the treatment and a reduction in the mass of the tumor was documented. It appears that the excessive Pt concentrations in the pleural fluid following the course of chemotherapy facilitated this significant response to treatment. We speculate that if

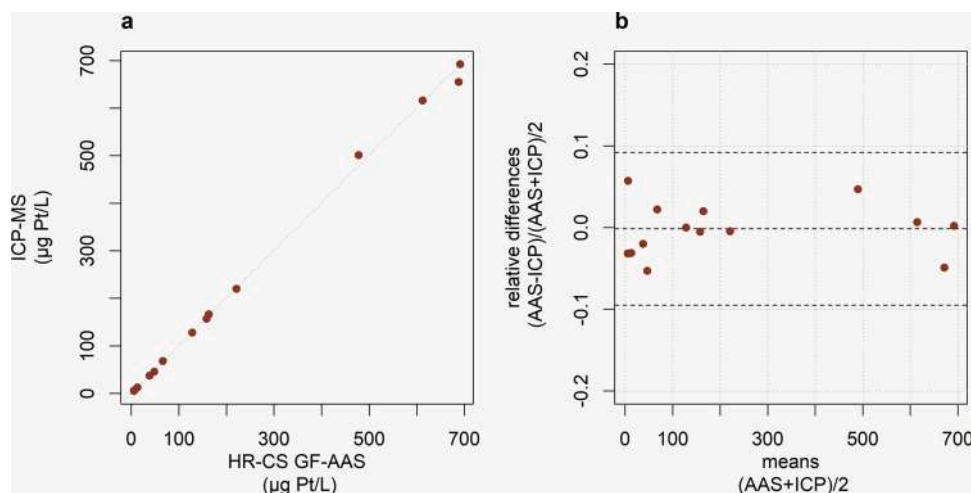


Fig. 4. Comparison of the results obtained by the developed method (HR-CS GF-AAS) and ICP-MS visualized using: a) an XY-plot, and b) a Bland-Altman-Plot showing relative differences between the two methods against the average Pt contents.

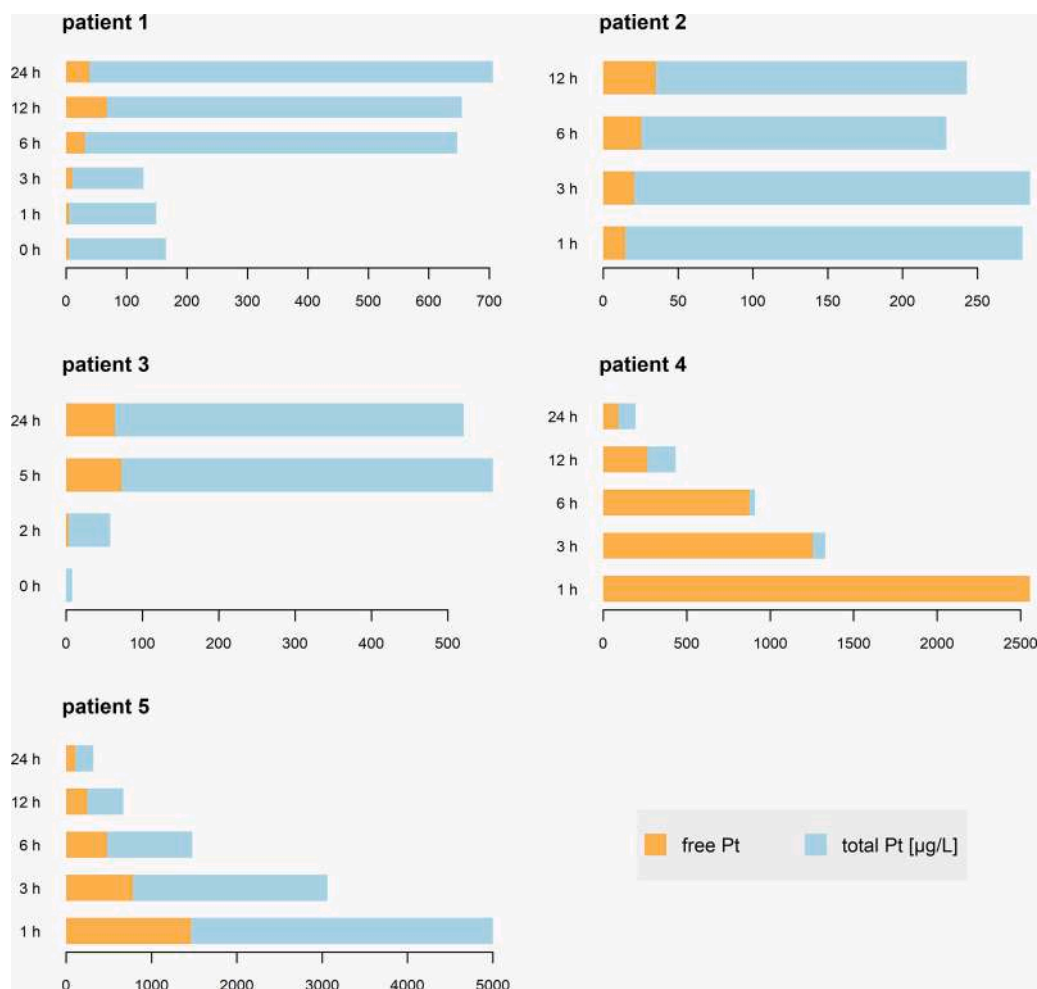


Fig. 5. Total Pt and free Pt in pleural effusions at different times after the intravenous application of the Pt derivative determined by HR-CS GF-AAS.

this hypothesis is correct, a pleural pharmacokinetic concentration curve similar to that of patient 4 might be a good predictor of a positive treatment response in similar patients. Patient 5 also clinically presented with massive pleural effusion and similarly to patient 4, responded well to the treatment. In case of patient 5, the concentration of total Pt was much higher than in patient 4. The question is, whether the differences between patients 1-3 and 4-5 are caused by the speed of production of the effusion, slightly different pharmacokinetics of cis-DDP/CBDCA, or both. The number of patients is still low to draw definite conclusions and further investigation is needed.

#### Author statement

**Ondřej Zvěřina:** Conceptualization; Investigation; Visualization; Supervision; Writing - original draft. **Ondřej Venclíček:** Conceptualization; Investigation; Methodology; Writing - original draft. **Jan Kuta:** Investigation; Writing- Reviewing and Editing. **Pavel Coufalík:** Conceptualization; Writing - original draft. **Ingrid Hagarová:** Writing- Reviewing and Editing. **Kristián Brat:** Investigation; Methodology; Writing- Reviewing and Editing, Supervision

#### Declaration of Competing Interest

There are no conflicts of interest.

#### Acknowledgements

Authors thanks to Research Infrastructure RECETOX RI (No

LM2018121) financed by the Ministry of Education, Youth and Sports, and Operational Programme Research, Development and Innovation - project CETOCOEN EXCELLENCE (No CZ.02.1.01/0.0/0.0/17\_043/0009632) for supportive background; Masaryk University (project MUNI/A/1608/2020); and the Ministry of Health of the Czech Republic (MH CZ-DRO FNBr 65269705). The involvement of Pavel Coufalík was supported by the Institute of Analytical Chemistry of the CAS under the Institutional Research Plan RVO: 68081715. We also thank Martin Pěkný for consulting with us throughout the project.

#### References

- [1] S.G. Spiro, G.A. Silvestri, One hundred years of lung cancer, *Am. J. Respir. Crit. Care Med.* 172 (09) (2005) 523–529, <https://doi.org/10.1164/rccm.200504-531OE>.
- [2] World Health Organisation, Cancer Facts Sheets: Lung Cancer (n.d.). <https://gco.iarc.fr/today/data/factsheets/cancers/15-Lung-fact-sheet.pdf> (Accessed April 1, 2020), 2021.
- [3] Institute of Health Information and Statistics of the Czech Republic, Cancer Incidence in the Czech Republic, Novotvary, 2016 (n.d.). <https://www.uzis.cz/sites/default/files/knihovna/novotvary2016.pdf> (Accessed February 8, 2021).
- [4] B. Jany, T. Welte, Pleural effusion in adults-etiology, diagnosis, and treatment, *Arztebl. Int.* 116 (2019) 377–386, <https://doi.org/10.3238/arztebl.2019.0377>.
- [5] W.W. Johnston, The malignant pleural effusion. A review of cytopathologic diagnoses of 584 specimens from 472 consecutive patients, *Cancer* 56 (1985) 905–909, [https://doi.org/10.1002/1097-0142\(19850815\)56:4<905::aid-cncr2820560435>3.0.co;2-u](https://doi.org/10.1002/1097-0142(19850815)56:4<905::aid-cncr2820560435>3.0.co;2-u).
- [6] A.O. Clive, H.E. Jones, R. Bhatnagar, N.J. Preston, N. Maskell, Interventions for the management of malignant pleural effusions: a network meta-analysis, *Cochrane Database Syst. Rev.* (2016), <https://doi.org/10.1002/14651858.CD010529.pub2>.
- [7] Kyushu Yamaguchi Thoracic Oncology Group, T. Seto, S. Ushijima, H. Yamamoto, K. Ito, J. Araki, Y. Inoue, H. Semba, Y. Ichinose, Intrapleural hypotonic cisplatin treatment for malignant pleural effusion in 80 patients with non-small-cell lung

- cancer: a multi-institutional phase II trial, *Br. J. Cancer* 95 (9) (2006) 717–721, <https://doi.org/10.1038/sj.bjc.6603319>.
- [8] V. Laszlo, T. Klikovits, A. Tisza, M. Bonta, M. Hoda, W. Berger, M. Grusch, W. Klepetko, B. Hegedus, A. Limbeck, B. Dome, P2.06-21 low intratumoral platinum concentration is associated with unfavorable clinical outcome in malignant pleural mesothelioma, *J. Thorac. Oncol.* 13 (10) (2018) S750, <https://doi.org/10.1016/j.jtho.2018.08.1276>.
- [9] W.J. van der Vijgh, Clinical pharmacokinetics of carboplatin, *Clin. Pharmacokinet.* 21 (1991) 242–261, <https://doi.org/10.2165/00003088-199121040-00002>.
- [10] W.I. Mortada, M.M. Hassanien, A.A. El-Asmy, Speciation of platinum in blood plasma and urine by micelle-mediated extraction and graphite furnace atomic absorption spectrometry, *J. Trace Elem. Med. Biol.* 27 (2013) 267–272, <https://doi.org/10.1016/j.jtemb.2013.04.004>.
- [11] I. Hagarová, M. Bujdoš, J. Kubová, P. Matúš, Direct spectrochemical determination of carboplatin species in human blood serum after their chemotherapy application for pharmacokinetic study, *Fresenius Environ. Bull.* 21 (2012) 343–350.
- [12] Z. Yang, X. Hou, B.T. Jones, Determination of platinum in clinical samples, *Appl. Spectrosc. Rev.* 37 (2002) 57–88, <https://doi.org/10.1081/ASR-120004747>.
- [13] M. Balcerzak, Methods for the determination of platinum group elements in environmental and biological materials: a review, *Crit. Rev. Anal. Chem.* 41 (07) (2011) 214–235, <https://doi.org/10.1080/10408347.2011.588922>.
- [14] M. Wójciak-Kosior, W. Szwerc, M. Strzemski, Z. Wichlacz, J. Sawicki, R. Kocjan, M. Latański, I. Sowa, Optimization of high-resolution continuum source graphite furnace atomic absorption spectrometry for direct analysis of selected trace elements in whole blood samples, *Talanta* 165 (04) (2017) 351–356, <https://doi.org/10.1016/j.talanta.2016.12.077>.
- [15] B. Welz (Ed.), *High-Resolution continuum Source AAS: the Better Way to Do Atomic Absorption Spectrometry*, Wiley-VCH, Weinheim; [Great Britain], 2005.
- [16] A.C. da Costa Jr, M.A. Vieira, A.S. Luna, R.C. de Campos, Determination of platinum originated from antitumoral drugs in human urine by atomic absorption spectrometric methods, *Talanta* 82 (2010) 1647–1653, <https://doi.org/10.1016/j.talanta.2010.07.029>.
- [17] R Core Team, *R: a Language and Environment for Statistical Computing*, R Foundation for Statistical Computing, Vienna, Austria, 2020. <https://www.R-project.org/>.
- [18] V.V. Eskina, O.A. Dalnova, D.G. Filatova, V.B. Baranovskaya, Y.A. Karpov, Direct precise determination of Pd, Pt and Rh in spent automobile catalysts solution by high-resolution continuum source graphite furnace atomic absorption spectrometry, *Spectrochim. Acta Part B At. Spectrosc.* 165 (03) (2020) 105784, <https://doi.org/10.1016/j.sab.2020.105784>.
- [19] G. Miserocchi, Physiology and pathophysiology of pleural fluid turnover, *Eur. Respir. J.* 10 (1997) 219–225, <https://doi.org/10.1183/09031936.97.10010219>.

# Analysis of mercury and other heavy metals accumulated in lichen *Usnea antarctica* from James Ross Island, Antarctica

Ondřej Zvěřina · Kamil Láška · Rostislav Červenka · Jan Kuta · Pavel Coufalík · Josef Komárek

Received: 12 February 2014 / Accepted: 16 September 2014 / Published online: 28 September 2014  
© Springer International Publishing Switzerland 2014

**Abstract** The study was designed to investigate the content and distribution of selected heavy metals (As, Cd, Co, Cr, Cu, Hg, Mn, Ni, Fe, Pb and Zn) in samples of fruticose macrolichen *Usnea antarctica* from James Ross Island. A special emphasis was devoted to mercury and its species (elemental mercury and methylmercury). It was found that mercury contents were relatively high (up to 2.73 mg kg<sup>-1</sup> dry weight) compared to other parts of the Antarctic Peninsula region, while the concentrations of most other elements were within reported ranges. Mercury contents in lichens originating from the interior were higher than those from the coast, which

is probably the result of local microclimate conditions. Similar trends were observed for Hg<sup>0</sup> and MeHg<sup>+</sup>, whose contents were up to 0.14 and 0.098 mg kg<sup>-1</sup> dry weight, respectively. While mercury did not show a significant correlation with any other element, the mutual correlation of some lithophile elements probably refers to the influence on thalli of resuspended weathered material. The influence of habitat and environmental conditions could play an essential role in the bioaccumulation of contaminants rather than just the simple presence of sources. Thus, the study of the thalli of this species can bring a new perspective on the interpretation of contaminant accumulation in lichens of the polar region.

O. Zvěřina · P. Coufalík · J. Komárek (✉)  
Department of Chemistry, Faculty of Science, Masaryk University, Kotlářská 2, 61137 Brno, Czech Republic  
e-mail: komarek@chemi.muni.cz

O. Zvěřina  
Department of Public Health, Faculty of Medicine, Masaryk University, Kamenice 5, 625 00 Brno, Czech Republic

K. Láška  
Department of Geography, Faculty of Science, Masaryk University, Kotlářská 2, 61137 Brno, Czech Republic

R. Červenka · J. Kuta  
Research Centre for Toxic Compounds in the Environment (RECETOX), Faculty of Science, Masaryk University, Kamenice 753/5, 62500 Brno, Czech Republic

P. Coufalík  
Institute of Analytical Chemistry, Academy of Sciences of the Czech Republic, v.v.i., Veveří 97, 602 00 Brno, Czech Republic

**Keywords** Antarctica · Heavy metal · Mercury · Lichen

## Introduction

Due to its remote location, Antarctica presents a unique opportunity to study the long distance transport and allocation of chemicals generated naturally or produced by humans on other continents. Although it is protected from the entry of lower latitude air masses by natural atmospheric circulation, Antarctica represents a potential sink for the deposition of long-range transported pollutants including mercury (Bargagli 2008). The atmospheric transport of pollutants is considered to be a significant pathway of Antarctic environment contamination (Montone et al. 2003; Bargagli 2008; Cipro et al. 2011). Therefore, studies on the amounts of particular chemicals

in different compartments of Antarctic ecosystems are of great importance.

Mercury is an atmospheric pollutant of global concern. Its biogeochemical cycle includes various physical, chemical and photochemical interactions, both wet and dry deposition, and reemission from environmental surfaces (Schroeder and Munthe 1998; Wängberg et al. 2001). In the atmosphere, mercury occurs mainly as  $\text{Hg}^0$  (elemental mercury vapour), along with reactive gaseous mercury ((RGM)— $\text{Hg}^{2+}$  divalent mercury compounds) and mercury associated with particulate matter. The presence of methylated mercury species has also been reported (Slemr et al. 1981, 1985; Fitzgerald et al. 1991; Lin and Pehkonen 1999).  $\text{Hg}^0$  is stable and its residence time of 6–24 months allows its transport over large distances on a global scale (Schroeder and Munthe 1998; William et al. 1998; Wängberg et al. 2001). The rate of deposition is largely affected by  $\text{Hg}^0$  to  $\text{Hg}^{2+}$  conversion, since RGM includes highly surface-reactive species and is rapidly deposited through both wet and dry deposition (Lindberg and Stratton 1998). It is known that, in polar regions, intensive Hg deposition occurs during and after the polar sunrise during mercury depletion events (MDEs). Elemental mercury undergoes photochemical oxidation to RGM by reactive halogens, and thereafter is rapidly deposited on the Earth's surface. MDE is considered to be a critical factor for mercury input in coastal polar ecosystems.

Concerns have been raised about the possible environmental effects of changes in the regional climate on the role of Antarctica as a “cold trap”. The warming of both land and ocean causes increased outgassing and also changes in sea-ice cover and in precipitation patterns (Lindberg et al. 2002; Bargagli 2005; Bargagli et al. 2005). The west side of the Antarctic Peninsula has experienced the largest increase in annual surface air warming over the last few decades. An annual temperature growth of +0.56 °C per decade was reported at the Faraday/Vernadsky station between 1951 and 2001 (Turner et al. 2005), while warming in the northwest Antarctic Peninsula was considerably greater than the mean Antarctic trend (Vaughan et al. 2001). The mean annual air temperatures also rose substantially along the eastern coast of the Antarctic Peninsula, accelerating glacier retreat and an increase in permafrost temperature (Strelin et al. 2006; Cook and Vaughan 2010). The recent breakup of the Prince Gustav shelf in 1995 (Rott et al. 1996) is one of the consequences of this temperature increase. It can also be assumed that open

water connected with sea aerosol input may additionally increase the deposition of Hg and other metals into the surveyed area.

As the retreating ice is uncovering bedrock in coastal areas, new terrestrial ecosystems are being established. Lichens are among the first colonisers of exposed rock and snow-free ground (Bargagli et al. 1999). Along with mosses, they are able to tolerate extreme temperatures together with long periods of desiccation and are the main components of Antarctic terrestrial flora (Bargagli et al. 1998; Wojtuń et al. 2013).

Lichens are known for their ability to capture and accumulate gaseous atmospheric pollutants and are commonly used as biomonitors of airborne metals including Hg (Bargagli and Barghigiani 1991; Loppi and Bonini 2000; Conti and Cecchetti 2001; Pisani et al. 2011; Mlakar et al. 2011; Lodenius 2013; Mão de Ferro et al. 2014). Five processes by which both nutrients and contaminants are deposited onto lichens are described. These are wet deposition (including snowfall), occult precipitation (fog, dew and mist), sedimentation (particles >1–4 mm), impaction (particles <1–4 mm carried by wind) and direct uptake (particularly when wetted) (Knops et al. 1991). Unlike higher plants, lichens have neither roots nor stomata, and a weak or absent cuticle enables easy exchange between the environment and their cell walls. Owing to their high cation exchange capacity, lichens have the ability to accumulate available ions of all gaseous, dissolved and particulate elements in air, snow and melting water (Bargagli et al. 1998). In addition, due to the lichens having a complicated surface structure, contaminants are absorbed over the whole thallus surface (Lupsina et al. 1992; Lodenius 2013). Different lichen morphotypes vary in their active surface for ion uptake. From this perspective, the fruticose type of thallus represents an ideal material with a large surface area. The fruticose macrolichen *Usnea antarctica* has already been utilised for monitoring the levels of heavy metals (Bargagli et al. 1993; Poblet et al. 1997; Osyczka et al. 2007; Cansaran-Duman 2011; Wojtuń et al. 2013).

There is a continuous need to monitor pollutants in the polar environment. In contrast to numerous studies on the Arctic, information on the levels of heavy metals in Antarctic lichens is still scarce. Moreover, most of the studies concerning this topic are focused on the South Shetland Islands and no similar report has been published on mercury levels in the Antarctic Peninsula and on James Ross Island in particular. The small amount of

available data from the Antarctic hinders the assessment of mercury (and other heavy metal) concentrations and the complex comparison of such concentrations and their trends between different geographical locations. James Ross Island represents an ideal area for the investigation of heavy metal concentrations and their geographical distribution, as it is one of the largest deglaciated areas along the eastern coast of the Antarctic Peninsula with only small glaciers remaining in the present landscape (Engel et al. 2012).

The objectives of this research were to determine the contents of Hg (including MeHg<sup>+</sup> and Hg<sup>0</sup> species) and some other heavy metals (As, Cd, Co, Cr, Cu, Mn, Ni, Fe, Pb and Zn) and to investigate their distribution in lichen samples originating from the northern part of James Ross Island. The geographical distribution of sampling points affected by local factors and climatic conditions (distance from the seashore, snow accumulation and fog occurrence) was expected to be the most influential factor.

## Materials and methods

### Sample origin and treatment

James Ross Island (JRI, 64° 10' S, 57° 45' W) is situated on the east side of the Antarctic Peninsula tip (Fig. 1). About 20 % of its total area of 2500 km<sup>2</sup> is recently deglaciated (Rabassa et al. 1982). The Ulu Peninsula, the northern part of JRI, represents the largest deglaciated area, with several lava-fed deltas, abundant outcrops of glacial sedimentary rock and exposures of Cretaceous marine sediments (Crame et al. 1991; Kristjánsson et al. 2005; Nývlt et al. 2014). The area of the Abernethy Flats was selected for sampling considering the articulation of the recently deglaciated terrain, which is characterised by a gradual increase in altitude from 0 to 134 m at San Jose Pass. The morphology of the valley is relatively flat and formed mostly by less resistant Cretaceous marine deposits. Local and small elevations in the central part of the valley are mostly formed by exhumed volcanic dykes. Monolith Stream, one of the largest watercourses in the area, is dewatering the vicinity of Monolith Lake towards the broad and shallow Brandy Bay. The river is located in the western and southern part of the asymmetric depression Abernethy Flats.

Climatic conditions of the Ulu Peninsula are characterised by a short summer (December–February) with positive air temperatures up to 10 °C and an annual mean air temperature of around −7 °C (Láska et al. 2011a). Total precipitation is estimated at between 300 and 500 mm water equivalent per year, with snowfall occurring even in the summer period (Bromwich et al. 2004; Dethloff et al. 2010). The snow-free period can vary from 1 to 3 months with large year-to-year variations. The daily mean incoming solar radiation is around 250 W m<sup>-2</sup> in summer, which significantly reduces snow cover (Láska et al. 2011b). In order to describe local wind conditions, 30-min surface wind observations from the nearby meteorological station at Johnson Mesa were used. The flat surface of Johnson Mesa at an elevation of 320 m a.s.l. was found as a representative site for evaluation of the prevailing wind direction. In the study, the relative frequency of wind direction measured at 6 m above ground was estimated for the period 2008–2010.

Samples were collected from the gravel plain Abernethy Flats and also in the area of the continuous and stable slope of Keller Stream and Monolith Lake during the 2012 Czech Antarctic expedition. Fruticose macrolichens *U. antarctica* were sampled along a 6-km transect beginning inland and running down across the Abernethy Flats to the seashore (Fig. 1). In the laboratory, the lichens were washed in deionised water in order to remove dust and any unwanted particles and dried for 48 h at 30 °C. Then, the thalli were homogenised in a ball mill and stored at −20 °C until analysis.

### Analytical procedures

Total mercury concentrations in the samples were determined by means of an AMA-254 analyser (Altec, Czech Republic). Determination is based on dry decomposition followed by preconcentration by amalgamation and AAS detection (Száková et al. 2004).

Elemental mercury was determined by means of thermal desorption. Aliquots of samples were heated at 105 °C for 48 h and the mercury concentrations subsequently measured. The contents of elemental mercury were calculated as the differences between total concentrations and those measured in treated aliquots. The pyrolytical determination of Hg<sup>0</sup> was first suggested by Biester and Scholz (1997) and applied as a single-step analysis by Nóvoa-Muñoz et al. (2008). This method was also conducted for Hg<sup>0</sup> determination

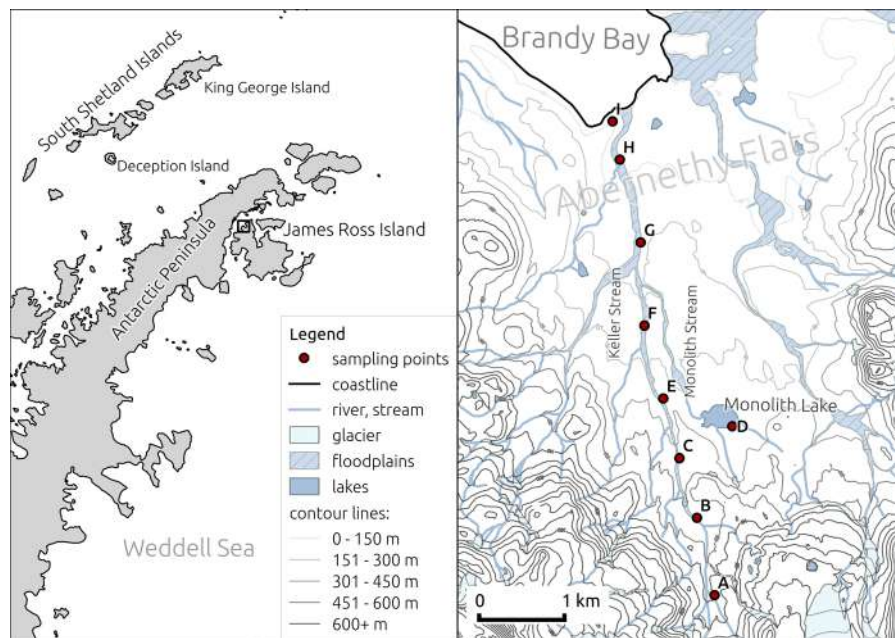


**Fig. 1** Maps of the Antarctic Peninsula region (*left*) and the Abernethy Flats sampling locality on James Ross Island (*right*). Modified map of James Ross Island-Northern part (Czech Geological Survey 2009)

in samples with a high content of organic carbon (Coufalík et al. 2013a).

For methylmercury determination, 300-mg samples were extracted with 10 mL of 6 mol L<sup>-1</sup> HCl (Sigma-Aldrich, Germany). The extraction was conducted for 2 h in an ultrasound bath and then for another 18 h on an end-over-end shaker (150 RPM). The obtained extracts were filtered through glass microfibre filters (Whatman) and the pH of the solution was adjusted to 5 with acetate buffer. The contained polar methylmercury was then converted to nonpolar volatile ethylated methylmercury using NaBEt<sub>4</sub> (Sigma-Aldrich, Germany), and the resulting solution was extracted with hexane (Sigma-Aldrich, Germany). Finally, an aliquot of 2 µl was injected into an Agilent 6890N gas chromatograph with a PSA 10.750 atomic fluorescence detector (Cai et al. 2000; Leermakers et al. 2005; Kuballa et al. 2008; Nevado et al. 2011; Červenka et al. 2011).

For the determination of selected metal contents (As, Cd, Co, Cr, Cu, Mn, Ni, Fe, Pb and Zn), the homogenised lichen thalli were digested in an HNO<sub>3</sub>/H<sub>2</sub>O<sub>2</sub> (both Sigma-Aldrich, Germany) mixture in a microwave digester (Berghof MSW3+ speedwave) according to EPA 3052 method. The contents of elements in digestions were subsequently measured using an Agilent 7500 CE quadrupole ICP-MS spectrometer (Agilent, Japan) according to the EPA 6020A method.

The spectrometer was equipped with an octopole reaction cell to avoid isobaric interferences, a Babington nebuliser and a double-pass Scott chamber. The conditions were optimised to obtain maximum sensitivity and minimum CeO<sup>+</sup>/Ce<sup>+</sup> and Ce<sup>++</sup>/Ce<sup>+</sup> ratios.

All analyses were performed in an ultra-clean laboratory equipped with HEPA filters. The used chemicals were ACS reagent grade, especially pure for mercury. Prior to use, all glassware was cleaned by two-stage decontamination in an HNO<sub>3</sub> bath and heated to 250 °C for 2 h.

The accuracy of the methods was verified by means of the following reference materials: IRMM BCR-482 Lichen (for elements As, Cd, Cr, Cu, Hg, Ni, Pb, Zn) and IAEA-336 Lichen (for elements As, Co, Cu, Hg, Fe, Mn, Zn). Recoveries of all elements were consistently within the ranges of certified values. Typical relative standard deviations for triplicate analysis of reference materials and lichen samples were within the order of units of percents. Contents of particular elements in samples were at least one order of magnitude higher than the method detection limits.

#### Statistical analysis

To summarise the collected data, general descriptive statistics including Spearman rank order correlation

and Bartels' rank test (investigation of trend occurrence) (Bartels 1982) were performed using R version 3.0.2 (R Development Core Team 2013). Nonparametric tests were used due to the non-normality of the data.

## Results and discussion

### Surface wind conditions

Figure 2 shows the relative frequency of the wind direction at the Johnson Mesa in the period 2008–2010. The prevailing wind directions were observed in the south-western sector. Southerly and westerly winds were the most common, with a frequency of occurrence of 18.8 and 14.4 % of all cases, respectively. On average, the summertime and wintertime wind directions were slightly different, but were observed within the same sector. Northerly, northwesterly and southeasterly winds had the lowest frequency of occurrence. From the observed wind pattern, it is evident that the orography of the Antarctic Peninsula affects the airflow along the eastern side of the Peninsula and the northern coast of James Ross Island.

### Total mercury contents

Figure 3 shows the total Hg contents in lichen samples. Hg concentrations ranged from 0.72 to 2.73 mg kg<sup>-1</sup> dry weight (d.w.) with a median value of 1.59 mg kg<sup>-1</sup> d.w. Bartels' test for randomness was used to examine the probability of trend occurrence (Bartels 1982). A *p*

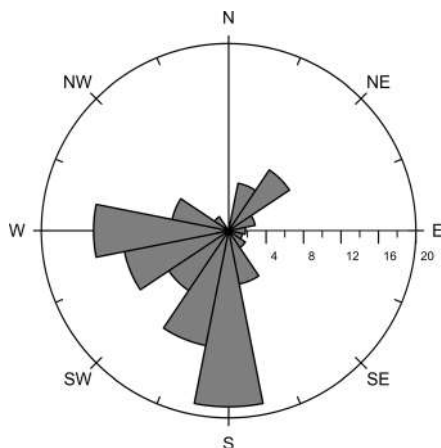


**Fig. 2** Relative wind frequency at the Johnson Mesa in the period 2008–2010

value of 0.82 indicates a gradual mercury content increase in the direction from the coast to the interior.

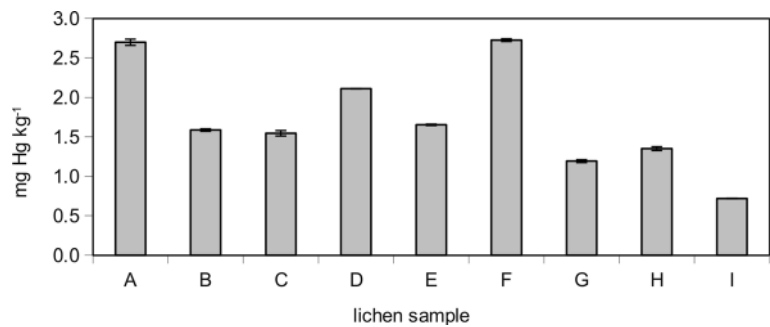
Marine aerosol has been suggested as the main contributor of mercury contamination in lichens together with volcanic emissions (Mão de Ferro et al. 2014). The lowest mercury content determined in coastal sample I, together with the above mentioned trend, indicates that sea spray does not represent a significant Hg source in this case. This fact can be partly attributed to the prevailing winds blowing towards the sea (Fig. 2). Moreover, lichens growing in localities further inland may be more affected by moisture at higher elevations. An increase in relative air humidity of 5 % from seashore to higher-elevated plateaus was observed in a previous study (Láska et al. 2011a). Increased mercury input into lichens caused by the effect of fog was already observed (Evans and Hutchinson 1996).

Abernethy Flats is a valley with suitable conditions for snow accumulation and subsequent melting. At the beginning of the sampling transect (in the vicinity of sampling points A and partially in the vicinity of B), there is the probability of increased accumulation of wind-blown snow from the glaciers south of the sampling area (e.g. Whisky Glacier). Dissolved Hg<sup>2+</sup> compounds are known to be readily absorbed by lichens when snow melts (Skov et al. 2004; Bargagli et al. 2005).

In fact, the concentrations of mercury in lichens are two to three orders of magnitude higher than those determined in soils from the same sampling localities (0.0073–0.011 mg kg<sup>-1</sup>) (Coufalík et al. 2013b). The enrichment factor between lichens and the underlying soil would reach a value of several hundred. This ratio excludes crustal aerosols as a strongly influential factor (Carignan et al. 2009). Therefore, atmospheric deposition could be considered the main source of mercury in lichens.

In comparison with mercury contents reported in lichens from the Antarctic Peninsula region, the values obtained in this work are substantially higher. Table 1 summarises published Hg levels for lichen samples originating from the South Shetland Islands, the closest area for which similar information has been published. The likely explanation is the fact that the environments of JRI and the South Shetlands are influenced by the circulation of different air masses. The climate of the South Shetlands is mainly affected by relatively warm (oceanic) air masses associated with synoptic-scale systems moving across the Bellingshausen Sea (Martin and

**Fig. 3** Total mercury concentrations in samples of *Usnea antarctica* ( $n=5$ ,  $\pm$ SD) from inland site (A) towards the seashore (I)



Peel 1978). JRI, however, is moderated by cold air masses of continental origin coming from the south and southwest, along the eastern coast of the Antarctic Peninsula. The advection of oceanic air masses towards James Ross Island is reduced by the pronounced orographic effect of the Peninsula (King 2003). Therefore, the frequency of the occurrence of continental and oceanic air masses determines the climate of the study site. These factors are assumed to play a crucial role in the distribution of long-range transported pollutants such as mercury.

#### Elemental mercury

An amount of up to 0.14 mg Hg kg<sup>-1</sup> d.w. was released by thermal desorption experiments, which presents less than 5 % of the total mercury in the samples (Fig. 4). The amounts of the desorbed portions correlate closely with total mercury contents (Spearman's correlation coefficient  $r_s=0.93$ ,  $p<0.001$ ). Similarly to the total Hg concentration, the desorbed fraction also increased

along the sampling transect from the coast to the interior ( $p$  value of Bartels' test is 0.78).

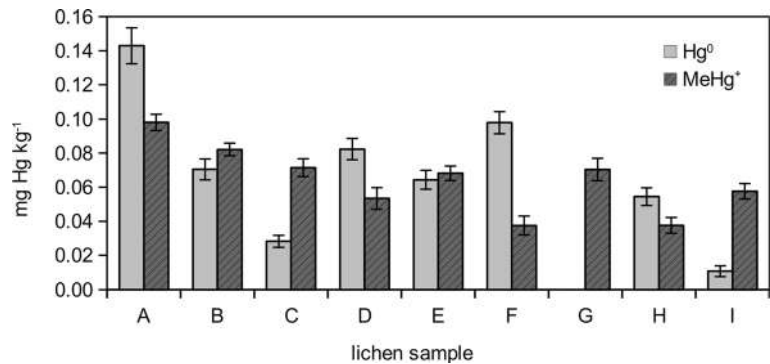
Recently, laboratory experiments have shown the ability of some plants to take up Hg<sup>0</sup> directly from the atmosphere and bond it strongly with almost no losses from evaporation or leaching (Lodenus et al. 2003). It has been demonstrated that, on the lichen surface, elemental mercury is converted into a strongly held form or diffuses into the lichen cells and is released less readily; possibly, it is converted into an inorganic form—Hg<sup>2+</sup> (Krishna et al. 2003, 2004). The high concentration of mercury in some plants could be created by an irreversible accumulation process determined by oxidation of the adsorbed Hg<sup>0</sup> followed by complexation of Hg<sup>2+</sup> by -SH groups of amino acids (Bacci et al. 1994). Some authors suggest that Hg is captured by lichens mainly after its atmospheric oxidation to the more soluble Hg<sup>2+</sup> (Krishna et al. 2003). The above-described processes are probably the reason for the small proportion of total mercury that was desorbed at 105 °C, although Hg<sup>0</sup>, the main mercury form in the atmosphere, is readily released under these conditions.

**Table 1** Reported mercury levels in lichens of *Usnea* species originating from the South Shetland Islands

Study, location	Lichen specie	Hg [mg kg <sup>-1</sup> ]	MeHg [mg kg <sup>-1</sup> ]
(Mão de Ferro et al. 2014)			
Deception Island	<i>Usnea sphacelata</i>	0.14–0.24	0.021–0.026
(Bargagli et al. 1993)			
King George Island	<i>Usnea antarctica</i>	0.026–0.061	–
Deception Island	<i>Usnea antarctica</i>	0.190–0.253	–
(Wojtuń et al. 2013)			
King George Island	Several lichen species including <i>Usnea antarctica</i>	0.18	–
(dos Santos et al. 2006)			
King George Island	<i>Usnea spp.</i>	0.0363	–

“–” means that methylmercury was not determined in this study

**Fig. 4** Elemental mercury and methylmercury contents in samples of *Usnea antarctica* ( $n=3, \pm SD$ ) from inland site (A) towards the seashore (I)



Locally, Hg vapours can be evaporated from the top soil layer. According to literature, the Hg evaporation rate from bare uncontaminated soils increases linearly from 10 °C (the lowest measured temperature) to 15–20 °C and then exponentially to 35 °C, while the volatile species (such as Hg<sup>0</sup> and (CH<sub>3</sub>)<sub>2</sub>Hg) are supposed to dominate Hg evaporation from soil (Schlüter 2000). However, previously reported results suggest that Hg content in Abernethy Flats soils is stable at temperatures up to 50 °C (Coufalík et al. 2013b). Moreover, a recent study showed that the mean monthly surface temperature on the Ulu Peninsula ranges from -11 to 6 °C (Láska et al. 2011a), which implies a low rate of Hg evaporation. Furthermore, a surface temperature higher than 10 °C is exceeded only for several days in the summer (December–February).

**Methylmercury**

The methylmercury concentration in samples ranged from 0.037 to 0.098 mg kg<sup>-1</sup> d.w. with a median of 0.068 mg kg<sup>-1</sup> d.w., which represents a portion of 1.4 to 8.1 % of total Hg. A trend of increasing MeHg<sup>+</sup> content from the coast to the interior was observed (Bartels’ test  $p$  value is 0.82).

So far, little data has been published on the occurrence of methylmercury in lichens. It was reported for lichen (*Usnea sphacelata* from Deception Island) to have a higher capacity for Hg and MeHg bioaccumulation than that observed for moss (*Polytrichum strictum* Brid. and *Sanionia georgico-uncinata*), while published MeHg<sup>+</sup> levels (Tab. 1) were slightly lower than those observed in this work (Mão de Ferro et al. 2014). Similar concentrations of MeHg<sup>+</sup> were also determined in *Hypogymnia physodes* lichens from Slovenia: 5–106 µg kg<sup>-1</sup> (0.06–3.70 % of total Hg). In addition, a good statistical correlation with total Hg was found

(Lupsina et al. 1992). In contrast, our data shows no correlation between total Hg and MeHg<sup>+</sup> ( $r_s = -0.05, p = 0.9$ ). Moreover, MeHg<sup>+</sup> contents were in anti-correlation with contents of most of the measured elements (Fig. 5).

Several processes of MeHg<sup>+</sup> production in the polar environment have been suggested, but the pathways and methylation/demethylation processes which occur are still not fully understood (Steffen et al. 2008). Snowmelt water has been identified as a significant source of MeHg<sup>+</sup> in the High Arctic, and elevated levels of bioavailable Hg were found in snow after the MDE (Loseto et al. 2004; Steffen et al. 2008).

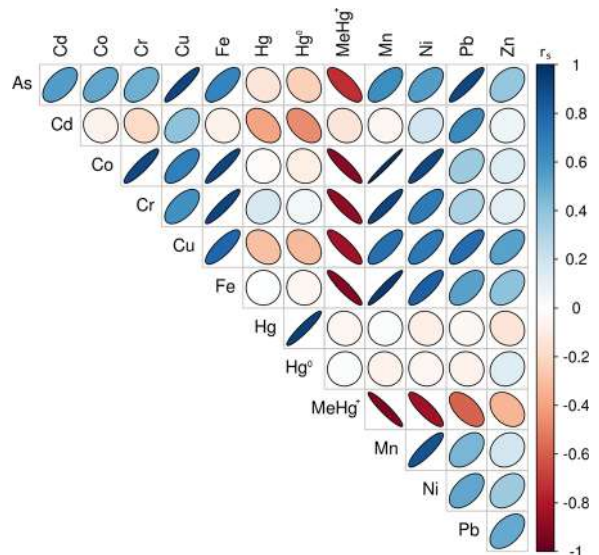


**Fig. 5** Matrix of Spearman rank correlations between measured elements. The  $r_s$  coefficients are denoted both by different shapes of ellipse and different colours (Murdoch and Chow 1996). Thin and deeply coloured ellipses refer to the strongest correlations, the inclination of an ellipse indicates the sign of the correlation. (Thin blue ellipses refer to the strongest positive correlations, thin red to the negative.)

**Table 2** Contents of heavy metals in samples and reported contents for *Usnea antarctica* [mg kg<sup>-1</sup> d.w.]

Element	As	Cd	Co	Cr	Cu	Mn	Ni	Fe	Pb	Zn
Range	0.9–2.3	0.03–0.05	0.3–1.6	1.9–4.6	1.8–6.7	10–47	1–5.1	1800–6400	0.9–3	12–27
Median	1.5	0.04	0.8	2.7	3.9	26	2.5	3900	2.0	20
Bartels' negative rank <sup>a</sup>	0.97	0.47	0.77	0.85	0.98	0.80	0.39	0.82	0.59	0.55
(Olech 1991) <sup>b</sup>	–	–	–	5.6	2.9	–	2	170	2	7
(Poblet et al. 1997)	–	0–0.03	–	–	–	16–56	2.2–9.5	283–1115	0–2.9	–
(Osyczka et al. 2007) <sup>b</sup>	–	<1.8	–	<1.7	6±1	25±5	–	–	<0.9	26±5

<sup>a</sup> *p* value of Bartels' negative rank test indicates the probability of a decreasing trend of element content from seashore to the interior

<sup>b</sup> reference samples of *Usnea antarctica* originating from areas remote to polar stations on the South Shetland Islands

“–” means that the element was not determined in this work

Ocean evasion of volatile Hg compounds (including dimethylmercury) was postulated as a source of these compounds in glacial meltwater streams (Vandal et al. 1998). The MeHg levels reported for Antarctic waters were some of the highest observed in the open ocean (Cossa et al. 2011). Unique conditions enable the oxidation of atmospheric Hg by halogens followed by its deposition into the sea. Subsequently, it is scavenged by organic particles and together with organic matter it presents a substrate for methylating bacteria in the hypoxic zone. The upwelling water is low in oxygen and rich in MeHg (Cossa et al. 2011). The sampling area is adjacent to Brandy Bay; therefore, the sea may represent a potential source of MeHg for lichens. However, no elevated MeHg levels were found in samples originating from the Brandy Bay seashore (Fig. 4).

In situ methylation in sediment, followed by diffusion into overlaying water, is another suggested cause of the presence of MeHg in the polar environment (Vandal et al. 1998). In the investigated area, conditions for methylation are expected in Monolith Lake and its close vicinity. The bottom of the lake is covered by a thick cyanobacterial mat accumulated on sediment, which allows particularly suitable conditions for microbial methylation. However, no elevated MeHg<sup>+</sup> level was observed in sample D. The highest level of MeHg<sup>+</sup> (0.098 mg kg<sup>-1</sup> d.w.) was detected in sample A, originating from the headwater area of Keller Stream with thicker snow accumulation. Lichens in this locality are frequently wetted by meltwater from both the glacial Keller Stream and also snow, which is brought by wind from the south-western sector, where the higher-located glaciers occur.

The methylation abilities of lichens themselves are not well explored. The methylation of arsenic compounds was confirmed for *Hypogymnia* lichen as a part of the detoxification process (Mrak et al. 2008). It was suggested that lichens do not act as simple passive biomonitors, but are actively involved in the uptake, accumulation and/or biotransformation of arsenic, and possibly other elements as well (Machado et al. 2006). Nevertheless, little is known about the transformation of mercury in lichens. Further research has to be undertaken to investigate the applicability of lichens as bioindicators of organometallic compounds.

#### Selected heavy metals

The concentrations of selected heavy metals (As, Cd, Co, Cr, Cu, Mn, Ni, Fe, Pb and Zn) are presented in Table 2. Generally, the contents of most metals were similar to those already reported for *U. antarctica* in other studies (Table 2). The only exception is Fe, which content is slightly higher than published values; however, it is still of the same order of magnitude. The significant correlation of lithophile elements (Co, Cr, Fe, Mn and Ni) indicate that lichen thalli may be affected by absorbed soil particles. Elevated Fe levels are likely caused by dust particles deposited onto lichen by impaction. A significant relationship has been reported to exist between the concentration of lithophile elements (including Fe and particularly Cu) in Antarctic soils and lichens (Bargagli et al. 1999). Therefore, bedrock composition is supposed to be an influencing factor, since most other metal levels are within the

ranges reported for *U. antarctica* from reference areas.

As follows from the Bartels' test  $p$  values (Table 2), the contents of As and Cu decrease with distance from the ocean. This indicates sea spray as a potential source of these metals. In contrast, no significant trend was observed for Cd, Ni, Pb or Zn.

There was no significant correlation found between the content of Hg and that of any other metal (Spearman's correlation coefficient  $r_s < 0.4$ ,  $p > 0.3$ , Fig. 5). The same lack of correlation between Hg and some other heavy metals (Pb, Cd) has been reported (Carignan et al. 2009), suggesting decoupling between these elements during emission and/or transport.

## Conclusion

Local climate and microclimate conditions are key determinants with respect to total mercury content and its variability in the Antarctic Peninsula region. While the levels of most monitored metals were within already published ranges, total Hg levels determined in the samples of *U. antarctica* originating from the area of Brandy Bay were some of the highest reported in Antarctica. According to the results of this research, elemental mercury and methylmercury accounted for up to 5.0 and 8.1 % of total mercury, respectively. It remains unclear whether these species were accumulated from the environment or whether they are products of lichen metabolism. The effects of atmospheric deposition and sea spray are most likely overlapped by the different abilities of individual thalli to effectively capture pollutants from their immediate surroundings. Nevertheless, lichen species selected for this purpose appeared to be suitable for the monitoring of heavy metals and their deposition patterns in the polar environment. Mercury speciation and the clarification of undergoing biotransformation in lichens should be important tasks for future studies.

**Acknowledgments** The authors are grateful to the CzechPolar project for the provision of infrastructure (Johann Gregor Mendel Station) and for financial support from the Grant Agency of the Czech Republic, project P503/12/0682. The work of K. Láška was supported by the Masaryk University project MUNI/A/0902/2012 "Global environmental changes and their impacts" (GlobE). The research has been co-funded from the European Social Fund and the state budget of the Czech Republic.

## References

- Bacci, E., Gaggi, C., Duccini, M., Bargagli, R., & Renzoni, A. (1994). Mapping mercury vapours in an abandoned cinnabar mining area by azalea (*Azalea indica*) leaf trapping. *Chemosphere*. doi:10.1016/0045-6535(94)90036-1.
- Bargagli, R. (2005). *Antarctic ecosystems: environmental contamination, climate change, and human impact*. Berlin: Springer.
- Bargagli, R. (2008). Environmental contamination in Antarctic ecosystems. *Science of the Total Environment*. doi:10.1016/j.scitotenv.2008.06.062.
- Bargagli, R., & Barghigiani, C. (1991). Lichen biomonitoring of mercury emission and deposition in mining, geothermal and volcanic areas of Italy. *Environmental Monitoring and Assessment*. doi:10.1007/BF00397614.
- Bargagli, R., Battisti, E., Focardi, S., & Formichi, P. (1993). Preliminary data on environmental distribution of mercury in northern Victoria Land, Antarctica. *Antarctic Science*. doi:10.1017/S0954102093000021.
- Bargagli, R., Sanchez-Hernandez, J. C., Martella, L., & Monaci, F. (1998). Mercury, cadmium and lead accumulation in Antarctic mosses growing along nutrient and moisture gradients. *Polar Biology*. doi:10.1007/s003000050252.
- Bargagli, R., Sanchez-Hernandez, J. C., & Monaci, F. (1999). Baseline concentrations of elements in the antarctic macrolichen *Umbilicaria decussata*. *Chemosphere*. doi:10.1016/S0045-6535(98)00211-2.
- Bargagli, R., Agnorelli, C., Borghini, F., & Monaci, F. (2005). Enhanced deposition and bioaccumulation of mercury in Antarctic terrestrial ecosystems facing a coastal polynya. *Environmental Science and Technology*. doi:10.1021/es0507315.
- Bartels, R. (1982). The rank version of von Neumann's ratio test for randomness. *Journal of the American Statistical Association*. doi:10.1080/01621459.1982.10477764.
- Biester, H., & Scholz, C. (1997). Determination of mercury binding forms in contaminated soils: mercury pyrolysis versus sequential extractions. *Environmental Science and Technology*. doi:10.1021/es960369h.
- Bromwich, D. H., Guo, Z., Bai, L., & Chen, Q. (2004). Modeled antarctic precipitation. Part I: spatial and temporal variability\*. *Journal of Climate*. doi:10.1175/1520-0442(2004)017<0427:MAPPIS>2.0.CO;2.
- Cai, Y., Monsalud, S., Jaffé, R., & Jones, R. D. (2000). Gas chromatographic determination of organomercury following aqueous derivatization with sodium tetraethylborate and sodium tetraphenylborate. Comparative study of gas chromatography coupled with atomic fluorescence spectrometry, atomic emission spectrometry. *Journal of Chromatography A*, 876, 147–155.
- Cansaran-Duman, D. (2011). Study on accumulation ability of two lichen species *Hypogymnia physodes* and *Usnea hirta* at iron-steel factory site, Turkey. *Journal of Environmental Biology*, 32, 839–844.
- Carignan, J., Estrade, N., Sonke, J. E., & Donard, O. F. X. (2009). Odd isotope deficits in atmospheric Hg measured in lichens. *Environmental Science and Technology*. doi:10.1021/es900578v.
- Červenka, R., Bednařík, A., Komárek, J., Ondračková, M., Jurajda, P., Vítek, T., et al. (2011). The relationship between

- the mercury concentration in fish muscles and scales/fins and its significance. *Central European Journal of Chemistry*. doi:10.2478/s11532-011-0105-8.
- Cipro, C. V. Z., Yogui, G. T., Bustamante, P., Taniguchi, S., Sericano, J. L., & Montone, R. C. (2011). Organic pollutants and their correlation with stable isotopes in vegetation from King George Island, Antarctica. *Chemosphere*. doi:10.1016/j.chemosphere.2011.07.047.
- Conti, M. E., & Cecchetti, G. (2001). Biological monitoring: lichens as bioindicators of air pollution assessment—a review. *Environmental Pollution*, 114, 471–492.
- Cook, A. J., & Vaughan, D. G. (2010). Overview of areal changes of the ice shelves on the Antarctic Peninsula over the past 50 years. *Cryosphere*. doi:10.5194/tc-4-77-2010.
- Cossa, D., Heimbürger, L.-E., Lannuzel, D., Rintoul, S. R., Butler, E. C. V., Bowie, A. R., et al. (2011). Mercury in the Southern Ocean. *Geochimica et Cosmochimica Acta*. doi:10.1016/j.gca.2011.05.001.
- Coufalík, P., Zvěřina, O., & Komárek, J. (2013a). Atmospheric mercury deposited in a peat bog, the Jeseníky Mountains, Czech Republic. *Journal of Geochemical Exploration*. doi:10.1016/j.gexplo.2013.06.005.
- Coufalík, P., Zvěřina, O., Komárek, J. (2013b). Ultra-trace analysis of mercury deposition in soils and sediments from James Ross Island, Antarctica. In: *poster Present. 11th Int. Conf. Mercur. as a Glob. Pollut. Edinburgh, Scotland, 28.7.-2.8.* (p 611). <http://www.mercury2013.com/view-abstract.php?id=447>
- Crame, J. A., Pirrie, D., Riding, J. B., & Thomson, M. R. A. (1991). Campanian Maastrichtian (Cretaceous) Stratigraphy of the James-Ross-Island Area, Antarctica. *Journal of the Geological Society (London)*. doi:10.1144/gsjgs.148.6.1125.
- Czech Geological Survey. (2009). *James Ross Island—northern part. Topographic map 1:25,000*. Prague: CGS.
- Dethloff, K., Glushak, K., Rinke, A., & Handorf, D. (2010). Antarctic 20th century accumulation changes based on regional climate model simulations. *Advances in Meteorology*. doi:10.1155/2010/327172.
- Development Core Team, R. (2013). *R: a language and environment for statistical computing*. Vienna: R Foundation for Statistical Computing.
- Dos Santos, I. R., Silva-Filho, E. V., Schaefer, C., Maria Sella, S., Silva, C. A., Gomes, V., et al. (2006). Baseline mercury and zinc concentrations in terrestrial and coastal organisms of Admiralty Bay, Antarctica. *Environmental Pollution*. doi:10.1016/j.envpol.2005.07.007.
- Engel, Z., Nývlt, D., & Láska, K. (2012). Ice thickness, areal and volumetric changes of Davies Dome and Whisky Glacier (James Ross Island, Antarctic Peninsula) in 1979–2006. *Journal of Glaciology*. doi:10.3189/2012JoG11J156.
- Evans, C. A., & Hutchinson, T. C. (1996). Mercury accumulation in transplanted moss and lichens at high elevation sites in Quebec. *Water, Air, and Soil Pollution*. doi:10.1007/BF00282663.
- Fitzgerald, W. F., Mason, R. P., & Vandal, G. M. (1991). Atmospheric cycling and air-water exchange of mercury over mid-continental lacustrine regions. *Water, Air, and Soil Pollution*. doi:10.1007/BF00342314.
- King, J. C. (2003). The spatial coherence of interannual temperature variations in the Antarctic Peninsula. *Geophysical Research Letters*. doi:10.1029/2002GL015580.
- Knops, J. M. H., Nash Iii, T. H., Boucher, V. L., & Schlesinger, W. H. (1991). Mineral cycling and epiphytic lichens: implications at the ecosystem level. *Lichenologist*. doi:10.1017/S0024282991000452.
- Krishna, B. M. V., Karunasagar, D., & Arunachalam, J. (2003). Study of mercury pollution near a thermometer factory using lichens and mosses. *Environmental Pollution*. doi:10.1016/S0269-7491(03)00041-1.
- Krishna, B. M. V., Karunasagar, D., & Arunachalam, J. (2004). Sorption characteristics of inorganic, methyl and elemental mercury on lichens and mosses: implication in biogeochemical cycling of mercury. *Journal of Atmospheric Chemistry*. doi:10.1007/s10874-004-1242-7.
- Kristjánsson, L., Gudmundsson, M. T., Smellie, J. L., McIntosh, W. C., & Esser, R. (2005). Palaeomagnetic, 40 Ar/39 Ar, and stratigraphical correlation of Miocene–Pliocene basalts in the Brandy Bay area, James Ross Island, Antarctica. *Antarctic Science*. doi:10.1017/S0954102005002853.
- Kuballa, T., Leonhardt, E., Schoeberl, K., & Lachenmeier, D. W. (2008). Determination of methylmercury in fish and seafood using optimized digestion and derivatization followed by gas chromatography with atomic emission detection. *European Food Research and Technology*. doi:10.1007/s00217-008-0949-0.
- Láska, K., Barták, M., Hájek, J., Prošek, P., & Bohuslavová, O. (2011a). Climatic and ecological characteristics of deglaciated area of James Ross Island, Antarctica, with a special respect to vegetation cover. *Czech Polar Reports*. doi:10.5817/CPR2011-1-5.
- Láska, K., Prošek, P., Budík, L., & Budíková, M. (2011b). Method of estimation of solar UV radiation in high latitude location based on satellite ozone retrieval with improved algorithm. *International Journal of Remote Sensing*, 32, 3165–3177.
- Leermakers, M., Baeyens, W., Quevauviller, P., & Horvat, M. (2005). Mercury in environmental samples: speciation, artifacts and validation. *TrAC Trends in Analytical Chemistry*. doi:10.1016/j.trac.2004.01.001.
- Lin, C.-J., & Pehkonen, S. O. (1999). The chemistry of atmospheric mercury: a review. *Atmospheric Environment*. doi:10.1016/S1352-2310(98)00387-2.
- Lindberg, S. E., & Stratton, W. J. (1998). Atmospheric mercury speciation: concentrations and behavior of reactive gaseous mercury in ambient air. *Environmental Science and Technology*. doi:10.1021/es970546u.
- Lindberg, S. E., Brooks, S., Lin, C. J., Scott, K. J., Landis, M. S., Stevens, R. K., et al. (2002). Dynamic oxidation of gaseous mercury in the Arctic troposphere at polar sunrise. *Environmental Science and Technology*. doi:10.1021/es0111941.
- Lodenius, M. (2013). Use of plants for biomonitoring of airborne mercury in contaminated areas. *Environmental Research*. doi:10.1016/j.envres.2012.10.014.
- Lodenius, M., Tulisalo, E., & Soltanpour-Gargari, A. (2003). Exchange of mercury between atmosphere and vegetation under contaminated conditions. *Science of the Total Environment*. doi:10.1016/S0048-9697(02)00566-1.
- Loppi, S., & Bonini, I. (2000). Lichens and mosses as biomonitors of trace elements in areas with thermal springs and fumarole activity (Mt. Amiata, central Italy). *Chemosphere*. doi:10.1016/S0045-6535(00)00026-6.

- Loseto, L. L., Lean, D. R. S., & Siciliano, S. D. (2004). Snowmelt sources of methylmercury to high arctic ecosystems. *Environmental Science and Technology*. doi:10.1021/es035146n.
- Lupsina, V., Horvat, M., Jeran, Z., & Stegnar, P. (1992). Investigation of mercury speciation in lichens. *Analyst*, 117, 673–675.
- Machado, A., Šlejkovec, Z., Elteren, J. T., Freitas, M. C., & Baptista, M. S. (2006). Arsenic speciation in transplanted lichens and tree bark in the framework of a biomonitoring scenario. *Journal of Atmospheric Chemistry*. doi:10.1007/s10874-006-9013-2.
- Mão de Ferro, A., Mota, A. M., & Canário, J. (2014). Pathways and speciation of mercury in the environmental compartments of Deception Island, Antarctica. *Chemosphere*. doi:10.1016/j.chemosphere.2013.08.081.
- Martin, P. J., & Peel, D. A. (1978). The spatial distribution of 10m temperatures in the Antarctic Peninsula. *Journal of Glaciology*, 20, 311–317.
- Mlakar, T. L., Horvat, M., Kotnik, J., Jeran, Z., Vuk, T., Mrak, T., et al. (2011). Biomonitoring with epiphytic lichens as a complementary method for the study of mercury contamination near a cement plant. *Environmental Monitoring and Assessment*. doi:10.1007/s10661-010-1825-5.
- Montone, R. C., Taniguchi, S., & Weber, R. R. (2003). PCBs in the atmosphere of King George Island, Antarctica. *Science of the Total Environment*. doi:10.1016/S0048-9697(02)00649-6.
- Mrak, T., Šlejkovec, Z., Jeran, Z., Jačimović, R., & Kastelec, D. (2008). Uptake and biotransformation of arsenate in the lichen *Hypogymnia physodes* (L.) Nyl. *Environmental Pollution*. doi:10.1016/j.envpol.2007.06.011.
- Murdoch, D. J., & Chow, E. D. (1996). A graphical display of large correlation matrices. *American Statistician*. doi:10.2307/2684435.
- Nevado, J. J. B., Martín-Doimeadios, R. C. R., Krupp, E. M., Bernardo, F. J. G., Fariñas, N. R., Moreno, M. J., et al. (2011). Comparison of gas chromatographic hyphenated techniques for mercury speciation analysis. *Journal of Chromatography A*. doi:10.1016/j.chroma.2011.05.036.
- Nóvoa-Muñoz, J. C., Pontevedra-Pombal, X., Martínez-Cortizas, A., & García-Rodeja Gayoso, E. (2008). Mercury accumulation in upland acid forest ecosystems nearby a coal-fired power-plant in southwest Europe (Galicia, NW Spain). *Science of the Total Environment*. doi:10.1016/j.scitotenv.2008.01.044.
- Nývlt, D., Braucher, R., Engel, Z., & Mlčoch, B. (2014). Timing of the Northern Prince Gustav Ice Stream retreat and the deglaciation of northern James Ross Island, Antarctic Peninsula during the last glacial–interglacial transition. *Quaternary Research*. doi:10.1016/j.yqres.2014.05.003.
- Olech, M. (1991). Preliminary observations on the content of heavy metals in thalli of *Usnea antarctica* Du Rietz (Lichenes) in the vicinity of the “H. Arctowski” Polish Antarctic Station. *Polish Polar Research*, 12, 129–131.
- Osyeczka, P., Dutkiewicz, E., & Olech, M. (2007). Trace elements concentrations in selected moss and lichen species collected within Antarctic research stations. *Polish Journal of Ecology*, 55, 39–48.
- Pisani, T., Munzi, S., Paoli, L., Bačkor, M., Kováčik, J., Piovár, J., et al. (2011). Physiological effects of mercury in the lichens *Cladonia arbuscula* subsp. *mitis* (Sandst.) Ruoss and *Peltigera rufescens* (Weiss) Humb. *Chemosphere*. doi:10.1016/j.chemosphere.2010.10.062.
- Poblet, A., Andrade, S., Scagliola, M., Vodopivec, C., Curtosi, A., Pucci, A., et al. (1997). The use of epilithic Antarctic lichens (*Usnea aurantiacoatra* and *U. antarctica*) to determine deposition patterns of heavy metals in the Shetland Islands, Antarctica. *Science of the Total Environment*. doi:10.1016/S0048-9697(97)00265-9.
- Rabassa, J., Skvarca, P., Bertani, L., Mazzoni, E. (1982). *Glacier inventory of James Ross and Vega islands, Antarctic peninsula\**. p. 260–264.
- Rott, H., Skvarca, P., & Nagler, T. (1996). Rapid collapse of Northern Larsen Ice Shelf, Antarctica. *Science*. doi:10.1126/science.271.5250.788.
- Schlüter, K. (2000). Review: evaporation of mercury from soils. An integration and synthesis of current knowledge. *Environmental Geology*. doi:10.1007/s002540050005.
- Schroeder, W. H., & Munthe, J. (1998). Atmospheric mercury—an overview. *Atmospheric Environment*. doi:10.1016/S1352-2310(97)00293-8.
- Skov, H., Christensen, J. H., Goodsite, M. E., Heidam, N. Z., Jensen, B., Wählin, P., et al. (2004). Fate of elemental mercury in the Arctic during atmospheric mercury depletion episodes and the load of atmospheric mercury to the Arctic. *Environmental Science and Technology*. doi:10.1021/es030080h.
- Slemr, F., Seiler, W., & Schuster, G. (1981). Latitudinal distribution of Mercury over the Atlantic Ocean. *Journal of Geophysical Research*. doi:10.1029/JC086iC02p01159.
- Slemr, F., Schuster, G., & Seiler, W. (1985). Distribution, speciation, and budget of atmospheric mercury. *Journal of Atmospheric Chemistry*. doi:10.1007/BF00053870.
- Steffen, A., Douglas, T., Amyot, M., Ariya, P., Aspmo, K., Berg, T., et al. (2008). A synthesis of atmospheric mercury depletion event chemistry in the atmosphere and snow. *Atmospheric Chemistry and Physics*. doi:10.5194/acp-8-1445-2008.
- Strelin, J., Sone, T., Mori, J., Torielli, C., Nakamura, T. (2006). New Data Related to Holocene Landform Development and Climatic Change from James Ross Island, Antarctic Peninsula. *Antarct SE*, 58. doi:10.1007/3-540-32934-X\_58.
- Szaková, J., Kolihová, D., Miholová, D., & Mader, P. (2004). Single-purpose atomic absorption spectrometer AMA-254 for mercury determination and its performance in analysis of agricultural and environmental materials. *Chemical Papers*, 58, 311–315.
- Tumer, J., Colwell, S. R., Marshall, G. J., Lachlan-Cope, T. A., Carleton, A. M., Jones, P. D., et al. (2005). Antarctic climate change during the last 50 years. *International Journal of Climatology*. doi:10.1002/joc.1130.
- Vandal, G. M., Mason, R. P., McKnight, D., & Fitzgerald, W. (1998). Mercury speciation and distribution in a polar desert lake (Lake Hoare, Antarctica) and two glacial meltwater streams. *Science of the Total Environment*. doi:10.1016/S0048-9697(98)00095-3.
- Vaughan, D. G., Marshall, G. J., Connolley, W. M., King, J. C., & Mulvaney, R. (2001). Climate change. Devil in the detail. *Science*. doi:10.1126/science.1065116.
- Wängberg, I., Munthe, J., Pirrone, N., Iverfeldt, Å., Bahlman, E., Costa, P., et al. (2001). Atmospheric mercury distribution in Northern Europe and in the Mediterranean region.

- Atmospheric Environment*. doi:10.1016/S1352-2310(01)00105-4.
- William, H. S., Munthe, J., & Schroeder, W. H. (1998). Atmospheric mercury—an overview. *Atmospheric Environment*. doi:10.1016/S1352-2310(97)00293-8.
- Wojtuń, B., Kolon, K., Samecka-Cymerman, A., Jasion, M., & Kempers, A. J. (2013). A survey of metal concentrations in higher plants, mosses, and lichens collected on King George Island in 1988. *Polar Biology*. doi:10.1007/s00300-013-1306-8.